1-1-1993

Molecular aspects of rubberlike elasticity :: a comparison of two different network systems/

Bert J. Reekmans
University of Massachusetts Amherst

MOLECULAR ASPECTS OF RUBBERLIKE ELASTICITY: A COMPARISON OF TWO DIFFERENT NETWORK SYSTEMS

A Dissertation Presented

by

BERT J. REEKMANS

Submitted to the Graduate School of the
University of Massachusetts in partial fulfillment
of the requirements for the degree of

DOCTOR OF PHILOSOPHY

September 1993

Department of Polymer Science and Engineering

MOLECULAR ASPECTS OF RUBBERLIKE ELASTICITY: A COMPARISON OF TWO DIFFERENT NETWORK SYSTEMS

A Dissertation Presented

by

BERT J. REEKMANS

Approved as to style and content by:

W. J. MacKnight, Chair

J. C. W. Chien, Member

C. P. Lillya, Member

W. J. MacKnight, Department Head
Department of Polymer Science and Engineering

To J.

I was to young to know you, but you always inspired me.

And therefore hath she brib'd the Destinies,
To cross the curious workmanship of nature,
To mingle beauty with infirmities,
And pure perfection with impure defeature;
Making it subject to the tyranny
of mad mischances and much misery;

from "Venus and Adonis" by William Shakespeare (1594)

ACKNOWLEDGMENTS

Acknowledgments of this form cannot be more than a superficial expression of my profoundest gratitude and admiration for the people that had an essential part in the realization of this work. Nevertheless, for lack of a social framework in which more appropriate expression of my feelings would fit, a few thanking words.

To Dr. MacKnight: for giving me the opportunity and the extreme latitude to experience the scientific and social USA; for allowing kinetics to be second to thermodynamics. The past five years are without a doubt the most important of my life.

To Dr. Chien and Dr. Lillya: for agreeing to be on my committee; for all the helpful comments along the way; and the patience with scheduling.

To Dr. Dickinson: for his support, in all its forms. Thanks, Charlie. Canonization would be the least.

To Dr. Dusek: for his help on a few crucial calculations.

To Dr. Petrovic: for showing me the difference between good science and better science.

To Dr. Koningsveld: for his initial support on getting my trip to the US organized; for the help with the swelling experiments.

To all the people at UMass that have helped with suggestions and actual work, and more specifically:

Meera Pyati: for the painstaking PIP synthesis.

Kimio Ichikawa: for help in the synthesis of the PPG-DRF networks.

Shifeng Xi: for help with the NMR.

Vicky White: for the fact that she always listened and helped, even though she is always overworked

To Jim Vizzini and Chris Costa: for never turning down an opportunity to lament about life over ice cream or a beer. The best friends and roommates a guy could want.

To Steve, Karen, An, Cindy, Louize, Kerri, Jerry, Kerri, Juli, and Heather: for being there when I needed it.

To all my friends: for making the experience complete.

To my family: last but not least, for the patience and support.

To worm burners, Baltimore chops, and Texas leaguers.

ABSTRACT

MOLECULAR ASPECTS OF RUBBERLIKE ELASTICITY:

A COMPARISON OF TWO DIFFERENT NETWORK SYSTEMS

SEPTEMBER 1993

BERT J. REEKMANS, B.S. UNIVERSITY OF ANTWERP, BELGIUM

Ph. D., UNIVERSITY OF MASSACHUSETTS AMHERST

Directed by Professor W. J. MacKnight

The glass transition temperature, the equilibrium modulus, the relaxation behavior in the glass transition region, and the swelling behavior in mixed solvents of two structurally different model network systems, the PPG-DRF system and the PIP-HDI system, were studied. These materials are important since they mimic the behavior of the theoretically described "perfect networks" closely. A range in material properties was induced by introducing stoichiometric imbalances and different molecular weights of the network components in the system.

Several theories for each aspect of the properties of these two systems were tested against the experiment.

It can be concluded that the PPG-DRF system behaves as a copolymer, following from the glass transition temperature and relaxation, and the swelling behavior. The end group contribution was important for the glass transition temperature. The PIP-HDI system does not behave as a copolymer.

The Constrained Chain model was applicable to the equilibrium modulus data for both systems. The trapped entanglement contribution was not explicitly relevant. The swelling in mixed solvents could only be explained when azeotropic behavior of the solvent mixture is assumed.

TABLE OF CONTENTS

Page

ACKNOWLEDGMENTS v

ABSTRACT viii

LIST OF TABLES xiii

LIST OF FIGURES xiv

Chapter

1. INTRODUCTION 1

General considerations 1
The model network 3
Homogeneity 5
The glass transition 6
Network-solvent interaction 8
Objectives 8
References 12

2. EXPERIMENTAL SECTION 14

Materials 14

The PPG-DRF system 14
The PIP-HDI system 15

Sample preparation 17
Calorimetry 18
Dynamic mechanical thermal analysis (DMTA) 18
Dielectric thermal analysis (DETA) 18
Equilibrium modulus: the Impulse technique 19
^{13}C- and ^{31}P-NMR $T_{1\rho}$ relaxation time measurements . . 19
Swelling 20
References 20

3. THE GLASS TRANSITION TEMPERATURE 21

Introduction 21
Theoretical background 24
Results and discussion 29

Conclusions 44
References 47

4. MECHANICAL MEASUREMENTS 49

Introduction 49
Theoretical background 50

The phantom network 50
The affine limit 52
The Constrained Junction model (CJ) 53
The parameter h 54
The Constrained Chain model (CC) 55
The trapped entanglement contribution 57
Other models 58

Results and discussion 59

The PPG-DRF system 59
The PIP-HDI system 66

Conclusions 71
References 73

5. RELAXATION IN THE GLASS TRANSITION REGION . 75

Introduction 75

Dynamic mechanical thermal analysis 75
Dielectric thermal analysis 77
$T_{1\rho}$ relaxation in NMR 78

Results and discussion 80

The DMTA results 80
The DETA results 85
The ^{13}C- and ^{31}P-$T_{1\rho}$ relaxation time results 87

Conclusions 95
References 96

6. SWELLING IN MIXED SOLVENTS 97

Introduction 97
Theoretical background and its application 100

The Gibbs free energy of elasticity ΔG_{el} 100
The Gibbs free energy of mixing ΔG_{mix} 101
The equilibrium swelling condition 104
Practical and computational considerations 107

Results and discussion 109
Conclusions 122
References 123

7. CONCLUSIONS 124

APPENDICES

A. CALCULATION OF STRUCTURAL PARAMETERS OF POLYURETHANE NETWORKS 127

B. SWELLING OF A NETWORK IN A MIXTURE OF SOLVENTS, A THEORETICAL APPROACH 132

BIBLIOGRAPHY 138

LIST OF TABLES

Table		Page
3.1	Experimental values for Tg of the PPG-DRF system	35
3.2	Experimental values for Tg of the PIP-HDI system	40
4.1	Mechanical and structural characteristics of the PPG-DRF networks	60
4.2	Mechanical and structural characteristics of the PIP-HDI networks	67
6.1	χ_{ab} for swelling in methanol and benzene	116
6.2	Solvent composition inside and outside the swollen PPG-DRF network at 25°C	118
6.3	Solvent composition inside and outside the swollen PIP-HDI network at 25°C	121

LIST OF FIGURES

Figure		Page
3.1	Plot of (Tg-Tg_∞) vs. 1/Mc for Tg_2 equal to (1) 500 K and (2) 1000K, using equation (2)	31
3.2	Plot of (Tg-Tg_∞) vs. 1/Mc where Tg_2 and k are (1) 400 K and 0.5; (2) 375 K and 1.0; and (3) 350 K and 1.5, respectively, using the Gordon-Taylor equation	32
3.3	The number of end groups n_e per gram vs. the temperature difference between the calculated and experimental Tg value for all samples	37
3.4	Tg of PMMA-EGDMA (squares) and PMMA-2,2-D-PDMA (circles), with fitted experimental values, vs. crosslink density 1/Mc	42
4.1	$(G - \xi RT)/T_e$ vs. $\nu RT/T_e$ for the PPG-DRF samples	62
4.2	log Δ vs. w_g for PPG-DRF	65
4.3	$(G - \xi RT)/T_e$ vs. $\nu RT/T_e$ for the PIP-DRF samples	69
4.4	log Δ vs. w_g for PIP-HDI	70
5.1	tan δ (DMTA) vs. temperature, for all PPG400-DRF samples	81

5.2 tan δ (DMTA) vs. temperature, for all PPG3000-DRF samples 82

5.3 tan δ (DMTA) vs. temperature, for all PIP2201-HDI samples 83

5.4 tan δ (DMTA) vs. temperature, for all PIP6117-HDI samples 84

5.5 tan ε (DETA) vs. temperature, for some of the PPG400-DRF samples 85

5.6 tan ε (DETA) vs. temperature, for all PPG3000-DRF samples 86

5.7 $T_{1\rho}$ relaxation times in msec vs. temperature, for the PPG2000-DRF sample 88

5.8 ^{13}C-$T_{1\rho}$ relaxation times vs. temperature for PPG-DRF3000 samples with stoichiometric imbalances 90

5.9 ^{31}P-$T_{1\rho}$ relaxation times vs. temperature for stoichiometrically balanced PPG-DRF samples 91

5.10 ^{13}C -$T_{1\rho}$ relaxation times in msec vs. temperature, for the stoichiometrically balanced PIP2201-HDI 92

5.11 ^{13}C-$T_{1\rho}$ relaxation times vs. temperature for PIP-HDI samples with different molecular weights for the backbone carbons 94

6.1 Degree of swelling in mixed solvents for PPG-DRF samples 109

6.2 Degree of swelling in mixed solvents for PIP-HDI samples 110

6.3 Plot of χ_{13} vs. φ_b for the PPG-DRF system at 25°C, extracted 114

B.1 χ_{12} for the methanol-benzene mixture 136

CHAPTER 1

INTRODUCTION

General considerations

Ever since Goodyear discovered the vulcanization process[1], the description of the elastic behavior of crosslinked materials has fascinated scientists. In the 19th century, when physical chemistry was still in its developmental stage and the concept of entropy had just been introduced, the study of elastomers confined itself to the experimental characterization of vulcanized natural rubbers of different kinds. Not until the notion that elastomers are associative materials of some kind was dispelled by Staudinger could the basis for rubberlike elasticity theory be laid. The crucial step was a number of experiments done by Meyer, von Susich, and Valko in 1932[1] that examined the near constancy of volume upon deformation. This indicated that entropy changes were governed by the configurational structure of polymers. The prominent conclusions of that time period hold in first approximation to this day, the most important one being that elastic force is proportional to the absolute temperature. Kuhn, Guth, and Mark originated the first stages of a quantitative theory, which involved the idea that polymers undergo configurational changes through bond rotation when a polymer is subjected to a stress. In 1941, the phantom network theory was formulated by James and Guth[2], and soon Flory and Wall followed with the affine network theory[3]. Two basic postulates have been of critical importance in the development of these theories and the subsequent ones. The most important

one states that although intermolecular interactions are present these interactions are independent of configuration and thus deformation. In essence, this means that rubberlike elasticity stems from an intramolecular phenomenon, i. e. an entropy reducing orientation of network chains. The second states the Gibbs free energy of the network can be written as a linear combination of the nonelastic and the elastic part of the network free energy. In the rest of this work the nonelastic part of the behavior of the network will be ignored for the reason of this postulate. Since the 1940s the scientists have generally confined themselves to refining the aforementioned theories to account for permanent topological constraints, most importantly trapped entanglements, in the form of for example the constrained junction[4], constrained chain[5], and trapped entanglement models[6]. This stage is still ongoing and part of the focus of this work is to shed more light on the subject. Other theories start from the principles of the tube models and apply them to rubberlike elasticity. It is clear that the jury is still out on which theoretical approach is the correct one to describe the complete picture of uniaxial extension and swelling data.

A brief summary of the terminology used in this work is necessary. A network is a three dimensional structure of permanently linked polymeric chains. The process of obtaining a network from the network components is called crosslinking, curing, or vulcanization, depending on the initial name for the particular process. Points of linking between chains are called junctions or crosslinks. They may be randomly located along the chain, or at specific locations along the chain. The crosslinking can be brought about by chemical reactions yielding covalently bonded structures, or physically, forming

aggregates, such as cluster formation in ionomers or crystallization in segmented polyurethanes. The average functionality of the crosslinks is >2. The process where a liquid of the network components solidifies upon reaction is called gelation, and the resulting network is often referred to as a gel. The unreacted portion that is usually present after reaction is called the sol fraction or sol. A dangling end is a network chain that is only connected to the network on one end. A loop is formed if two ends of one chain are connected to one junction point.

The model network

A very important aspect in this general controversy is the influence of molecular structure of both the polymer chain and the crosslinker on the elastic behavior. Outlining the assumptions behind the rubberlike elasticity theories explains this. The structure of the network is assumed to be "perfect", which is defined as follows: "a network with no dangling ends or loops and in which all junction points have a functionality greater than 2"[7]. For the purpose of elasticity theories some additional assumptions are made: a Gaussian end-to-end distribution between crosslinks, a perfect point crosslink. A molecular weight between crosslinks that is high enough to ensure the Gaussian behavior, perfectly homogeneous distribution of the chains and crosslinks, no free ends present, a neglect of the volume considerations, and theta conditions. These conditions have yet to be met by an experimentally accessible network system. Ever since the initial formulation of the network theories, a search has been ongoing for the

perfect network. In attempts to approach the perfect network and to study the omnipresent structural deviations from these assumptions, the model network has taken an important place. A model network is defined as a network system that resembles the perfect network structure as closely as possible, and for which a number of structural parameters needed for the theories are easily calculated. Most of the model network systems consist of a difunctional telechelic polymer of molecular weight > 1000 and a tri- or tetrafunctional crosslinker. Examples of such systems are: (1) condensation of telechelic dibasic acid polymers with glycerol; (2) addition of α,ω-divinyl polydimethyl siloxane to a tetrafunctional alkoxysilane such as $Si(OC_2H_5)_4$; (3) addition reaction of hydroxyterminated poly isobutylene tristars having a phenyl group at the crosslink point, with a diisocyanate, such as TDI. Since the molecular weight distribution has been shown to have an effect on the elastic properties of the networks, most of these systems are practically monodisperse, or fractionated to exclude the low molecular weight portion. This also ensures close compliance with the Gaussian end-to-end distribution requirement, if one assumes full flexibility of the polymer chain. The point crosslink is also inherently present. The molecular weight between crosslinks of the formed networks is fixed when full reaction is assumed. In summary, the choice of the structure of the network system offers substantial opportunity to approach the perfect network with reasonable approximation. Full reaction is hardly ever achieved, however. This has a substantial influence on the properties. Dangling ends and loops are formed. Depending on the system used and the stoichiometric imbalance, their structure can be extensively branched. The importance of the study of dangling ends

becomes clear when comparing model networks with commercial networks. There, perfection is hardly ever approached, and dangling ends will be present in substantial numbers and sizes. They do not contribute to the elasticity of the network since full relaxation is possible. Maximum extensibility of the network is found to be higher since the molecular weight between crosslinks is increased. The modulus of a network with an increased amount of dangling ends is lower because the concentration of elastically active network chains is higher. In addition, an extractable portion of some size may occur when reaction is incomplete. Both dangling ends and soluble fraction are assumed to have a plasticizing effect on a number of physical properties.

An interesting aspect of non-Gaussian behavior is highlighted by the study of bimodal networks. They are prepared by end-linking very short telechelic chains with relatively long chains[8 9 10]. The difference in average molecular weight of these polymers is a factor 10-100. This process results in unusually tough elastomers. It is still somewhat unclear what the reasons for this toughening is.

Homogeneity

Another aspect of structural problems is the lack of homogeneity and its influence on the physical properties. Crystallization is the most prominent source of inhomogeneity. Usually manifested upon stretching, it stems from the alignment of the chains with elongation, which makes crystallization preferable. It causes significant stiffening of the network sample at high elongation[11 12]. This is undesirable when studying model network properties, since homogeneity is

assumed. It is easily detected and has been studied extensively. In model network systems polymer chains are used that are inherently non-crystalline. This is usually accomplished by applying polymerization techniques that result in atactic polymers, or by random copolymerization to eliminate crystallizing potential Other kinds of inhomogeneity manifest themselves on a far smaller scale, and the effect of most of them, if identified at all, is less understood. They cause differences in rigidity on a molecular level, and may thus influence the Gaussian end-to-end distribution. Some of them are "hard segments"; hydrogen bonding; crosslink functionality; helix formation; deviations from point crosslinking. These inhomogeneities may cause differences in the elastic behavior, or may just be neglected, for reasons involving the equilibrium state. To shed some light on the influence of these molecular inhomogeneities, ^{13}C- and ^{31}P-NMR relaxation studies[13 14 15] were done, in addition to dielectric measurements[16]. X-ray diffraction was also used[17].

The glass transition

The glass transition region in temperature or frequency is important since structural features are highlighted, either in the relaxation behavior or in the glass transition temperature.

The glass transition temperature of networks is influenced by a number of structural features. The common denominator of most theoretical descriptions is the free volume in the system. Since Flory[18] defined the glass transition as an iso-free volume state, the factors that influence free volume are important in the

study of Tg. Different structural groups in the network contribute differently to Tg. This can be described by considering the network as a copolymer[19]. Crosslinking in the sense of vulcanization results in a loss of free volume. Tg generally increases with the crosslink density in the network[20]. The unreacted end groups or dangling ends have a different free volume contribution, and therefore decrease the Tg[21]. The presence of the unreacted sol fraction can act as a plasticizer to the sample. Plasticization generally lowers Tg[22].

The effect of the phenomena enumerated here generally reflect upon the relaxation behavior through the glass transition in a number of different physical properties[23]. Mechanical relaxation, dielectric relaxation, and NMR's spin-spin relaxation in the rotating frame have been used to examine the relaxation behavior through the glass transition. The applicability of each depends on the system. At Tg the storage modulus E'' in dynamic mechanical measurements and the storage dielectric constant ε'' in dielectric measurements exhibit a maximum. This maximum is shifted with frequency from the Tg determined by differential scanning calorimetry. The NMR $T_{1\rho}$ relaxation time exhibits a minimum. These maxima and minima correspond roughly to the temperature where the frequency of a certain motion in the system is the same as the technique-specific measurement frequency. Inhomogeneities may cause motions of different frequencies. Study of the relaxation behavior will provide information on the homogeneity on different length scales in the system, since the different techniques at different frequencies are sensitive to different motions.

Network-solvent interaction

When a network is submersed in a good solvent, swelling of the network by the solvent will occur. The degree of the swelling will be determined by the interaction parameter between the network chain and the component, and the crosslink density. Swelling is used to determine either the interaction parameter or the crosslink density, given that one is known. Since a study has suggested that the PPG-DRF system described hereafter behaves as a copolymer[24], interactions between crosslinker and chain need to be taken into account, as well as those between the network components and the solvent. Generally, in swelling experiments the network is considered to consist of one polymer only and the copolymer contribution is ignored. Also the influence of swelling in a mixture of solvents is studied.

Objectives

Reported studies of elastomeric systems have centered around experimental determination of mechanical properties of model networks. Even though certain imperfections were acknowledged and studied, most of the experimental work was performed under the assumption that the network system used was actually a model network. When looking more closely at the properties of the networks prepared it is often found that a large number of dangling ends are present that are not taken into account in the analysis. Also imperfections in polydispersities and functionality are seen.

A study of two model network systems is performed. The two systems are:

1. α,ω-dihydroxy poly(propyleneoxide) of nominal molecular weights of 400 , 1000 , 2000 , and 3000 , crosslinked with tris(isocyanatophenyl) thiophosphate (Desmodur RF):

PPG

DRF

2. hydroxyl terminated poly (isoprene) tristars, with approximately 6-7 repeat units of poly (butadiene) near the Si atom at the crosslink point (hereafter referred to as PIP), crosslinked with 1,6-hexamethylene diisocyanate (HDI):

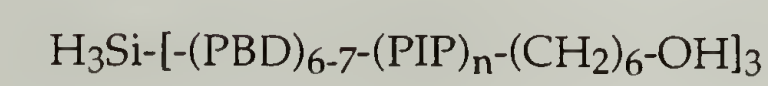

PIP

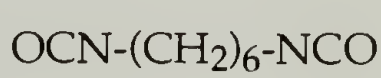

HDI

It is the objective to study a number of samples of these two different model network systems, over a range of molecular weight of the starting components and over a range of stoichiometric imbalances. This gives full information of the influence of dangling ends and Mc on the different properties examined. Examination of the relaxation behavior by the DMTA, DETA[16], $T_{1\rho}$ NMR[13,14] techniques gives information of the inhomogeneity on a molecular scale of the

polymer chains, chains close to and far from the crosslink, and crosslinks and chains, respectively.

Recently a number of complex theories have arisen to describe the Tg behavior of polymer networks. One suggests that the Tg depends on the total number of crosslink molecules[25] that are in the system, while another suggests that it depends on the total number of elastically active crosslinks[26]. This controversy perpetuates the question of the dependence of certain physical properties of the network on its equilibrium elasticity. The debate centers around the observation that the elasticity is an equilibrium quantity, while the relaxation phenomenon is a dynamic one.

A long standing problem is the inclusion of permanent topological constraints, such as trapped entanglements, into the network theories for rubberlike elasticity. Flory[27] and Langley[28] have pointed out each side of the issue. Flory contends that the influence is merely a constraining factor on the junction points, while Langley thinks that it has to be described from a phenomenological perspective, claiming that entanglements act as additional crosslinks in the system. Recently, Erman and Monnerie[6] expanded on the idea, following Flory, yet including the influence of the constraints on the chain as well, yielding a higher theoretically possible value for the equilibrium modulus. The samples made are ideally suited to shed some more light in the case. A number of studies of PDMS networks[29], which is a very "messy" system, has supported Langley's approach that explicitly treats trapped entanglements as crosslinks.

Since most examinations of swelling theories are also done with PDMS networks[7], it is necessary to search for a different system for verification. Since the PPG-DRF system behaves like a copolymer, a large number of interaction parameters need to be determined. Studying the swelling behavior in a mixture of solvents (methanol and benzene) with an appropriate theory is proposed to study the validity of the previous approach. As a verification the same experiments were performed on the PIP-HDI system.

References

1. L. R. G. Treloar, The physics of Rubber Elasticity, 3rd. ed., Clarendon Press, Oxford

2. E. Guth, H. M. James, Ind. Eng. Chem. 33, 624 (1941)

3. F. T. Wall. P. J. Flory, J. Chem. Phys, 19, 1435 (1951)

4. P. J. Flory, J. Chem. Phys, 66, 5720 (1977)

5. B. Erman, L. Monnerie, Macromolecules, 22, 3342 (1989)

6. N. R. Langley, Macromolecules, 1, 348 (1968)

7. J. E. Mark, B. Erman, Rubberlike Elasticity, a Molecular Primer, John Wiley & Sons, New York, (1988)

8. J. E. Mark , Adv. Pol. Sci. 44, 1 (1982)

9. J. E. Mark, Rubber Chem. Techn., 55, 762 (1982)

10. J. E. Mark, Acc. Chem. Res., 18, 202 (1985)

11. J. E. Mark, Pol. Eng. Sci., 19, 254 (1979)

12. J. E. Mark, Pol. Eng. Sci., 19, 409 (1979)

13. L. C. Dickinson, P. L. Morganelli, C. W. Chu, Z. Petrovic, W. J. MacKnight, J. C. W. Chien, Macromolecules, 21, 338, (1988).

14. L. C. Dickinson, J. C. W. Chien, W. J. MacKnight, 23, 1279 (1990)

15. I. M. Ward, Structure and Properties of Oriented Polymers, Appl. Science Publ., London (1975)

16. K. Ichikawa, W. J. MacKnight, submitted for publication

17. T. G. Fox, P. J. Flory, J. Appl. Phys., 21, 581 (1950)

18. T. G. Fox, P. J. Flory, J. Appl. Phys., 21, 581 (1950)

19. G. Lee, B. Hartmann, J. Appl. Polym. Sci., 28, 823 (1983)

20. T. G. Fox, S. Loshaek, J. Polym. Sci., 15, 371, (1955)

21. P. Meares, Trans. Far. Soc., 53, 31 (1957)

22. P.D. Ritchie, ed., Plasticizers, Stabilizers, and Fillers, Iliffe Books Ltd. (1972)

23. J. D. Ferry, Visocelastic Properties of Polymers, John Wiley & Sons, New York, (1980)

24. Z. S. Petrovic, W. J. MacKnight, R. Koningsveld, K. Dusek, Macromolecules, 20, 1088 (1987)

25. A. Shefer, M. Gottlieb, Macromolecules, 25, 4036 (1992)

26. A. Hale, C. W. Macosko, H. E. Bair, Macromolecules, 24, 2610 (1991)

27. P. J. Flory, Polymer, 20, 1317 (1979)

28. N Langley, J. Non-Cryst. Solids, 131, 894 (1991)

29. J. P. Queslel, J. E. Mark, Adv, Pol. Sci. 65, 135, (1984), and references therein.

CHAPTER 2

EXPERIMENTAL SECTION

Materials

The PPG-DRF system

The system consists of α,ω-dihydroxy poly(propylene oxide) of nominal molecular weights of 400 (PPG400), 1000 (PPG1000), 2000 (PPG2000), and 3000 (PPG3000), obtained from Aldrich Chemical Co., and tris(isocyanatophenyl) thiophosphate (Desmodur RF), generously supplied by Mobay Chemical Corp.

The PPGs were dried azeotropically in benzene and stored under dry nitrogen. Before using, the PPGs were placed under reduced pressure for several days to remove residual benzene. Hydroxyl group functionality was determined by titration of excess added phtalic anhydride (ASTM D4274). The PPG samples were tested for monofunctional species by thin layer chromatography. The glycols were dissolved in ethyl acetate containing 1% sec butanol to obtain a glycol concentration of 0.1%. The developer was iodine. Despite some tailing no evidence of monofunctional species was found. Assuming ideal difunctionality the molecular weight of the PPGs are 402, 1002, 2004, and 2901 for PPG400, 1000, 2000, and 3000, respectively, as determined from titration.

Tris(4-isocyanatophenyl) thiophosphate (Desmodur RF) was recrystallized twice from dry toluene after removal under reduced pressure of the initial solvent, methylene chloride. The isocyanate content was determined by titration of the excess of added dibytylamine with HCl following ASTM D1638-74. The titration was performed on three different samples, and the average taken. The functionality was 3.00 ± 0.03, which is well within the error margin of the technique.

The PIP-HDI system

All polymerizations were done in Schlenk type of glassware. A 10% monomer to solvent ratio was used for the solutions.

To a stoppered round bottom flask equipped with a glass stir bar, initiator solution (Butyl 6-Lithiohexyl Acetaldehyde Acetal) was added. The initiator solution was diluted with solvent. The solution was cooled to -10° C. Isoprene was added and the polymerization was continued for 1 day. The polymer solution was cooled to 0° C. An amount of butadiene, equivalent to about 7 repeat units per polymer, was added and the polymerization was continued for 1 day. The coupling agent, methyltrichlorosilane was added in aliquots at 0° C. 50% of the coupling agent was added the first day. The rest of the coupling agent was added in aliquots over the next day. Methyl lithium was added to quench excess chlorosilane and methanol was added to quench excess methyl lithium. The solvent was evaporated, the polymer redissolved in ether, washed with water, and subsequently a saturated NaCl solution, and

dried over Na_2CO_3. The solvent was evaporated to obtain colorless, viscous polymer. The resulting tristar polymers were fractionated (benzene/methanol) to remove uncoupled material (5-10%).

The acetal blocking group was removed by acid hydrolysis. 80g of polymer was dissolved in toluene (750 ml). Distilled water (250 ml) was added. Dicloroacetic acid (1g in 7 ml of water) was added. The solution was refluxed for 30h. A stream of nitrogen was continuously passed through the solution. The reaction mixture was cooled and the layers separated. The toluene layer was washed consecutively with water (250 ml, 2X), 10% aqueous Na_2CO_3 solution(250 ml,3X) and a saturated NaCl solution (250 ml). The solvent was evaporated and dried under vacuum at 60^o C for 2 days.

Number average molecular weight of the three samples was 2201, 2641, and 6117 as measured by GPC calibrated with low molecular weight, low polydispersity polybutadiene as standards. The polydispersity was 1.07, 1.08, and 1.03 respectively. The respective molecular weight as measured by VPO are 2000, 2518, and 5804. The discrepancy between the two measurements is within limits usually observed.

From solid state ^{13}C-NMR, the 3,4-content of the polyisoprene portion for all tristars is approximately 65%, with the 1,4-content at 25% and the 1,2-content at 10%. The polybutadiene portion makes up 41%, 36%, and 15% of the PIP2201, PIP2641, and PIP6117 tristars respectively. This corresponds to approximately 7 repeat units of butadiene in each case, as intended during the polymerization. The 1,2-content of the polybutadiene is approximately 65%.

Sample preparation

The network samples were prepared by dissolving at room temperature under dry nitrogen the appropriate amounts of trifunctional and difunctional materials in an equivolumetric amount of dry toluene (Aldrich Chemical) to achieve proper mixing of the components. For the samples prepared with excess isocyanate, an equimolar amount to the excess of cyclohexanol (Aldrich Chemical) was added to prevent side reactions. Solutions were placed under reduced pressure to remove the toluene. For the PPG-DRF samples the solvent could be fully removed before the gel point was reached, except for the PPG400 samples. These samples and the PIP-HDI samples became highly viscous and unpourable before all solvent was removed. All samples were transferred while still pourable to Teflon lined Al molds, 5 cm in diameter, and then heated to 90°C under reduced pressure for 7 days. The residual 5-20% toluene still present after transfer was thus removed before the gel point was reached. The sample thickness was 0.7-1 mm.

The weight fraction w_s of the extractable sol fraction was determined by weighing a portion of the sample before and after extraction with toluene for 6 days. Fresh solvent was provided each day. The samples were dried under reduced pressure at 50°C in a vacuum oven for 3 days.

The samples were stored under vacuum in a desiccator. Occasionally, the samples were redried by placing them in a vacuum oven at 50°C for a period of time.

Calorimetry

DSC measurements were carried out with a Perkin-Elmer DSC-4 over a temperature range of -100°C to 50°C. The heating rate was 20°C/min. The glass transition temperature Tg was defined as the midpoint of the heat capacity change. The measurement was taken after the third run. The weight of the samples was 7-12 mg.

Dynamic mechanical thermal analysis (DMTA)

DMTA equipment from Polymer Laboratories was used for dynamic mechanical analysis. The measurements were carried out in single cantilever mode with a free length of 2-5 mm, appropriate to the thickness and width of the sample used (width between 0.5 and 1.3 mm). A frequency of 1 Hz was applied. The heating rate was 2°C/minute in all cases. The sample chamber was constantly purged with nitrogen gas. A small strain (<2%) was applied when clamping the sample to prevent slippage above the glass transition temperature. Samples were run at least twice to verify proper clamping and reproducibility.

Dielectric thermal analysis (DETA)

DETA equipment from Polymer Laboratories with a digital Wheatstone bridge from GenRad Corporation were used to determine dielectric behavior

with changing temperature. Plate electrodes with a diameter of 20 mm were used. A frequency of 1 kHz was applied, with a heating rate of 3°C/minute for all samples. The sample chamber was constantly purged with nitrogen gas. Slight pressure was applied to the top electrode to ensure proper contact between the electrodes and sample.

Equilibrium modulus: the Impulse technique[1]

The Dynastat mechanical analyzer was used to measure the equilibrium modulus. A square wave deformation with an amplitude corresponding to <5% deformation and a frequency of .05 Hz was applied. The analysis and integration were carried out on an IBM-XT computer with software, courtesy of Dr. Farris, Dr. Vratsanos, and Dr. Goldfarb. The samples were reclamped a number of times to ensure reproducibility. The actual value of the modulus is an average of at least 5 consecutive experiments.

^{13}C- and ^{31}P-NMR $T_{1\rho}$ relaxation time measurements

The ^{13}C- and ^{31}P-NMR $T_{1\rho}$ relaxation measurements were done with a Bruker AF-200 NMR spectrometer with solid state accessories. CP-MAS and DP-MAS $T_{1\rho}$ relaxation pulse sequences were used to determined the relaxation times of all samples. No statistically significant difference was found between the resulting relaxation times from the cross-polarizing and direct polarizing techniques. The cross-polarizing technique was applied

below the temperature of the minimum in relaxation times, while the direct polarizing technique was used at and above. This was done for expedience purposes, since the CP technique increases resolution substantially below the minimum. A series of delays of up to 60 msec were used to determine the relaxation time.

Swelling

Stoichiometrically balanced samples of all molecular weights of both systems were swollen in mixtures of methanol (Aldrich) and benzene (Aldrich) in a desiccator. Full swelling was usually accomplished within 7 days. Swelling longer resulted in degradation of the samples. The swollen samples were transferred very fast from the swelling bottle to the balance, with a quick drying of the surface with a paper towel. The time from removal from the bottle to the actual weighing was less than 30 seconds.

References

1. R. J. Farris, C. Lee, Polym. Eng. Sci., 23, 586 (1983)

CHAPTER 3

THE GLASS TRANSITION TEMPERATURE

Introduction

In the study of structure-property relationships of networks, the knowledge of the glass transition temperature, Tg, takes an important place. For post-synthesis cured systems, such as rubber vulcanizates, the Tg defines the lower limit of usefulness in their application as elastomers, while in thermosetting polymers the Tg usually marks the top limit. In addition, physical and mechanical properties of network polymers change greatly at Tg.

A number of theoretical approaches have been proposed to relate the glass transition temperature to the structure of networks. Most are based on free volume theory and configurational entropy, differing only in the modifications where necessary for certain imperfections or limits, specific to a particular network system. The complexity of these theoretical approaches has increased with the search for universality. The number of polymer-specific experimentally determined parameters needed to fully describe the Tg behavior of a network system has increased. A larger number of experiments needs to be performed to accurately describe the Tg behavior of a network. In an effort to shed some light on the matter we have broken down the problem into three parts, namely the effect of crosslinking on Tg; the copolymer effect on Tg; and the effect of free end groups on Tg. These three effects are difficult to separate. The use of model networks, giving limited control over certain

structural and topological network parameters, offers an opportunity to study the influence of the three effects on Tg.

Model networks usually exhibit moderate to high crosslink densities and relatively high glass transition temperatures. A number of structural and topological parameters necessary in Tg theories for thermosetting polymers, such as the end group concentration and conversion, can be determined for model networks from a simple extraction experiment using branching theory[1]. The molecular weight between crosslinks, Mc, which is an essential experimental parameter for the theories applying to post-synthesis cured systems, is known here from the molecular weight of the network component. The choice of the model network components offers an ideal opportunity to the study of physical properties, such as Tg, for both post-synthesis cured network systems or their structural equivalents, and thermosetting network systems.

The current study compares the glass transition temperature of two model network systems. The first is the thoroughly studied poly(propylene glycol)-Desmodur RF (PPG-DRF) system[2 3 4]. Structurally, this system resembles thermosetting polymers, since the DRF crosslinker is very bulky, and for high crosslink density the glass transition temperature is above room temperature. The second consists of hydroxyl terminated poly isoprene (PIP) tristars with a range of molecular weights, which is crosslinked with the difunctional hexamethylene diisocyanate (HDI). This system corresponds more to the post-synthesis cured polymers, since crosslink density is somewhat lower and

it exhibits a true point crosslink, lacking the bulkiness and the structural differences in the chain.

To study their Tg behavior, samples were prepared with stoichiometric and off-stoichiometric ratios of hydroxyl and isocyanate terminated components of each system, with different molecular weights of the hydroxyl terminated components. This yields networks with a range of molecular weights between crosslinks (Mc), and a range of concentrations of dangling ends in the ensuing samples.

The effect of crosslinking on Tg is influenced by a number of additional parameters. For a given network system the Tg is proportional to the functionality of the crosslinks. In both systems studied here the crosslinks are trifunctional, but data for vulcanized polyisoprene which has tetrafunctional crosslinks are available for comparison. The influence of crosslinking units that are not considered elastically active but are merely branching units in dangling ends, is unclear. One study[5] suggests that they should not be considered crosslinks for the purpose of Tg determination, while another suggests the opposite[6]. Recently, it was suggested that the assumption depends on crosslink density[7].

The copolymer effect on Tg can easily be investigated with these two systems, since one is clearly a copolymer, while the other is not. The Tg of samples prepared from stoichiometric feeds of the DRF-PPG system has been described by considering the copolymer effect only[8]. The PIP-HDI system does not

exhibit the structural difference between the crosslink and the chain. For Tg purposes PIP and PBD behave very similarly. In the samples prepared from stoichiometrically imbalanced feeds of network components, the importance of the copolymer effect will become apparent since all other parameters are constant.

The effect of end groups on Tg is much better understood because it also influences the Tg of linear and branched polymers. Fewer parameters influence the Tg of linear polymers. The transfer of this knowledge to crosslinked polymers has therefore not posed a problem. The hydroxyl end group in PPGs negates the effect of differing molecular weight on their Tg. Regardless of the molecular weight of the PPG, the Tg remains the same[9]. This has been attributed to hydrogen bonding. For polyisoprene the behavior is similar since the presence of a terminal hydroxyl group reduces the molecular weight effect on Tg by approximately 60 %[10]. The end group contribution, even though the concentration of end groups is relatively large, will be negligible for the PPG-DRF system and on the order of 1-2K for the PIP-HDI system.

Theoretical background

At the basis of most theoretical approaches for explanation of Tg behavior of polymer networks is the dependence of Tg on free volume. After the definition of Tg as an iso-free volume state by Fox and Flory[11] the principle

has been applied to characterize the influence of three fundamental structures of polymers on Tg; chain ends[12], crosslinking[13], and copolymers[14]. All three factors play a role in Tg of network polymers.

The influence of chain ends is very important in thermosets, where the reaction of low molecular weight molecules with a large number of end groups seldom reaches complete conversion. In post-synthesis cured polymers, the crosslinks are introduced in high molecular weight polymers with a relatively low concentration of end groups, making their influence on Tg negligible. Tg of a network is directly proportional to the number of end groups, and directly following Meares[12] the dependence can be expressed as:

$$Tg = Tg_\infty - KC_e \qquad (1)$$

Tg_∞ is the Tg of the network without end groups, K a polymer-specific constant, and C_e the concentration of end groups.

A similar equation, first formulated by Fox and Loshaek[13], can be written for the dependence of Tg on crosslinking:

$$Tg = Tg_\infty + k/Mc \qquad (2)$$

with Tg_∞ the Tg of the linear equivalent of the network polymer, k a network system-specific constant, and Mc the molecular weight between crosslinks. Two other theoretical approaches[15 16] describe the crosslinking effect in a similar fashion, namely as a crosslink density dependent deviation from the

Tg of the linear polymer, although the equations are arrived at in a slightly different way. Several experimental difficulties may occur in assessing Tg with equation (2). The determination of the Tg of the linear equivalent polymer, especially for thermosets, can be difficult because of lack of availability of difunctional or monofunctional equivalents to some of the network components. Tg_∞ is therefore often an additional fitting parameter. K is dependent on the functionality and structure of the crosslink. Deviations from point crosslinks can seriously alter Tg behavior, as demonstrated by a study of crosslinked acrylates with various different di-acrylates[17].

The network can be treated as a copolymer of crosslinks, chains, and chain ends. A modified Gordon-Taylor equation[14], or a modified version of its simplified version, the Fox equation[18]:

$$1/Tg = \Sigma w_i/Tg_i \qquad (3)$$

with w_i the weight fraction of and Tg_i the Tg of the homopolymer of the network components, has been used to determine the Tg of thermosets[19] [20] [21]. The difficulty with applying this equation to thermosetting networks is again the accessibility of the Tg's of the appropriate homopolymers.

The decision to use either the crosslink density or the copolymer equation depends on the network system used, and whether one of the effects is negligible. The inclusion of the end group contribution also depends on the importance versus the other effects in a particular system. Therefore, equation (2) gives very good results for networks with low crosslink density,

low concentration of end groups, and point crosslinks. Equation (3) works well for thermosets with high crosslink density where it is easy to determine the Tg of the homopolymers of the network components.
For network systems where these ideal situations are not met, the assessment of Tg is more difficult and an amalgamated equation, combining all effects, is necessary. The theories by Stutz et al.[6], by Hale et al.[5], and the modification by Shefer and Gottlieb[7] are good examples. Each approach affords several experiments to determine conversion, Tg of the homopolymer, crosslink density, and a few polymer-specific constants.

The theory by DiBenedetto[22], as applied to our DRF-PPG system, is an interesting example because it yields an equation with terms addressing each of the three effects discussed here. DiBenedetto used a model based on the principle of corresponding states and modified it to describe the Tg behavior of the PPG system:

$$Tg = \frac{Tg_{p=0}}{1 + \frac{c^{E}_{e} \cdot p}{X} - \frac{1}{3}\frac{c_D}{c_{p=0}} \varphi_D \frac{p(1+2p^2)}{(1-p+p^2)}} \qquad (4)$$

c_D is related to the degrees of freedom of the crosslinker. $c_{p=0}$ is the weighted average of c_D and c_P before reaction, with c_P is related to the average degree of freedom of the rotatable bond of the PPG molecule. $Tg_{p=0}$ is the glass transition temperature of the initial reaction mixture, φ_D is the fraction of

lattice sites occupied by the crosslinker, and p is the conversion of isocyanate groups. Analysis of the ratio $c_D/c_{p=0}$ gives information on the relative mobility of the crosslinker to the chain segments. The three terms in the denominator incorporate the copolymer effect, the end group effect, and the crosslinking effect, respectively. This approach gives information on the dependence of Tg on the composition of the network and takes into account differing mobilities of network components. This approach will be tested for the DRF-PPG system. The structural difference between the crosslinker and network chain is absent in the PIP system, rendering the DiBenedetto equation inapplicable.

Networks prepared from stoichiometrically imbalanced mixtures of network components will exhibit an increasing extractable sol fraction of partially reacted components. Tg of the extracted samples was measured. Extraction results in a difference between the weight fractions of the components in the extracted network from those in the unextracted network. This difference has to be taken into account in the calculations of Tg of the extracted samples. All parameters needed for the calculation of the weight fractions and the number of end groups in the extracted and unextracted samples are calculated in Appendix A.

Results and discussion

The trends in Tg of the PPG system are consistent and can be described as follows. For samples with higher molecular weight PPG the Tg is lower for the same stoichiometric imbalance. For samples prepared from a single molecular weight PPG the Tg decreases with the stoichiometric imbalance. This holds for all molecular weights of the PPG and all off-stoichiometric ratios, including the samples prepared with excess isocyanate. The Tg of unextracted samples is always lower than that of the equivalent extracted sample. The difference is larger for samples with higher stoichiometric imbalances, and larger for samples prepared from low molecular weight PPG. These observations confirm that the composition is of significance in explaining the Tg of this system.

It seems prudent first to attempt to analyze the Tg behavior of the stoichiometrically balanced networks after which an extrapolation will be attempted to the stoichiometrically imbalanced networks.

As Andrady and Sefcik[23] accurately stated, Tg in this system is difficult to assess. They applied equation (2) in their calculations. To find Tg_∞ , linear equivalents of similar structure to the structural unit between crosslinks were synthesized. It was concluded that by this method the copolymer contribution, which was deemed important, could successfully be separated out and analyzed. Criticism on this method is the presence of a large number of end groups, which is not accounted for.

Another method to introduce the copolymer contribution into the theory is to evaluate Tg as a copolymer equation, such as equation (3) or the Gordon-Taylor equation:

$$Tg = [Tg_1 + (\kappa Tg_2 - Tg_1) w_2]/[1 - (1 - \kappa) w_2] \qquad (5)$$

Tg_1 and Tg_2 are Tgs of the linear equivalent homopolymers of the network components, w_2 is the weight fraction of component 2, and k is related to the expansion coefficients of the linear equivalent homopolymers. The obvious problem in using these equations stems from the lack of knowledge of the Tg of the linear equivalent homopolymer of the crosslinker. It is therefore considered as an adjustable parameter. Tg_1 was taken to be 200 K[24]. A number of values for Tg_2 in both equation 2 and 5, and k in equation 5 were attempted. Figure 3.1 shows a plot of $(Tg-Tg_\infty)$ vs. 1/Mc for Tg_2 equal to 500 K and 1000K, using equation (2). Figure 3.2 shows a plot of $(Tg-Tg_\infty)$ vs. 1/Mc where Tg_2 and κ are 400 K and 0.5, 375 K and 1.0, and 350 K and 1.5, respectively, using equation (5). No linear plots for these and a wide range of additional values for Tg_2 and κ were obtained, with larger deviations from linearity for networks with smaller Mc. Upon closer examination it was found that a value for Tg_2 of 1734 yielded good linearity with equation (2) and with $\kappa = Tg_1/Tg_2$, this has to be the case for equation (5) as well. This value is far higher than would reasonably be expected, and it cannot be checked experimentally. However, this suggests that the crosslinker has a profound impact on Tg, validating a further look into a different copolymer approach.

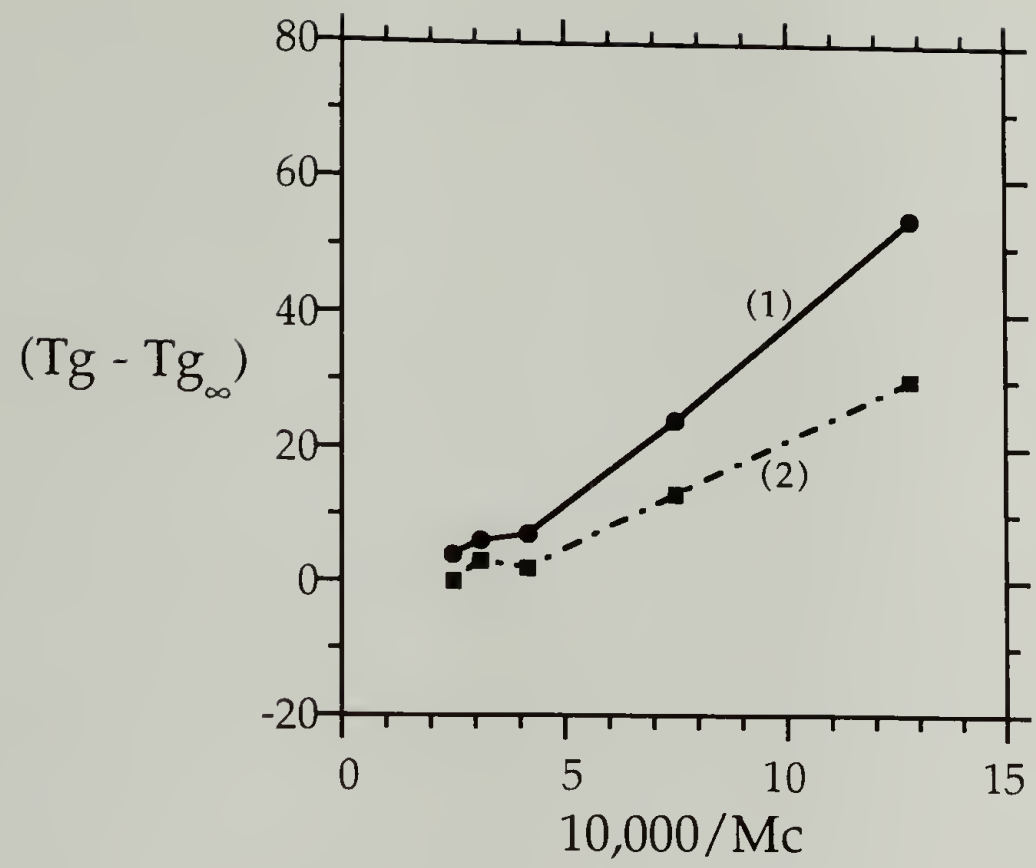

Figure 3.1 Plot of ($Tg-Tg_\infty$) vs. 1/Mc for Tg_2 equal to (1) 500 K and (2) 1000K, using equation 2.

The order of magnitude of Tg_2 found does not correspond to that expected for Tgs of linear equivalents of network components from the work of Lee and Hartmann[20,21]. The highest values for such Tgs never exceeded 1000K, and those were found for components lacking rotatable bonds. The value here, while useful, seems physically unfounded.

In order to find a predictive expression Tg that would relate Tg and Mc, a different approach is adopted. The approach is based on the Fox copolymer equation (2). A different set of "linear equivalent homopolymers" is assumed to describe the system. These networks are considered as copolymers of a "crosslinking unit" (CLU) and a "chain

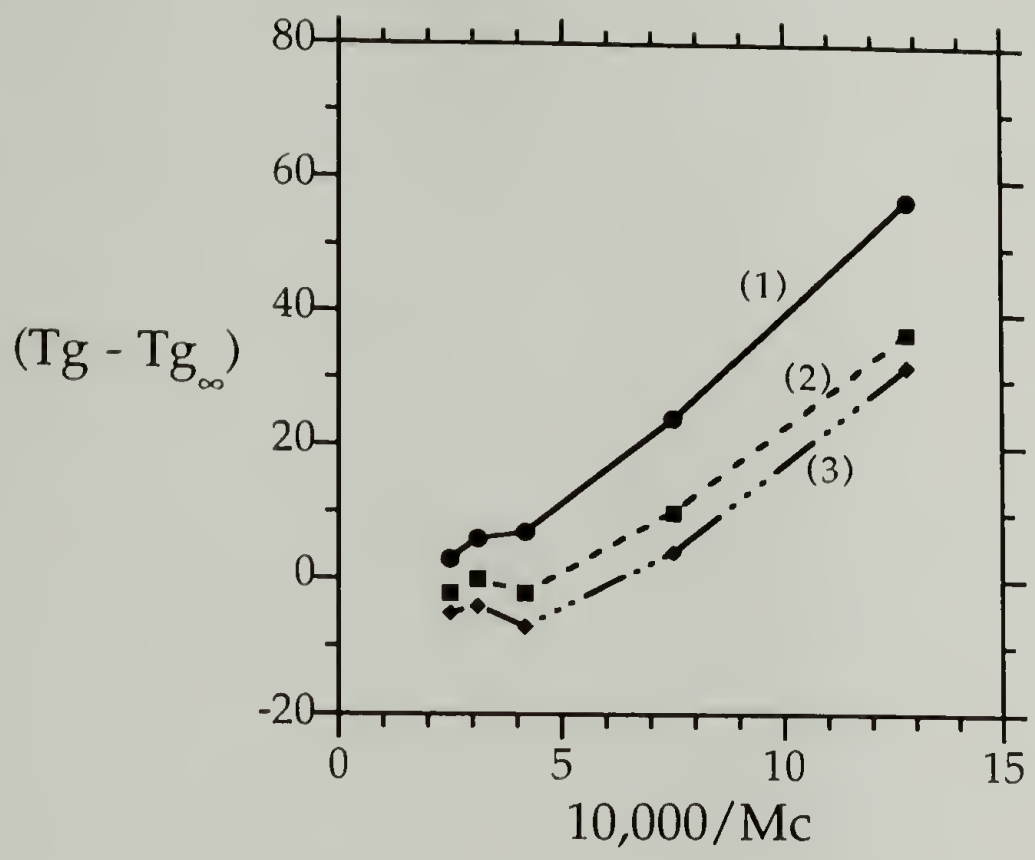

Figure 3.2 Plot of ($Tg-Tg_\infty$) vs. 1/Mc where Tg_2 and κ are (1) 400 K and 0.5; (2) 375 K and 1.0; and (3) 350 K and 1.5, respectively, using the Gordon-Taylor equation.

unit" (CU). The crosslinking unit consists of the crosslinker and a part of the chain. Its molecular weight becomes $M_{CLU} = M_{DRF} + 3x$, with M_{DRF} the molecular weight of DRF, and x the molecular weight of the PPG segment assigned to the CLU. The "chain unit" is the portion of the PPG chain that is not assigned to the CLU. Its molecular weight is $M_{CU} = M_{PPG} - 2x$. M_{PPG} is the molecular weight of the PPG. By definition the weight fraction of the chain unit, w_1 is:

w_1 = weight of the network chain/total weight of the sample

For samples prepared from a stoichiometrically balanced feed of hydroxyl groups and isocyanate groups 3 moles of PPG are reacted with 2 moles of triisocyanate, so that w_1 becomes:

$$w_1 = 3\,(M_{PPG} - 2x)/(3\,M_{PPG} + 2\,M_{DRF}) \qquad (6)$$

Since the glass of the networks vary with Mc, which is related to M_{PPG}, by combining equation 6 and 2 we can write:

$$Tg = 200\,Tg_2/[((Tg_2 - 200)\,3\,(M_{PPG} - 2x)/(930 + 3\,M_{PPG})) + 200] \qquad (7)$$

By inserting different experimental values of Tg for different M_{PPG}, Tg_2 and x can be optimized to get the best fit for Tg vs. Mc.

By using several different optimization methods, it was observed that Tg_2 and x are not independent variables, i. e. for each chosen value of x a value of Tg_2 can be found which will result in a fit of the Tg data with the same precision. This is supported by mathematical manipulation of equation (7) which fails to separate Tg_2 and x in all cases. An additional assumption needs to be made.

When x is taken to be half the length of the shortest PPG chain, PPG 400, Tg_2 is equal to the Tg of the network prepared from PPG 400: 310 K. Tg_1, the Tg of the chain unit, remains the Tg of pure PPO: 200K.

Using equation (2) with the proper values for w_1 and w_2, Tg of the copolymers, i.e. networks, was calculated. Excellent correspondence (within the experimental error) with the experimental values was found. Tg can therefore be determined by describing the network as a copolymer of a "crosslinking unit" and a "chain unit". All results for the PPG-DRF system are represented in Table 3.1.

Expanding the approach to the stoichiometrically imbalanced samples shows excellent correspondence for the higher molecular weights over the entire range of imbalances. For the low molecular weight PPG samples the discrepancy between theory and experiment becomes larger with imbalance. Nevertheless, the differences are relatively small. This analysis is valid for both extracted and non-extracted samples. The trend of the calculated values for both extracted and non-extracted samples is consistent over the entire range of molecular weights and stoichiometric imbalances. The applicability of the copolymer approach to samples prepared from stoichiometrically imbalanced feeds , especially those with excess isocyanate, confirms the validity of the approach. The deviation from the copolymer approach is most likely due to a plasticizing effect from the soluble fraction and the dangling ends. Describing this deviation theoretically, using plasticization phenomena as the basis[25 26 27 28], has failed. All of these theories describe the plasticization effect on Tg in function of the weight fraction of a fairly low molecular weight plasticizer. In our case the molecular weight and composition of the soluble fraction and dangling ends changes

Table 3.1 Experimental values for Tg of the PPG-DRF system

Mw 400

r	ws	p	Tg(1)	Tg(2)	Tg(3)	Tg(4)	Tg(5)
1.81	0.355	1.00	367	380	380	428	380
1.66	0.185	1.00	353	368	361	400	367
1.43	0.075	0.99	334	348	340	363	343
1.11	0.019	0.93	319	320	322	323	317
1.00	0.006	0.93	310	310	310	310	298
0.869	0.028	0.97	291	296	297	298	292
0.769	0.083	0.98	279	287	291	293	283
0.729	0.121	0.99	274	283	288	291	280
0.689	0.185	0.99	270	279	286	289	275
0.657	0.240	1.00	263	275	284	288	272
0.625	0.313	1.00	259	272	283	287	269
0.588	0.444	1.00	256	268	282	286	265

Mw 1000

r	ws	p	Tg(1)	Tg(2)	Tg(3)	Tg(4)	Tg(5)
1.00	0.013	0.91	247	248	247	248	246
0.90	0.038	0.94	240	243	244	244	243
0.80	0.095	0.96	231	238	241	241	239
0.70	0.172	0.99	227	233	237	238	236
0.60	0.421	1.00	224	229	233	236	231

Table 3.1 continued on next page

Table 3.1 (continued)

Mw 2000

r	ws	p	Tg(1)	Tg(2)	Tg(3)	Tg(4)	Tg(5)
2.00	0.230	1.00	238	247	242	269	244
1.25	0.085	0.93	228	230	231	232	230
1.11	0.065	0.91	223	227	224	228	227
1.00	0.013	0.92	222	224	223	225	223
0.87	0.069	0.93	221	221	222	222	221
0.69	0.252	0.97	214	217	220	220	217

Mw 3000

r	ws	p	Tg(1)	Tg(2)	Tg(3)	Tg(4)	Tg(5)
1.00	0.011	0.92	216	217	216	217	216
0.90	0.040	0.94	214	215	215	216	215
0.80	0.121	0.95	212	214	215	215	213
0.70	0.253	0.97	211	212	214	214	212
0.60	0.604	0.97	209	210	213	213	210

Tg(1) = experimental, unextracted.

Tg(2) = calculated, unextracted.

Tg(3) = experimental, extracted.

Tg(4) = calculated, extracted, end groups not considered.

Tg(5) = calculated Tg, for unextracted samples using DiBenedetto.

considerably with stoichiometric imbalance. The discrepancy between the modified copolymer approach and the experimental Tg values is proportional to the concentration of unreacted end groups left in the system, rather than the weight fraction of the respective fractions. Figure 3.3 illustrates the number of end groups per gram and the difference between the copolymer

number of end groups per gram and the difference between the copolymer approach and the experiment. The number of end groups for both extracted and unextracted samples was calculated using equations derived in Appendix A.

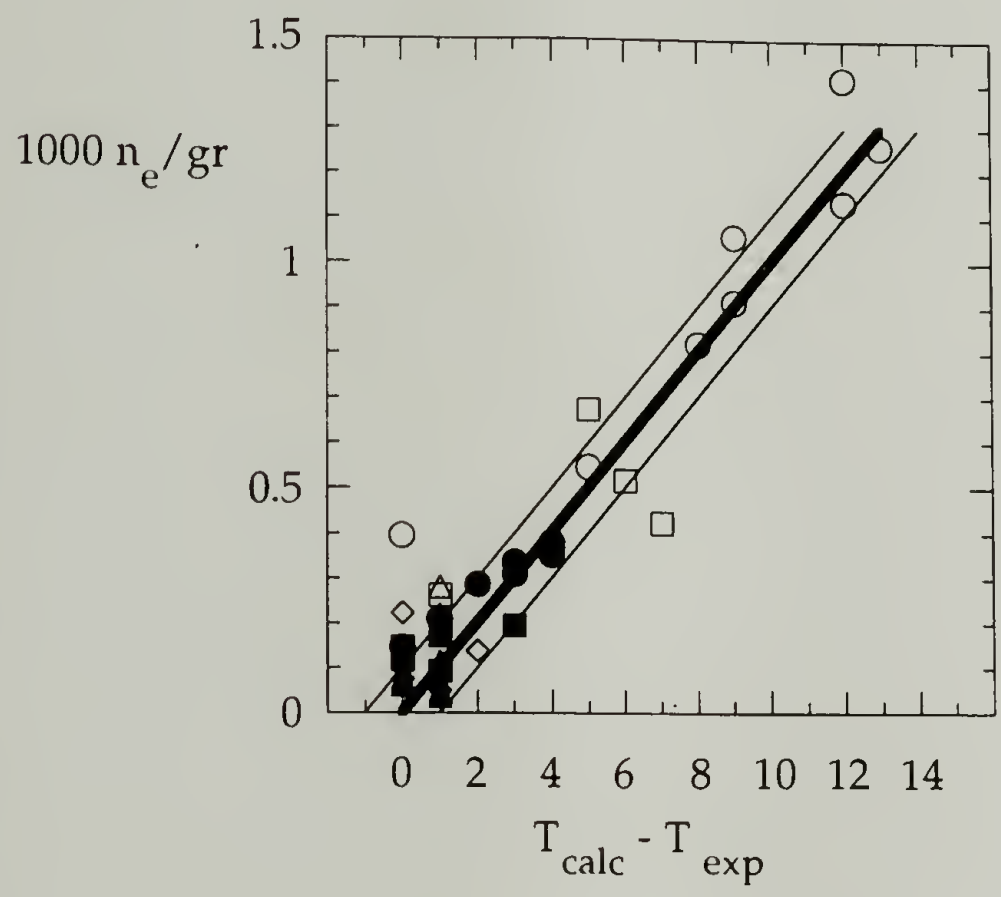

Figure 3.3 The number of end groups n_e per gram vs. the temperature difference between the calculated and experimental Tg value for all samples. PPG400: circles; PPG1000: squares; PPG2000: diamonds; PPG3000: triangles. Extracted samples (filled symbols) and unextracted samples (open symbols). Lines: best fit and error margins

A relatively good correlation can be concluded for all molecular weights. The deviations still present are hard to explain. The number of variables involved in the plasticization of these networks is too large to effectively separate each out and assess their contribution quantitatively. An additional

consideration is the possible difference of the end group contribution between linear and network polymers. The value for K in equation (1) that can be calculated from the best fit is approximately 10^4. This is well within the range of the values found for constants of this nature. This proves again that the copolymer and end group contributions are very important in the description of Tg of networks.

While the previous outline describes the Tg of the PPG-DRF system well, the DiBenedetto equation already has been used successfully before. To apply this equation 4 to the PPG system the $Tg_{p=0}$ needs to be determined. Feger[3] suggested the use of the Fox equation with Tg_1 = 200K for PPG and Tg_2 = 244K for the Tg of tri-isocyanate, and w_1 and w_2 the actual weight fractions of PPG and DRF, respectively. It is necessary to specify that this equation with these values for Tg_1 and Tg_2 is only applicable to the Tg of the unreacted mixture of the network components. The volume fraction of the crosslinker was determine from its molar volume as 6.33 times the molar volume of the PPG monomer unit. The unknown parameters are c_e^E, c_D and c_P. These parameters are independent of the composition of the sample and the molecular weight of the PPG. Using a value of c_P = 0.45-0.75 per repeat unit (as estimated from the -CH_2- unit), a value for c_D between 0.375-0.625 results in good correlation between theory and all experimental values. Any value other than 0 for c_e^E gave increasingly poor fits with the experimental data, and was therefore kept at 0, as suggested by DiBenedetto. For stoichiometric samples, very good correspondence with the theory is found. The deviations

are slightly beyond the experimental error of the DSC technique in the case of the samples prepared with the largest stoichiometric imbalance, and of the order of the deviations found with the modified copolymer approach. The same assessment of the plasticization contribution as previously made applies here. No accurate assessment can be made with this approach of the extracted samples. The equation is only applicable to networks as prepared from the feed. Additional parameters for the dangling ends would have to be taken into account to describe the behavior of the extracted samples.

A conclusion on the relative mobility of the network components can be drawn from a closer look at the c_D and c_P values. A c_P value of 0.45-0.75 per repeat unit corresponds to 1.35-2.25 degrees of external freedom, while a value of c_D of 0.375-0.625 corresponds to 7-12 degrees of external freedom for the tri-isocyanate. The PPG repeat unit has 3 rotatable bonds while the crosslinker has 6. The volume occupied by the crosslinker is 6.33 times that of the PPG repeat unit. The rotational mobility of the crosslinker bonds is slightly higher than that of the PPG bonds, while the crosslinker is less mobile than the PPG repeat units, due to a lower density of rotatable bonds in the crosslinker. This treatment confirms the earlier conclusion[29] of differences in mobility between crosslinker and chain in the PPG system.

For the PIP system, the results can be easily summed up. A singular glass transition was observed for all samples, and no evidence of phase separation was found. All results are shown in Table 3.2. For a particular molecular weight of the pre-cure tristar all samples have, within the experimental error limit, identical Tg's independent of the off-stoichiometric ratio of the starting

components. The Tg of the prepolymer tristars of MW 2201, MW 2641, and MW 6117, is 235K, 236K, and 237K, respectively. The Tg of the networks

Table 3.2 Experimental values for Tg of the PIP-HDI system

r	MW 2201 Tg	MW 2671 Tg	MW 6117 Tg
1.00	242	241	239
0.90	242	241	238
0.80	242	241	239
0.70	242	241	238
0.60	241	240	238

prepared from them is 242K, 241K, and 238.5K, respectively. From the order of magnitude of the deviation in Tg before and after curing, it can be concluded that the crosslinking effect is the predominant factor in describing the Tg behavior of the PIP system. A dependence of Tg on the copolymer effect or differing mobilities of the network components is negligible. The system exhibits a true point crosslink. Except for the urethane group, little structural difference exists between the PIP and HDI, since PIP contains 2 $-CH_2-$ units per repeat unit. Equation 2 can be applied for this system. As outlined before, the difficulty in using this equation lies in the assessment of Tg_∞. From NMR, the 3,4-content of the polyisoprene portion for all tristars is approximately 65%, with the 1,4-content at 25% and the 1,2-content at 10%. The polybutadiene portion makes up 41%, 36%, and 15% of the PIP2201,

PIP2641, and PIP6117 tristars respectively. The 1,2-content of the polybutadiene is approximately 65%. Factoring in the reported contribution of the hydroxyl end groups on the Tg of the tristars[10], combined with the composition dependence of Tg on 3,4-content of the polyisoprene[30], yields a Tg of the linear equivalent polyisoprene of 238K±2K. Mc was calculated by adding up the molecular weight of two arms of the PIP tristar, plus the molecular weight of HDI. The constant K in the Fox-Loshaek equation, as determined from samples with stoichiometric ratio is 9,200. This value is smaller than the value of 18,000 as calculated from vulcanized natural rubber[31]. The discrepancy may be due to the difference in functionality of the current system and vulcanized rubber. Indeed, it was suggested that two trifunctional crosslinks are equivalent to one tetrafunctional crosslink for the purpose of calculating the mobility of the chain[32]. This approach was successfully applied to Tg of crosslinked polymers recently[5]. The k value for our samples assuming tetrafunctional crosslinks is 18,400, which is well with the experimental error of the vulcanized rubber value.

The validity of the modified copolymer approach yielding equation (7) can be tested for this system as well, even though the copolymer effect seems of lesser importance. If the Tg of the "crosslinking unit" is taken to be the Tg of the PIP2201 sample of stoichiometric ratio r=1, 242K, and the Tg of the chain unit as 238K, the modified copolymer approach can be used. The Tg of the stoichiometric PIP2641 and PIP6117 then are calculated to be 241K, and 238.5K, respectively. These are indeed the experimental values found. The influence

of the HDI is neglected since the weight fraction is less than 10% of the weight of the networks, and changes little between samples.

Further evidence of the usefulness and universality of the modified copolymer approach can be found from data presented in the literature. As an example the Tg data presented by Loshaek will be used. He crosslinked methylmethacrylate with a number of dimethacrylates. Figure 3.4 shows a plot of the experimental and calculated Tg of poly methylmethacrylate crosslinked with ethylene glycol dimethacrylate (EGDMA), and 2,2-methyl

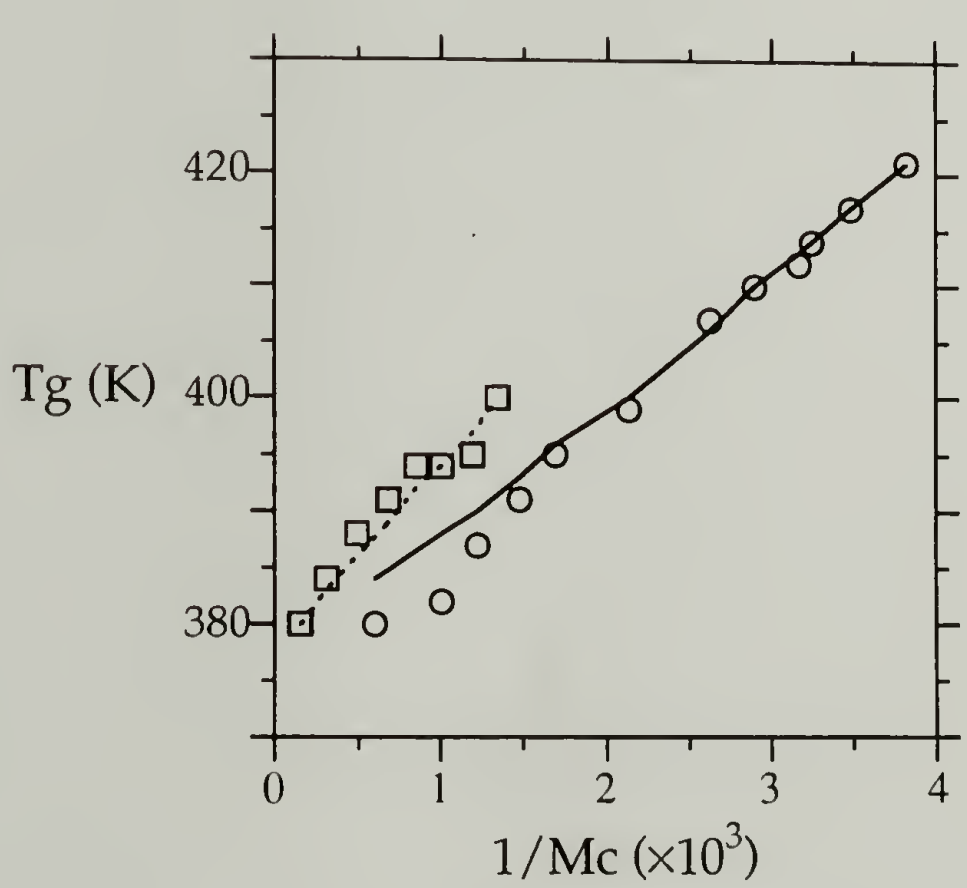

Figure 3.4 Tg of PMMA-EGDMA (squares) and PMMA-2,2-D-PDMA (circles), with fitted experimental values, vs. crosslink density 1/Mc.

propanediol 1,3 dimethacrylate (2,2-D-PDMA). These are obviously not point crosslinks. The fact that the Tg differs substantially for the same crosslink density but a different crosslinker, even though the polymer is the same, is additional evidence for the importance of the copolymer effect. The calculated data are within the experimental error of the technique. This confirms the assumption behind the modification of the copolymer equation. The crosslinking effect can be included in the copolymer equation in the form of using the Tg of a crosslinked polymer as the Tg for the crosslinking unit. It is likely that the effect on Tg of other phenomena like hydrogen bonding can be addressed in this way, as long as a the proper copolymer units can be defined for which the homopolymers, or networks can be found.

The fact that essentially no difference was found in Tg of samples made from the same prepolymer with different ratios of HDI draws two remarks. First, since the weight fraction of HDI is small in all samples, and HDI is chemically and structurally similar (except for the urethane group), influence of the copolymer effect is expected to be small. Comparing these PIP system Tg data to similar data for the PPG system merely confirms the notion that the copolymer effect is very important in the PPG system, while of insignificant consequence here. Second, the free volume of the unreacted hydroxyl end groups in the stoichiometrically imbalanced PIP networks is of little consequence to decrease Tg. As explained earlier, hydrogen bonding between unreacted hydroxyl end groups significantly decreases the end group contribution to Tg. Additionally, hydrogen bonding between the urethane and the unreacted hydroxyl end group is expected to yield the same effect.

The extractable portion, consisting of low molecular weight reaction products, and unreacted components, seems to have little or no effect on the Tg of these networks. This can be explained by the small difference in Tg between network components before reaction and the network after reaction.

Conclusions

The Tg behavior of stoichiometrically balanced and imbalanced PPG-DRF and PIP-HDI networks was studied. It can be concluded that the chemical structure has profound influence on the Tg. For the PPG-DRF system, the Tg decreases significantly with stoichiometric imbalance. This is not found in the PIP-HDI system. When the crosslinker differs in chemical structure from the chain, the copolymer effect becomes the predominant factor in the description of the Tg behavior. Otherwise, the crosslinking effect is the crucial factor.

The DiBenedetto equation describe the Tg behavior of the PPG system well, with slight deviations for highly stoichiometrically imbalanced samples. A lower number of external degrees of freedom, and hence mobility, of the crosslinker than for the PPG chain is found from the analysis of the c_D and c_P values in the DiBenedetto equation. This confirms the importance of the copolymer effect to the description of the Tg in this system.

The Fox-Loshaek equation, which is based on crosslinking effect, describes the Tg behavior in the PIP system reasonably well, given the relatively small range of crosslink densities available. The value of k, the experimental constant, corresponds to that of vulcanized PIP when the difference in functionality of the crosslink is taken into account.

The crosslinking effect was successfully combined with the copolymer effect for both systems by considering the network to be a copolymer of a "crosslinking unit" and a "chain unit". This approach eliminates the necessity to determine the Tg of the linear equivalent of the entire network chain, which is often difficult. The diversity in some network-specific constants due to differences in the actual crosslinker or its functionality is inherently present in the theory because the Tg of the "crosslinking unit" depends on it. The Tg of a network system can be predicted from the determination of Tg of a sample with high crosslink density, which is then applied as Tg of the "crosslink unit" in the copolymer equation. The Tg of most network "chain unit" polymers, which are usually equivalent to regular polymers, is known.

The concentration of the unreacted end groups is of significant consequence to the Tg in the PPG-DRF system, since it can be correlated to the deviation between the modified copolymer approach and the experimental value. The influence of the increased amount of dangling ends on Tg of stoichiometrically imbalanced networks is small in the PIP-HDI system, and

large for the PPG-DRF system as it is related to the composition of the network.

For both systems the Stutz assumption holds that no differentiation needs to be made between crosslink units that are elastically active and those that are merely branching points in the dangling ends.

References

1. K. Dusek, Adv. Polym. Sci., 78, 1, (1986)

2. C. Feger, S. E. Molis, S. L. Hsu, W. J. MacKnight, Macromolecules, 17, 1830, (1984).

3. C. Feger, W. J. MacKnight, Macromolecules, 18, 280 (1985).

4. L. C. Dickinson, P. L. Morganelli, C. W. Chu, Z. Petrovic, W. J. MacKnight, J. C. W. Chien, Macromolecules, 21, 338, (1988).

5. A. Hale, C. W. Macosko, H. E. Bair, Macromolecules, 24, 2610, (1991).

6. H. Stutz, K.-H. Illers, and J. Mertes, J. Polym. Sci. Phys. , 28, 1483, (1990).

7. A. Shefer, M. Gottlieb, Macromolecules, 25, 4036, (1992).

8. Z. Petrovic, B. J. Reekmans, W.J. MacKnight, submitted for publication.

9. J. A. Faucher, Polym. Letts., 3, 143, (1965).

10. C. Kow, M. Morton, L. J. Fetters, N. Hadjichristidis, Rub. Chem. Techn., 55, 245, (1982).

11. T.G. Fox, Jr., P. J. Flory, J. Appl. Phys., 21, 581, (1950).

12. P. Meares, Trans. Far. Soc., 53, 31, (1957)

13. T.G. Fox, S. Loshaek, J. Polym. Sci., 15, 371 (1955).

14. M. Gordon, J. S. Taylor, J. Appl. Chem., 2, 493, (1952).

15. K. Shibayama, Kobunshi Kagaku, 18, 183 (1961).

16. E.A. DiMarzio, J. Res., 68A, 611 (1964).

17. S. Loshaek, J. Polym. Sci., 15, 390 (1955).

18. T. G. Fox, Bull. Am. Phys. Soc. 1, 123, (1956).

19. V. Bellenger, J. Verdu, E. Morel, J. Pol. Sci., B25, 1219, (1987)

20. G. Lee, B. Hartmann, J. Appl. Polym. Sci. 28, 823, (1983).

21. G. Lee, B. Hartmann, J. Appl. Polym. Sci. 29, 1471, (1984).

22. A. T. DiBenedetto, J. Polym. Sci. Phys., 25, 1949, (1987).

23. A. L. Andrady, M. D. Sefcik, J. Pol. Sci. Phys. Ed., 21, 2453 (1983)

24. R. H. Beaumont, B. Clegg, G. Gee, J. M. Hebert, D. J. Marks, R. C. Roberts, D. Sims, Polymer, 7, 401 (1966)

25. R. F. Boyer, TAPPI, 34, 357, (1951).

26. S. N. Zhurkov, C. r. Acad. Sci., URSS, 47, 475, (1945)

27. F. N. Kelley, F. Bueche, J. Polym. Sci., 50, 549, (1961).

28. T. S. Chow, Macromolecules, 13, 362, (1980).

29. L. C. Dickinson, P. Morganelli, C. W. Chu. W. J. MacKnight, J. C. W. Chien, Macromolecules, 21, 338, (1988).

30. J. M. Widmaier, G. C. Meyer, Macromolecules, 14, 450, (1981).

31. P. Mason, J. Chem. Phys., 35, 1523, (1962).

32. N. R. Langley, K. E. Polmanteer, J. Pol. Sci., Pol. Phys. Ed., 12, 1023, (1974).

CHAPTER 4

MECHANICAL MEASUREMENTS

Introduction

The main purpose of the study of model networks is to examine the validity and applicability of the theories of rubber elasticity. Initially the molecular theories defined and described the elasticity of the phantom network[1] in which the network chains may move freely through one another, and the affine network in which the network junction points move proportionally with the macroscopic dimensions of the sample[2]. The most important modifications to these basic theories are based on the Constrained Junction (CJ) model[3] and the Constrained Chain (CC) model[4]. Both assume that the phantom network approach accurately describes the elasticity when topological constraints are neglected. The influence of topological constraints, such as trapped entanglements, on the junction point and on the network chain, respectively, is characterized by these modifications. The phenomenon of trapped entanglements is more explicitly represented in Langley's approach[5]. There, it is assumed that the contribution of a trapped entanglement to the elasticity of a network is the same as that of a permanent entanglement to the plateau modulus of the linear equivalent of the network polymer. Some discussion has arisen over the extent and the influence of topological constraints on elasticity. By testing our equilibrium modulus data with the theories at hand, each of which highlights the influence of a particular topological constraint, some determination on the subject may be expected. The

study of stoichiometrically imbalanced samples is therein crucial since the number of trapped entanglements decreases with increasing imbalance, while keeping the structure between crosslinks the same. Langley[6] pointed out a way to examine the importance of trapped entanglements vs. constrained chains. When the ratio between the theoretical CC modulus value and the trapped entanglement modulus value, both in the affine limit, is taken, it becomes clear that a large range of the fraction of trapped entanglements over the elastically active network chains provides the proper test. This condition is met here in the use of stoichiometrically imbalanced samples.

A brief description of each theory is given and subsequently integrated in the discussion of the data. Volume change upon stretching will be ignored in this treatment since its contribution is negligible in the low strain limit considered here. Also, all of the equations are written for networks with junctions of functionality equal to 3, since both systems under consideration exhibit trifunctional crosslinks.

Theoretical background

The phantom network

At the basis of all theories discussed here is the phantom network. The assumptions made in this model can be summed up as follows. Pairs of junction points are connected by Gaussian chains. The junction points fluctuate around their mean position with Brownian motion. Upon application of a strain the mean position of the junction points is deformed affinely, while the fluctuations

around the mean position are independent of the strain. This intrinsically assumes that chains are allowed to move through one another, and that inter-chain interactions do not change with strain. An active junction is defined as one joined by at least three paths to the gel network, and an elastically active network chain (EANC) as one terminated by an active junction on both ends.

The elastic free energy ΔA_{ph} relative to the undeformed state, can be calculated from the Gaussian distribution of the end-to-end vector as it relates to the conformational entropy. It is given by[7]:

$$\Delta A_{ph} = 1/2\ \xi\ kT \sum (\lambda_t^2 - 1) \qquad t = x, y, z \qquad (1)$$

T is the temperature, λ_t are the principal extension ratios, and ξ is the cycle rank. Flory defined the cycle rank as the number of chains which have to be cut to reduce the network to an acyclic structure or tree[8]. It is the difference between the number ν of EANCs and the total number μ of elastically active junctions (EAJ) with functionality $\varphi>2$:

$$\xi = \nu - \mu \qquad (2)$$

The general relationship between ν and μ is defined as[9]

$$\mu/\nu = 2/\varphi \qquad (3)$$

The equilibrium shear modulus for the phantom network (G_{ph}) can then be shown to be:

$$G_{ph} = \xi RT \tag{4}$$

R is the gas constant. The equilibrium modulus is sometimes called the small strain modulus, which is a more accurate description, since it is theoretically and oftentimes experimentally determined by extrapolation from the small strain deformation.

The affine limit

In real networks, the fluctuations around the mean position of the junction points is restricted by neighboring chains and junction points. The affine limit describes the extreme case where the fluctuations are completely suppressed. The elastic free energy in the affine limit (ΔA_{aff}) is given by:

$$\Delta A_{aff} = 1/2\ \nu\ kT \sum (\lambda_t^2 - 1) \qquad t = x, y, z \tag{5}$$

The equilibrium shear modulus in the affine limit (G_{aff}) is then given by

$$G_{aff} = \nu RT \tag{6}$$

Note that G_{aff} is always larger than G_{ph}.

The Constrained Junction model (CJ)

According to the Constrained Junction model, the deviation of a real network from the phantom network model stems from constraints affecting the fluctuations of junctions. Inherent in the model is the approximation that the influence of entanglements works to restrict only the fluctuation of the junction. The elastic free energy of deformation, ΔA_{el}, is given by the elastic free energy of the phantom network, ΔA_{ph}, with a correction to the phantom network term, ΔA_c:

$$\Delta A_{el} = \Delta A_{ph} + \Delta A_c \qquad (7)$$

The Constrained Junction theory defines ΔA_c as:

$$\Delta A_c = 1/2\, \mu\, kT \sum [B_t + D_t - \ln (1 + B_t) - \ln (1 + D_t)] \qquad (8)$$

The new parameters in equation (8) are defined as:

$$B_t = \kappa^2 (\lambda_t^2 - 1)(\lambda_t^2 + \kappa)^{-2} \qquad (9)$$

$$D_t = \lambda_t^2 B_t / \kappa \qquad (10)$$

with $$\kappa = \langle(\Delta R)^2\rangle_0 / \langle(\Delta s)^2\rangle_0 \qquad (11)$$

which is a quantitative measure of the strength of the constraints. For

$\kappa = 0$, $\Delta A_c = 0$ and the elastic free energy reverts to that found for the phantom network. When $\kappa = \infty$ the constraints are infinitely strong and fluctuations are suppressed and ΔA_{el} becomes:

$$\Delta A_{el} = 1/2\ (\mu + \xi)\ kT \sum (\lambda_t^2 - 1) \qquad (12)$$

This is equivalent to the solution found in the affine limit. The resulting equilibrium shear modulus is equivalent to equation (6). The value of κ is usually between 5-10[10 11 12 13].

Equation (12) is often used for stress-strain measurement in elongation. Another parameter ζ needs to be introduced to describe the non-affine transformation of the domains of constraints with strain. The influence, as is expected from its definition is small or negligible in the low strain limit.

The parameter li

To explain the intermediate behavior between the affine limit and the phantom limit, Graessley[14] proposed the use of the experimental parameter h. The equilibrium modulus is then defined as:

$$G = (\nu - h\mu)\ RT \qquad (13)$$

An analytical expression for h can be found by calculating the value of the sum in equation (8) in the limit of λ approaching 1. The parameter h is then given by:

$$h = 1 - \kappa^2 (\kappa^2 + 1)(\kappa + 1)^{-4} \qquad (14)$$

and is clearly a function of κ. For $\kappa = 0$, h becomes 1 and the equation (13) reverts to equation (4) for the phantom network. When κ approaches ∞, h approaches 0 and the equation for the affine limit is found. For polybutadiene and polyethylene-propylene copolymers[15], Graessley found h to equal 0, while Macosko found $0.7<h<1$ for PDMS networks[16].

The Constrained Chain model (CC)

In this model the notion of the influence of entanglements on junction points is expanded to their influence on the elastically active network chains. Rather than assuming that the topological influence is only noticeable as a restriction of the junction fluctuations, here it assumed that this influence is felt along the entire length of the chain. The introduction of these strain-dependent constraints affects the instantaneous distribution of the mass centers of chains relative to their location in the phantom network. The basic premise of the theory is that each chain can be subdivided in a number of Gaussian subchains, each of which contributes to the elastic free energy of the constraints. The incapability to determine the Gaussian subchains constitutes a minor criticism to the theory, which was rendered immaterial by the mathematical construction. Intuitively one would expect the elastic free energy due to constraints to be very similar to that given by the CJ model, with a mere modification for the number of chains. Indeed, it is given by:

$$\Delta A_c = 1/2\ \nu\ kT\ \Sigma\ [B_t + D_t - \ln\ (1 + B_t) - \ln\ (1 + D_t)] \qquad (15)$$

with $B_t = h(\lambda_t)^2\ (\lambda_t^2 - 1)(\lambda_t^2 + h(\lambda_t))^{-2}$ (16)

$$D_t = \lambda_t^2\ B_t/h(\lambda_t) \qquad (17)$$

and $h(\lambda_t) = \kappa_G\ [1 + (\lambda_t^2 - 1)\ \Phi]^{-1}$ (18)

Φ is dependent on the functionality of the junction points. $\kappa_G = <(\Delta X)^2>_0/<(\Delta x)^2>_0$ is defined similarly to the κ in the CJ model, but referring to the average position of the chain segment. The total elastic free energy of deformation is then given by:

$$\Delta A_{el} = 1/2\ \xi\ kT\ \Sigma\ \{\lambda_t^2 - 1 + (\nu\ /\xi)[B_t + D_t - \ln\ (1 + B_t) - \ln\ (1 + D_t)]\} \qquad (19)$$

Analysis of the CC model's equation in its limits yields the following. When no constraints on chains or junction points are present, $\kappa_G = 0$ and equation 19 reduces to equation 1, the elastic free energy of the phantom network. When $\kappa_G = \infty$ the elastic free energy becomes:

$$\Delta A_{el} = 1/2\ (\nu + \xi)\ kT\ \Sigma\ (\lambda_t^2 - 1) \qquad (20)$$

Note that $\Delta A_{el} > \Delta A_{aff}$ for large κ_G. The empirical approach to the h parameter can be modified to account for the constraints on chains as follows:

$$G = ((\nu + \xi) - h_G\nu)\ RT \qquad (21)$$

h_G describes the influence of the constrained chains in a similar way as h. For $h_G = 0$ all fluctuation is restricted and hor $h_G = 1$ the phantom network equation is found.

The trapped entanglement contribution

All aforementioned theories fail to take into account the contribution of long-range topological interactions to the modulus. During reaction a fraction, T_e, of the entanglements are permanently trapped, rendering them unable to relax. Langley[17] described their contribution to the modulus in a phenomenological way as:

$$G = G_C + G_e T_e \qquad (22)$$

Herein, G_C is the contribution of the chemical crosslinks, i.e. given by either equation (13) or (20), depending on which approach is taken in describing constraints. G_e is closely related to the plateau modulus G_N^o of the linear equivalent of the network chain polymer. In the case at hand it is very difficult to determine this value. Langley proposed to rewrite equation (21) (for the case of the Constrained Junction model) to account for that lack of knowledge in the following way:

$$G/T_e = (1 - h\,\mu/\nu)\,\nu\,RT/T_e + G_e \qquad (23)$$

The unknown parameters h and Ge can be determined from the slope and intercept, respectively, of a plot of G/T_e vs. $\nu RT/T_e$. Mark[18] crystallized the criticism of this method as follows. First, h is assumed independent of molecular weight of the network chain before crosslinking. Secondly, no maximum is set for the value of G_e with molecular weight, which is in disagreement with the findings for linear polymers. He suggested a different form of equation (21) which was used extensively[19, 20]. His form was suggested previous to the inception of the Constrained Chain model. Therefore it seems reasonable to follow his tact with the inclusion of the CC model considerations to come to the following:

$$(G - \xi RT)/T_e = G_e + h_{CC}\nu RT/T_e \qquad (24)$$

A plot of $(G - \xi RT)/T_e$ vs. $\nu RT/T_e$ yields a slope h_{CC} and an intercept G_e. Here, contrary to previous models, $h_{CC} = 0$ results in the phantom limit, and at $h_{CC} = 1$ all fluctuations are restricted.

Other models

Additional approaches to describe the elasticity behavior of networks are given in the slip-link model by Ball[21], the tube model by Gaylord[22], and a van der Waals model[23 24].

The proper calculations to calculate the structural parameters needed are given in Appendix A.

Results and discussion

The PPG-DRF system

Table 4.1 is a listing of the experimentally determined equilibrium shear modulus, the corresponding calculated value in the affine limit (as a reference point), the sol fraction, the number of elastically active network chains, N_e, and the trapping factor T_e. The results can be easily summed up. The highest modulus for a particular molecular weight is found for the stoichiometrically balanced sample. For either the samples with excess or deficiency in PPG the modulus is decreases with stoichiometric imbalance. For a particular stoichiometric imbalance the moduli decrease with increasing molecular weight of the PPG.

Table 4.1 Mechanical and structural characteristics of the PPG-DRF networks

PPG Mw = 400

r	w_s	N_e	G(exp)	G(calc)	T_e
1.818	0.3550	0.0086	0.06	0.0331	0.0100
1.667	0.1850	0.0919	0.64	0.1964	0.0837
1.428	0.0750	0.1322	0.92	0.7763	0.3484
1.111	0.0199	0.2975	2.07	1.7813	0.6237
1.000	0.0065	0.3604	3.13	2.4665	0.7492
0.869	0.0279	0.2589	1.57	1.7585	0.3473
0.769	0.0829	0.1462	0.86	0.9862	0.1408
0.729	0.1208	0.1072	0.46	0.7307	0.0891
0.689	0.1850	0.0666	0.27	0.4418	0.0470
0.657	0.2400	0.0458	0.16	0.3046	0.0276
0.625	0.3131	0.0282	0.05	0.1908	0.0141
0.588	0.4441	0.0114	0.02	0.0768	0.0042

PPG Mw = 1000

r	w_s	N_e	G(exp)	G(calc)	T_e
1.000	0.0130	0.3106	0.99	1.0573	0.6349
0.900	0.0382	0.2303	0.68	0.7707	0.3045
0.800	0.0946	0.1409	0.30	0.4634	0.1156
0.700	0.1727	0.0837	0.12	0.2701	0.0390
0.600	0.4212	0.0158	0.03	0.0501	0.0034

Table 4.1 continued on next page

Table 4.1 (continued)

PPG Mw = 2000

r	w_s	N_e	G(exp)	G(calc)	T_e
1.250	0.085	0.02006	0.397	0.3523	0.3116
1.111	0.065	0.2428	0.500	0.4394	0.4258
1.000	0.0113	0.3290	0.565	0.6119	0.6465
0.869	0.0693	0.1722	0.285	0.3090	0.1820
0.689	0.2519	0.0505	0.079	0.0858	0.0172

PPG Mw = 3000

r	w_s	N_e	G(exp)	G(calc)	T_e
1.000	0.0115	0.3290	0.588	0.4326	0.6406
0.900	0.0402	0.2352	0.393	0.2998	0.2786
0.800	0.1207	0.1196	0.157	0.1475	0.0809
0.700	0.1207	0.0503	0.074	0.0599	0.0169
0.600	0.6045	0.0039	0.010	0.0045	0.0004

r = [NCO]/[OH] in the reaction mixture.

w_s = weight fraction of the extractable sol fraction.

N_e = mole fraction of elastically active network chains

G(exp) = equilibrium shear modulus, experimental value as measured by the Impulse technique. (in MPa)

G(calc) = equilibrium shear modulus, theoretical value, calculated in the affine limit. (in MPa)

T_e = number fraction of entanglements trapped in the network structure

Further data analysis is necessary to evaluate the influence of constraining factors on either the junctions or the chains. Equation (23) is ideally suited for that purpose.

Figure 4.1 shows a plot of $(G - \xi RT)/T_e$ vs. $\nu RT/T_e$ for the PPG-DRF samples. The lines represent linear least square fits for the three highest molecular weights. A proper fit for the PPG400 data could not be achieved. The slope h_{CC} and intercept G_e of these fitted curves are 0.465 and -0.11 for PPG1000; 0.638 and -0.001 for PPG2000; and 0.725 and 0.01 for PPG3000. The fits become increasingly more accurate with molecular weight. Within the limit of error of the fits, the modulus related to the trapped entanglements is equal to 0. This in essence means that trapped entanglements do not

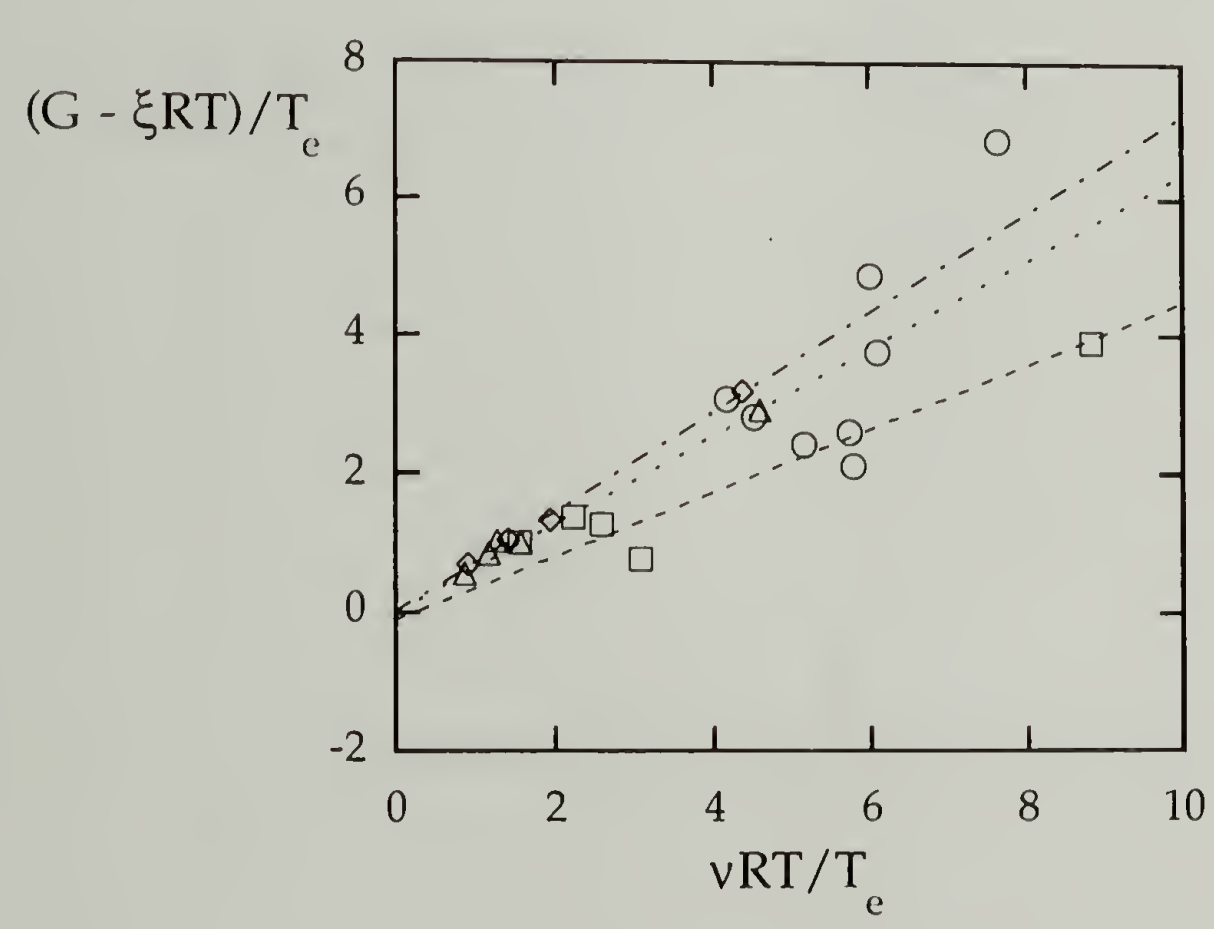

Figure 4.1 $(G - \xi RT)/T_e$ vs. $\nu RT/T_e$ for the PPG-DRF samples. PPG400: circles; PPG1000: squares, dashed fitted curve; PPG2000: triangles, dotted fitted curve; PPG3000: diamonds, dash-dotted fitted curve.

contribute to the equilibrium modulus for the PPG-DRF system. The slopes h_{CC}, representing the extent of restriction of fluctuations of chains and junctions, increase with molecular weight of the PPG. However, upon closer examination of Figure 4.1, it is clear that the difference between the three fitted curves is minimal when a reasonable error margin on the values for $(G - \xi RT)/T_e$ is taken into account. The observation of an increase in h with molecular weight of the PPG is consistent with the findings for other network systems.

This result is not in agreement with the results found for similar networks prepared with poly propylene oxide triols, crosslinked with MDI, yielding networks with molecular weight between crosslinks of approximately 700 and 2000[25]. The equilibrium modulus results were interpreted by assuming that the contribution of topological constraint consists of trapped entanglements only. The contribution of permanent interchain interactions $\Delta = G_r - \nu_g/3$ was plotted versus w_g, the weight fraction of the gel in the network. G_r is defined as the experimentally determined EANC in the gel: $G_r = G/w_g RT$. ν_g is the calculated value for EANC in the gel. Values for εT_e, which represents the number of elastically active trapped entanglements, were calculated with ε as an adjustable parameter. Good fits were obtained with $\varepsilon = 5 \cdot 10^{-4}$ mol cm^{-3} for the networks with Mc = 700, while this value was reduced to $\varepsilon = 3 \cdot 10^{-4}$ mol cm^{-3} for the samples with Mc = 2000. These values were both higher than the one estimated from linear poly propylene oxides[26], $\varepsilon = 2 \cdot 10^{-4}$ mol cm^{-3}.

The same treatment was undertaken for the present PPG-DRF samples. Figure 4.2 shows a plot of log Δ vs. w_g for the samples prepared from PPG400 and

PPG3000. The curves connect calculated values for log Δ with a value for ε that fits the result for the stoichiometrically balanced sample best. The resulting ε is $13 \cdot 10^{-4}$ mol cm^{-3} for the PPG 400 samples, which is significantly larger than the values previously found, and far exceeds any plausible value for the number of trapped entanglements. Indeed, this value corresponds to a permanent entanglement molecular weight in the linear equivalent polymer of 700, which is far below values generally found. The fit with the experimental values is very good for all stoichiometric imbalances. For the PPG3000 samples, ε is $3.25 \cdot 10^{-4}$ mol cm^{-3} which is on the order of magnitude

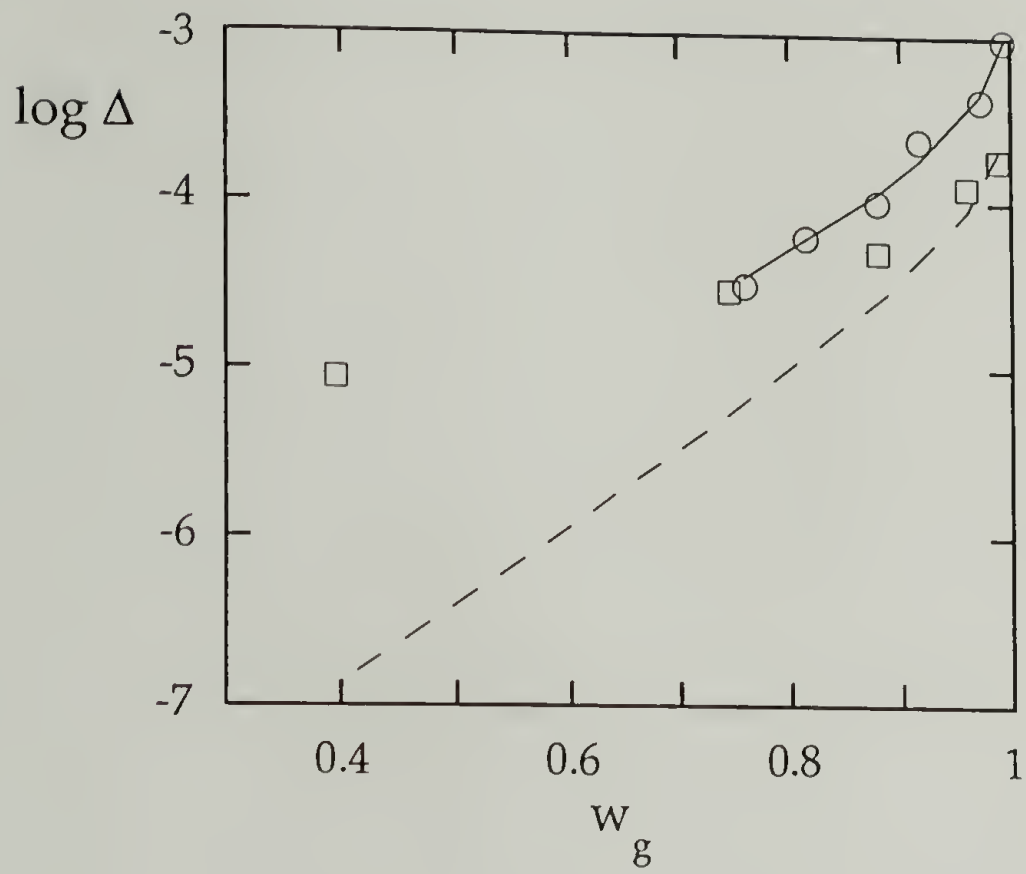

Figure 4.2 log Δ vs. w_g for PPG-DRF. PPG400: experimental values: circles; calculated values for ε is $13 \cdot 10^{-4}$ mol cm^{-3} : solid line; PPG3000: experimental values : squares; calculated values for ε is $3.25 \cdot 10^{-4}$ mol cm^{-3} : broken line

of the previously observed value. The fit with the experimental data is exceedingly poor with increasing stoichiometric imbalance. A similar plot for the samples of intermediary molecular weights can be produced. This yields values for ε of $4.2 \cdot 10^{-4}$ mol cm^{-3} for the PPG1000 samples, and $2.3 \cdot 10^{-4}$ mol cm^{-3} for the PPG2000 samples. The fit with the experimental data takes an intermediary place between the data plotted in figure 4.2.

From this treatment it can be concluded that considering the trapped entanglement contribution the only topological constraint is too narrow. The observation that the experimental values of Δ are always higher than the calculated ones underscores the notion that another factor contributes to the equilibrium modulus. In fact, from the earlier treatment, which considered the contribution of topological constraint to consist of both a suppression of chain and junctions, and trapped entanglements, it was concluded that the trapped entanglements do not significantly ad to the equilibrium modulus.

The PIP-HDI system

Table 4.2 is a listing of the experimentally determined equilibrium shear modulus, the corresponding calculated value in the affine limit (as a reference point), the sol fraction, the number of moles of elastically active network chains, N_e (EANC), and the trapping factor T_e. The results can be easily summed up. The highest modulus for a particular molecular weight is found for the stoichiometrically balanced sample. For the samples with increasing stoichiometric imbalance the modulus is decreased. For a particular stoichiometric imbalance the moduli decrease with increasing molecular weight of the initial PIP tristar.

The same track of analysis as for the PPG-DRF system will be followed here. Figure 4.3 represents a plot of $(G - \xi RT)/T_e$ vs. $\nu RT/T_e$ for the PIP-DRF samples. Considering that the margin of error on these values is of the order of the size of the dots in the plot, the values for the three sets of samples can be fitted with the same line. The scatter of the data is far less than for the PPG-DRF data. The

slope of the fitting line, h_{CC}, equals 0.91. A value over 0.67 indicates the necessity to consider the reduction of the fluctuation of the chain in addition to the junction point restriction. The intercept of the line, G_e, is 0.06. Within the margin of error, it can therefore be said that trapped entanglements are of negligible direct influence on the equilibrium modulus of these samples, similar to the conclusion for the PPG-DRF system.

The lack of a contribution of the trapped entanglements is a surprising result given that h_{CC} was found to be 0 for polybutadienes and ethylene-propylene

Table 4.2 Mechanical and structural characteristics of the PIP-HDI networks

PIP Mw = 2201

r	w_s	N_e	G(exp)	G(calc)	T_e
1.000	0.0024	0.3960	0.883	0.6603	0.5833
0.900	0.0114	0.2608	0.669	0.4195	0.3535
0.800	0.0518	0.1265	0.351	0.1960	0.1497
0.700	0.1652	0.0425	0.122	0.0633	0.0412
0.600	0.5450	0.0025	0.056	0.0035	0.0012

PIP Mw = 2641

r	w_s	N_e	G(exp)	G(calc)	T_e
1.000	0.0037	0.3668	0.286	0.5139	0.5280
0.900	0.0216	0.2107	0.260	0.2845	0.2908
0.800	0.0371	0.1522	0.153	0.1978	0.1871
0.700	0.1192	0.0608	0.083	0.0759	0.0637
0.600	0.3860	0.0082	0.043	0.0098	0.0056

Table 4.2 continued on next page

Table 4.2 (continued)

PIP Mw = 6117

r	w_s	N_e	G(exp)	G(calc)	T_e
1.000	0.0035	0.3668	0.530	0.2271	0.5259
0.900	0.0186	0.2228	0.350	0.1327	0.2847
0.800	0.0578	0.1196	0.280	0.0684	0.1345
0.700	0.1708	0.0416	0.150	0.0227	0.0375
0.600	0.4764	0.0044	0.050	0.0023	0.0023

r = [NCO]/[OH] in the reaction mixture.
w_s = weight fraction of the extractable sol fraction.
N_e = mole fraction of elastically active network chains
G(exp) = equilibrium shear modulus, experimental value as measured by the Impulse technique. (in MPa)
G(calc) = equilibrium shear modulus, theoretical value, calculated in the affine limit. (in MPa)
T_e = number fraction of entanglements trapped in the network structure

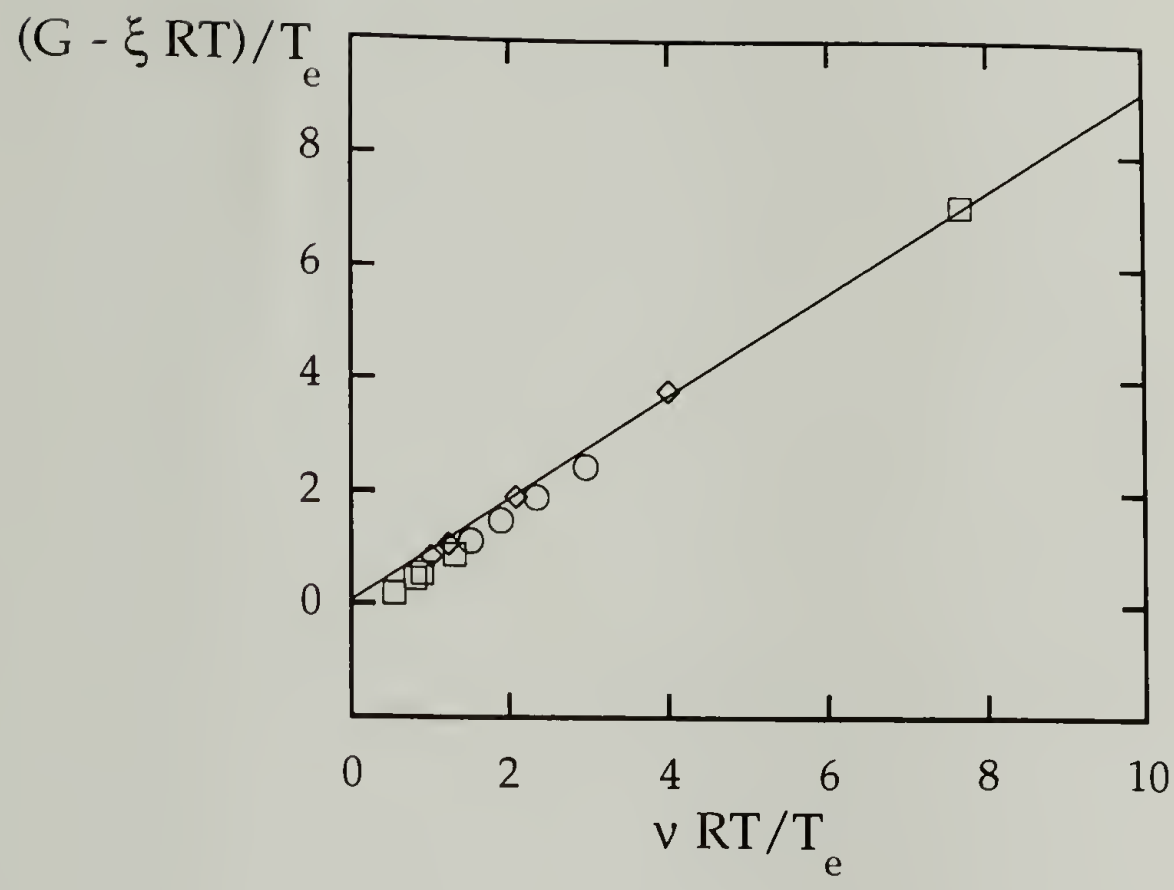

Figure 4.3 $(G - \xi RT)/T_e$ vs. $\nu RT/T_e$ for the PIP-DRF samples. PIP2201: circles; PPG2641: squares; PPG6117 diamonds; solid line represents best fit of all data with intercept $G_e = 0.06$ and slope $h = 0.91$.

copolymers, while less than 0.66 for PDMS. The value for Ge has been reported for a few different systems and was found to be close to the plateau modulus of the linear equivalent[15].

To verify that phenomena other than trapped entanglements are crucial in the explanation of the topological constraints in this system as in the PPG-DRF system, a similar development as previously used is undertaken for the PIP-HDI system. Figure 4.4 shows a plot of $\log \Delta$ vs. w_g. Δ and w_g were defined earlier.

A similar behavior is observed. The ε value that properly describes the entanglement contribution for the stoichiometrically balanced samples gives increasingly poor fits with the Δ values for the stoichiometrically imbalanced samples. The value for ε that provides a reasonable fit for the stoichiometrically balanced samples is $4.7 \cdot 10^{-4}$ mol cm^{-3}. This value corresponds to an

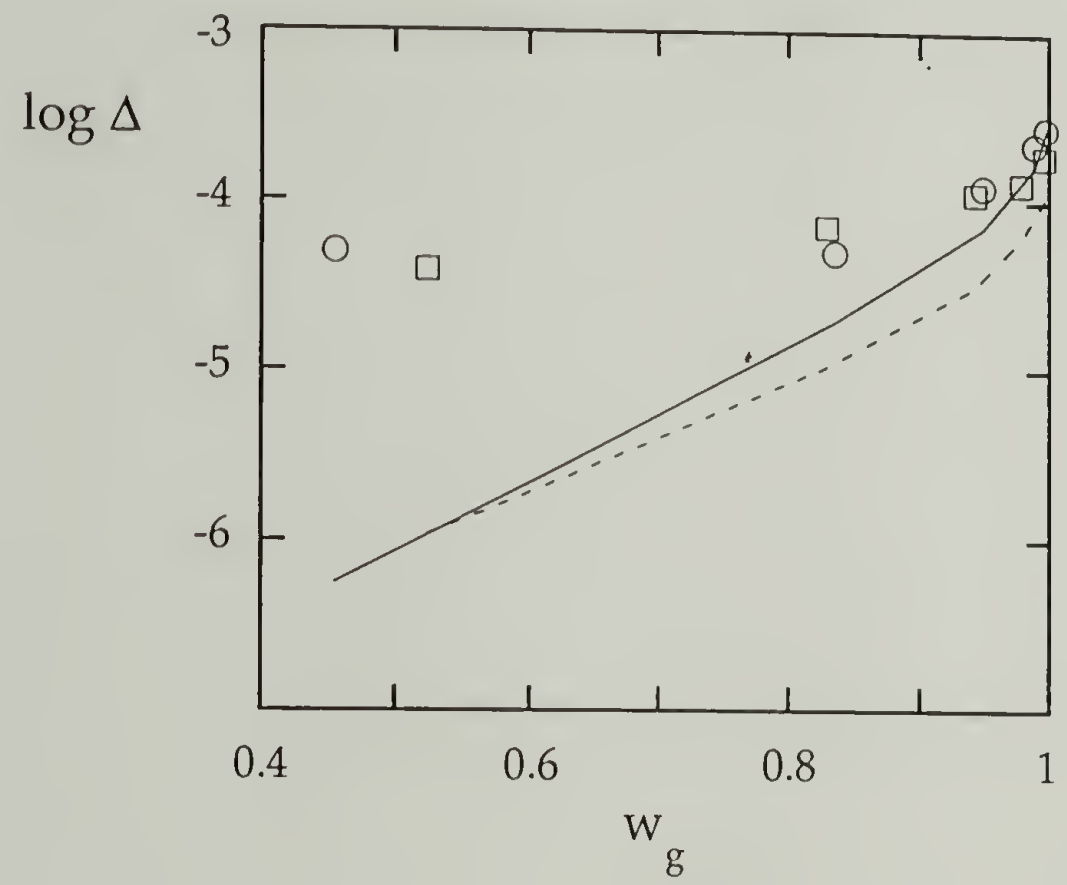

Figure 4.4 log Δ vs. w_g for PIP-HDI. PIP2201: experimental values: circles; calculated values for ε is $4.7 \cdot 10^{-4}$ mol cm^{-3} : solid line; PIP6117: experimental values : squares; calculated values for ε is $4.7 \cdot 10^{-4}$ mol cm^{-3} : broken line

entanglement molecular weight in the corresponding linear poly isoprene of approximately 2150 which is well below the 5000-6000 as estimated from rheological experiments[27] for polyisoprenes with high 3,4 content. The difference in entanglement molecular weights found for the networks and the linear equivalents is of the order of the difference found for the PPG-DRF system.

Conclusions

The combined findings of the PPG-DRF system and the PIP-HDI system can be summed up as follows. The direct contribution of trapped entanglements to the equilibrium modulus is negligible for these two systems. The key to this conclusion is found in the comparison of calculated and observed values of Δ. To fit the data for the stoichiometrically imbalanced samples an increasing value for ε is needed. This corresponds to a lower entanglement molecular weight. The entanglement molecular weight is a constant for a polymer. Even if the network structure were to influence this number, values necessary to fit the data are physically very unlikely.

To explain the contribution of the topological constraints to the equilibrium modulus, the plot of $(G - \xi RT)/T_e$ vs. $\nu RT/T_e$ has proven very useful. The value h_{CC} for the PIP-HDI system is higher than those found for the PPG-DRF system. This suggests that the chain motion is more restricted in the PIP-HDI system, possibly due to the larger number of branches by virtue of the structure of the prepolymer. The observation that h_{CC} is larger than 0.67 for PIP-HDI and PPG3000-DRF samples, which corresponds to the affine limit in the Constrained

Junction model, proves the validity and applicability of the Constrained Chain theory for rubber elasticity.

References

1. H. M. James, E. Guth, J. Chem. Phys., 15, 669 (1947).

2. P. J. Flory, Principles of Polymer Chemistry, Cornell University Press, Ithaca, NY (1953).

3. P. J. Flory, J. Chem. Phys., 66, 5720 (1977).

4. B. Erman, L. Monnerie, Macromolecules, 22, 3342 (1989).

5. N. R. Langley, Macromolecules, 1, 348 (1968)

6. N. R. Langley, J. Non-Cryst. Solids, 131, 894 (1991)

7. P. J. Flory, Proc. R. Soc. Lond. A351, 351 (1976)

8. F. Harari, Graph Theory, Addison-Wesley, Reading MA (1971)

9. W. W. Graessley, Macromolecules, 8, 186, (1975)

10. B. Erman, P. J. Flory, J. Pol. Sci. Pol. Phys. Ed., 16, 1115 (1978)

11. H. Pak, P. J. Flory, J. Pol. Sci. Pol. Phys. Ed., 17, 1845 (1979)

12. B. Erman, W. Wagner, P. J. Flory, Macromolecules, 15, 806 (1982)

13. P. J. Flory, Macromolecules, 12, 119 (1979)

14. L, M. Dossin, W. W. Graessley, Macromolecules, 12, 123, (1979)

15. L, M. Dossin, D. S. Pearson, W. W. Graessley, Abstracts, International Rubber Conference, Kiev (1978)

16. M. Gottlieb, C. W. Macosko, G. S. Benjamin, K. O. Meyers, E. W. Merrill, Macromolecules, 14, 1039, (1981)

17. N.R. Langley, K. E. Polmanteer, J. Pol. Sci. Pol. Phys. Ed., 12, 1023 (1974)

18. J. P. Queslel, J. E. Mark, Adv. Pol. Sci. 65, 135 (1984)

19. M. Gottlieb, C. W. Macosko, T. C. Lepsch, J. Pol. Sci. Pol. Phys. Ed.,19, 1603 (1981)

20. M. I. Aranguren, C. W. Macosko, Macromolecules, 21, 2484, (1988)

21. R. C. Ball, M. Doi, S. F. Edwards, Polymer, 22, 101 (1981)

22. R. J. Gaylord, Polym. Bulletin, 8, 325, (1982)

23. H.-G. Kilian, H. F. Enderle, K. Unseld, Colloid Pol. Sci., 264, 866 (1986)

24. F. Boue, T. Vilgis, Colloid Pol. Sci., 264, 285 (1986)

25. M. Ilavsky, K. Dusek, Polymer, 24, 981 (1983)

26. W. W. Graessley, S. F. Edwards, Polymer, 22, 1329 (1981)

27. J. T. Gotro, W. W. Graessley, Macromolecules, 17, 2767 (1984)

CHAPTER 5

RELAXATION IN THE GLASS TRANSITION REGION

Introduction

The glass transition region in temperature or frequency is important since structural features are highlighted, either in the relaxation behavior or in the glass transition temperature. It is defined as the temperature region from Tg - 50° to Tg + 50°. Relaxation or freeing of motional restrictions in the glassy state occurs when heating the sample to temperatures above the glass transition. This increase in motion at Tg has several repercussions on the magnitude of certain material characteristics. The ones considered here are the dielectric constant, the modulus, and the NMR intensity. These can be measured as a function of temperature or frequency (although the frequency is a machine specific constant in NMR). The two measurements can with certain limitations be related by the principle of time-temperature superposition.

Dynamic mechanical thermal analysis

The knowledge of the influence of certain structural features of the network on the mechanical properties is important. The dynamic mechanical technique offers insights in the viscoelastic behavior of the polymers studied[1] [2]. It identifies the regions of transition from a mechanical perspective. In the transition region DMTA offers information of the mechanical influence of the molecular motions.

The applicability of the DMTA technique is in a limited frequency range, due to limits on resonance of the machinery. The available frequencies are in the range of 10^{-2} -10^{2} Hz. The usual frequencies used are in the range of 1-10 Hz this results in a glass transition temperature shift of 10-20° over the DSC data. A DMTA measurement in the temperature domain measures the elastic and storage moduli. Their ratio, tan δ, is used here as a means of comparison between samples. The DMTA technique is ideally suited to investigate (largely on a qualitative basis for polymer networks) the influence of a number of structural features on the viscoelastic behavior.

DMTA is sensitive to most β transitions, where DSC and DETA are less important. Secondary transitions are of little importance in the rubber elasticity theory, but may indicate an inhomogeneity on a molecular level.

The influence of dangling ends can be described as a plasticizing effect. The incorporation of low molecular weight soluble compounds in a polymer changes the viscoelastic behavior to a greater or lesser extent, depending on the polymer -plasticizer system. The temperature of the maximum in tan δ decreases with higher concentration of the diluent. The half-width of the tan δ spectrum increases significantly indicating a larger distribution of the molecular mobilities in the system, and thus of correlation times.

A difference in molecular weight between crosslinks can cause reduction of the half width of the tan δ.

Crystallinity in the sample results in a melting transition peak, and a widening of the tan δ spectrum.

Dielectric thermal analysis

It is crucial to investigate the molecular homogeneity of the networks at hand. Any inhomogeneity found can serve as an extra crosslink and cause discrepancies in the elasticity behavior. An extensive study was done on stoichiometrically balanced samples of the PPG-DRF networks[3]. It was found that two relaxation processes take place. The high frequency process is due to motions mainly involving the ether oxygen in the group and the low frequency process stems from motions mainly involving the urethane group. This analysis was done on the basis of the Kirkwood-Frolich equation[4] defined as:

$$\varepsilon_R - \varepsilon_u = \kappa_1 \kappa_2^2 \, 4\pi \, N^2 \mu^2 g / 3kT \qquad (1)$$

Herein $\kappa_1 = 3\,\varepsilon_R / 2\varepsilon_R + \varepsilon_u$, and $\kappa_2 = \varepsilon_u + 2/3$, ε_R is the limiting value of the dielectric constant at long times, ε_u is the instantaneous component of the dielectric constant, μ is the dipole moment of the sample, N is the number of molecules per unit volume, k is the Boltzmann constant, and T is the temperature. g, the correlation factor, describes the directional contribution to the dipole moment and is defined as:

$$g = 1 + 1/N \sum \langle \cos \gamma_{1j} \rangle \qquad (2)$$

with γ_{1j} the angle between th first unit of chain 1 and the jth unit, and N the number of repeat units in the chain. g depends on the chain geometry. A g-

factor analysis on the dielectric data obtained on the PPG-DRF system suggested the two relaxations to correspond to the chain and the crosslinker, respectively. Dr. S. Havriliak[5] recalculated the g-factor using elaborate computer programs. His analysis showed that both relaxations were attributable to the motion of the PPO chain. According to him, the double relaxation behavior is explainable by assuming a relatively high compliance of the network, which results in a consecutive "freezing out" of the dipole upon heating. This does not mean that one portion of the chain has a different mobility and that a second relaxation is occurring from a mechanical perspective. For a full description of the influence of matrix compliance on dielectric relaxation we refer to the literature[6 7].

$T_{1\rho}$ relaxation in NMR

Nuclear magnetic resonance has been shown to be a good technique to investigate molecular motion in networks. The PPG-DRF system is ideally suited for the analysis of the difference of chain mobility vs. crosslink mobility. This is due to the NMR active phosphorus atom at the crosslink point. The relaxation behavior of the PPG-DRF network system for stoichiometrically balanced samples is well understood[8 9]. Both ^{13}C- and ^{31}P- experiments were performed. The observed decrease in line widths with increasing temperature or Mc is interpreted as increased mobility of the crosslink point. The crosslink point does not tumble isotropically, even well above the Tg. This was concluded from the actual value of the minimal $T_{1\rho}$versus the theoretical one. The theoretical value is given by:

$$T_{1\rho}^{-1} = (4/45)\,\gamma^2\,B_o^2\,(\sigma_{pa} - \sigma_{pe})^2\,\tau/(1+\omega_e^2\tau^2) \qquad (3)$$

where τ is the correlation time, ω_e is the spin lock frequency (the frequency at which the frame rotates), σ_{pa} is the shift tensor component parallel to the magnetic field while σ_{pe} is the perpendicular component. $(\sigma_{pa} - \sigma_{pe})$ is influenced by the reorientation of the P=S bond. If no full sweep of the molecular axis through 90° is observed, then the experimental relaxation time is larger then the theoretical one since $(\sigma_{pa} - \sigma_{pe})$ will remain too large.

The frequency of the crosslink point reorientation is a factor 3-5 slower than the chain segmental motion, based on a difference in the temperature at which the minimum in $T_{1\rho}$ relaxation time occurs. For samples made of PPG1000 and PPG2000 a second longer relaxation time is observed below the glass transition temperature. This suggests that the crosslink has an "anchoring effect" on the network.

This anchoring effect is not expected in the PIP-HDI system since the bulkiness of the crosslinker is absent. The influence of the increase in the amount of dangling ends with increasing imbalance is investigated here. Also, for the PPG-DRF system the ^{31}P $T_{1\rho}$ relaxation time will be examined for changes with stoichiometric imbalance.

Results and discussion

The DMTA results

The results shown in Figures 5.1-5.4 represent the tan δ results vs. temperature, obtained by DMTA at 1 Hz and at a heating rate of 2°/minute. For all samples of both network systems the same observations can be made. The other data were omitted for clarity. The temperatures at the maxima in tan δ shift with Tg, corresponding to the Tg shift with composition as described in Chapter 3. Broadening of the tan δ peak is apparent with increasing stoichiometric imbalance, Both the shift and the broadening are smaller for the PIP-HDI system samples.

It can be seen that the DMTA results corroborate all of the results found for Tg by DSC. The Tg shift with stoichiometric imbalance is of the order of a few degrees here, while negligible in DSC. This can be explained by assuming a plasticizing effect of the extractable portion and the dangling ends. The tan δ spectra widen with increasing stoichiometric imbalance. This also can be attributed to the plasticizing effect of the sol fraction and dangling ends.

In all cases a single transition is observed. No β transitions were expected or found in the temperature range studied. This is additional evidence that both of these network systems are homogeneous over the entire range of molecular weights and stoichiometric imbalances.

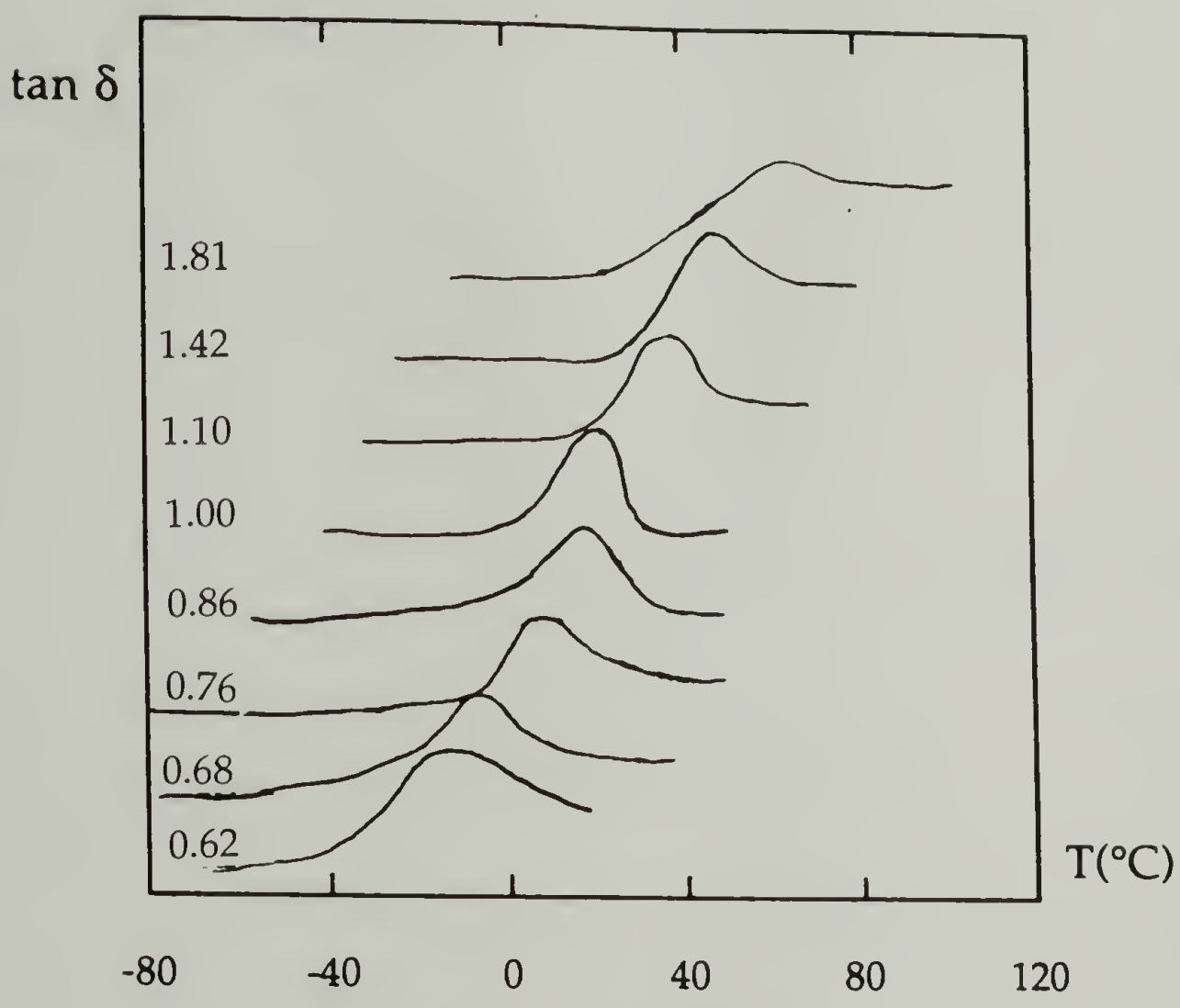

Figure 5.1 tan δ (DMTA) vs. temperature, for all PPG400-DRF samples. Stoichiometric imbalance indicated.

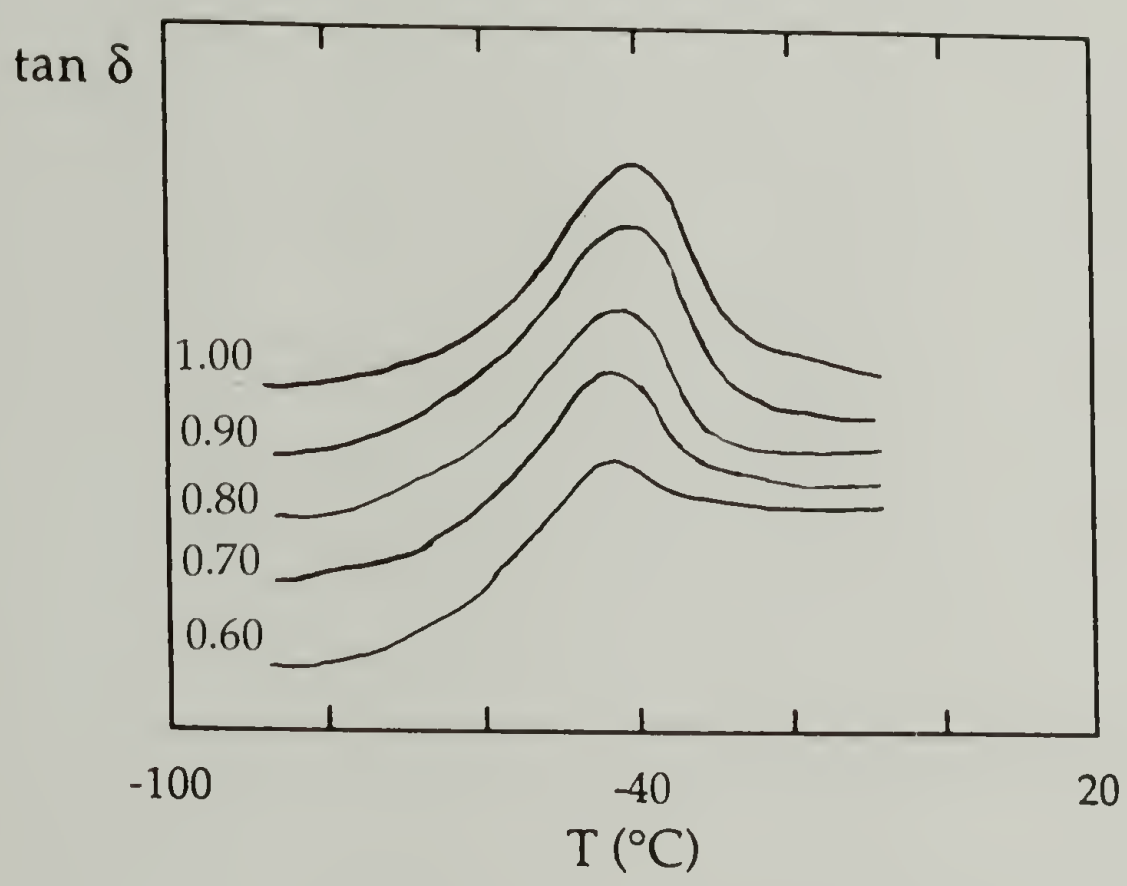

Figure 5.2 tan δ (DMTA) vs. temperature, for all PPG3000-DRF samples. Stoichiometric imbalance indicated.

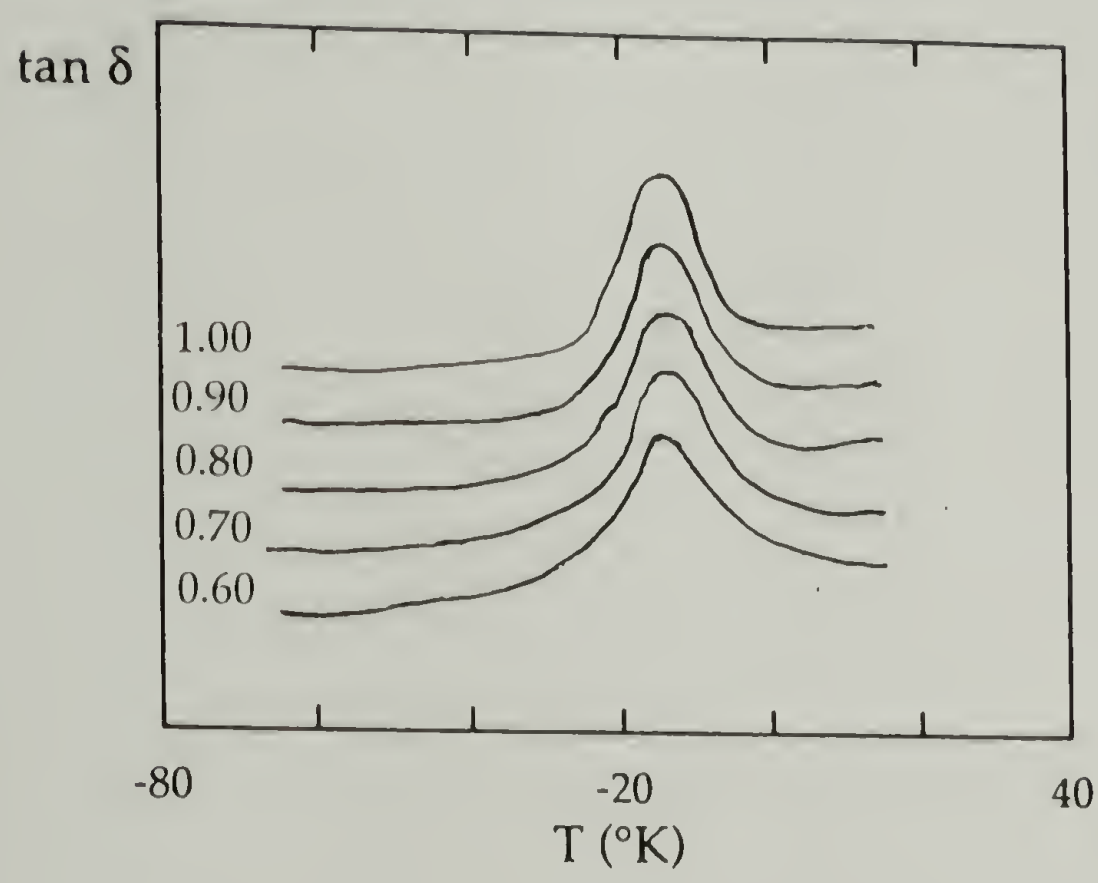

Figure 5.3 tan δ (DMTA) vs. temperature, for all PIP2201-HDI samples. Stoichiometric imbalance indicated.

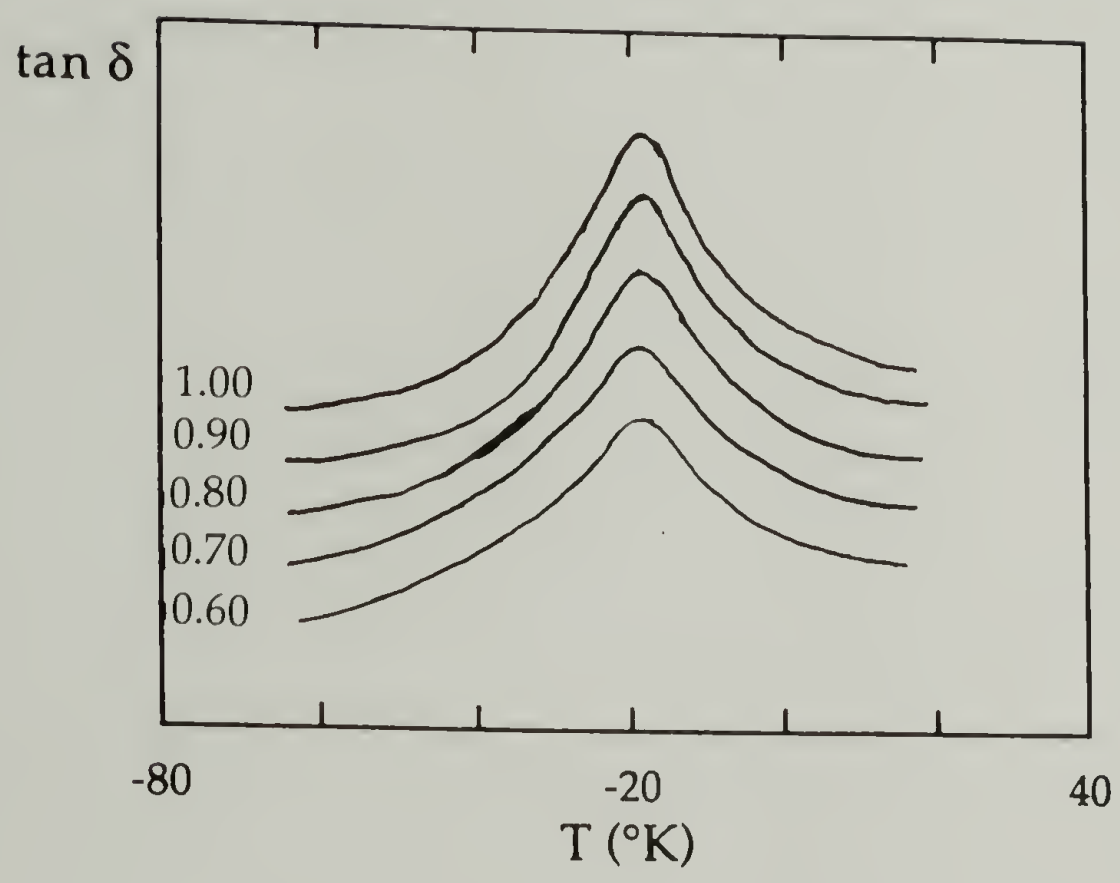

Figure 5.4 tan δ (DMTA) vs. temperature, for all PIP6117-HDI samples. Stoichiometric imbalance indicated.

The DETA results

Figure 5.5 and 5.6 depict the tan ε spectra versus temperature, measured at 1 kHz for the PPG-DRF samples. For the PPG400 samples a single relaxation is found. No influence from the "anchoring" of the crosslinker is seen. The temperature shift of the maximum which corresponds to the glass transition temperature is larger than that found in the DSC measurements. This is completely consistent with the temperature shift corresponding to the frequency difference of the DSC and DETA measurements.

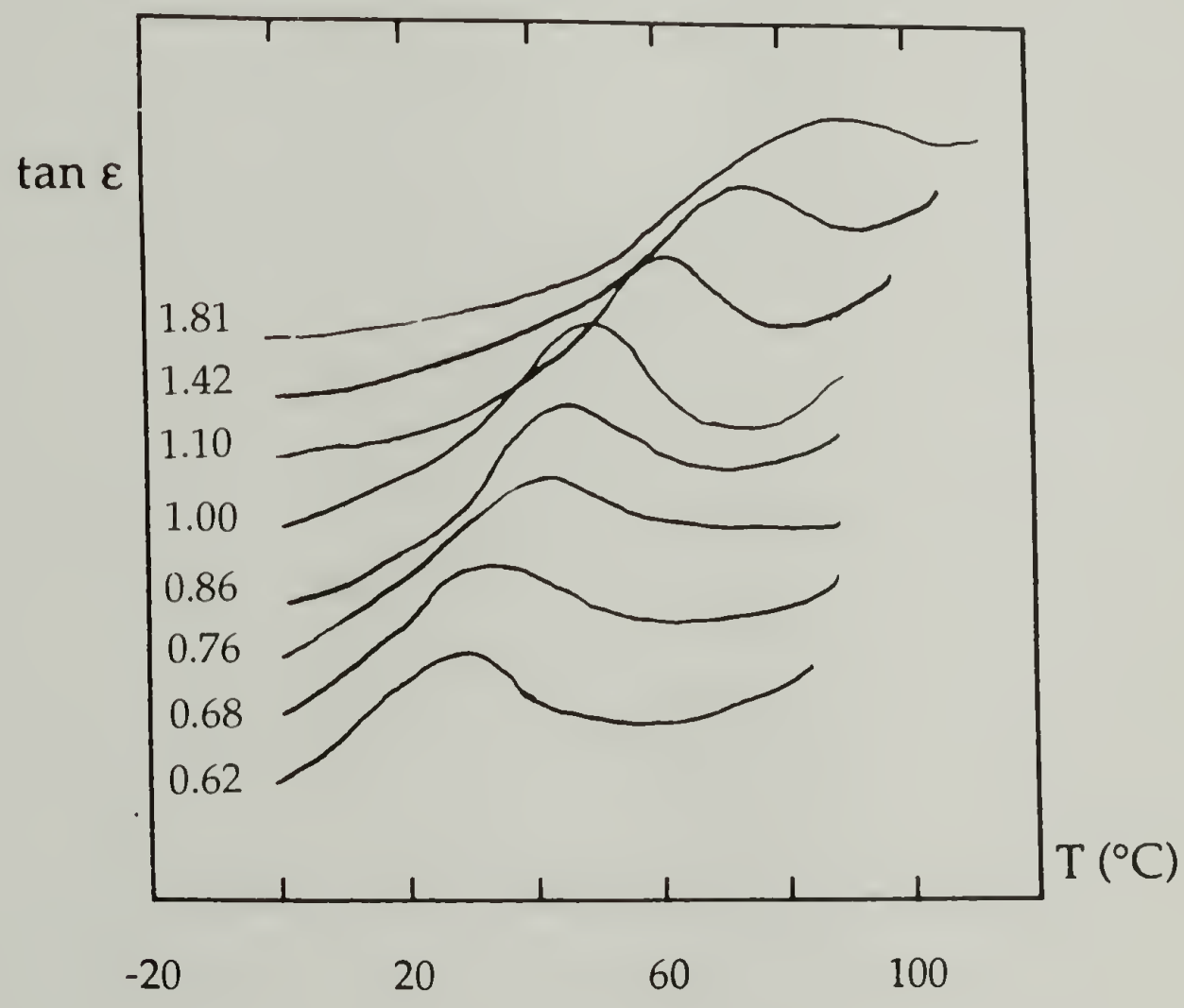

Figure 5.5 tan ε (DETA) vs. temperature, for some of the PPG400-DRF samples. Stoichiometric imbalance indicated.

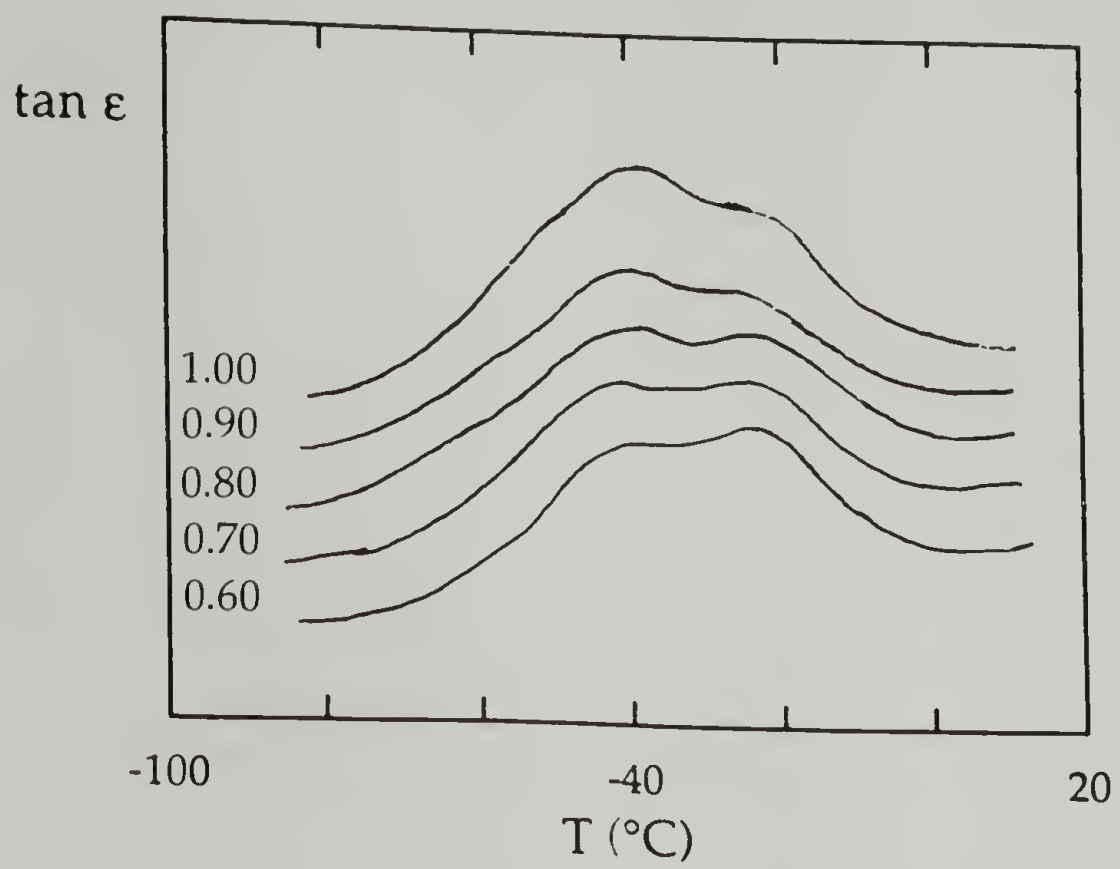

Figure 5.6 tan ε (DETA) vs. temperature, for all PPG3000-DRF samples. Stoichiometric imbalance indicated.

The results for the PPG3000-DRF samples show two relaxations. The peak height of the two relaxations changes with the composition of the sample. The other data were omitted for clarity. The same was observed for the PPG1000 and PPG2000 samples, only the peak at the lower temperature is merely a shoulder. It is clear however that the relative peak height is proportional to the composition of the samples. The higher temperature peak was previously correlated to the crosslinker, while the lower was suggested to the stem from the PPO chain. Again, that conclusion was questioned by Dr. Havriliak, who suggested that both relaxations belong to the chain, but that one corresponds to

the chain close to the crosslinker (the higher temperature one) and the other to the bulk PPO. This difference in interpretation of the data does not alter the conclusion that the bulkiness of the crosslinker has a distinct effect on dielectric relaxation. This however does not necessarily mean that the samples are heterogeneous on a molecular level larger than the chain. As pointed out in the introduction, a double relaxation phenomenon in dielectric measurements can be explained by taking into account the compliance of the network, while still assuming homogeneity. The shift in peak position of the high temperature peak corresponds more closely to the DSC data, taking into account the frequency difference. The frequency shift is smaller than for the PPG400 data. This serves as corroborating evidence for the analysis by Havriliak.

The ^{13}C- and ^{31}P-$T_{1\rho}$ relaxation time results

Figures 7-11 show assorted highlights of the ^{13}C- and ^{31}P-$T_{1\rho}$ relaxation time measurements for both systems. The other data were omitted for clarity. The trends shown here are consistent over the entire range of molecular weights and stoichiometric imbalance for both systems.

Figure 5.7 shows a plot of $T_{1\rho}$ relaxation times for both ^{13}C and ^{31}P in msec vs. temperature, for the PPG2000-DRF sample. All relaxations show a minimum with temperature. The temperature corresponds to the Tg for the technique used. The methyl group carbons have a higher relaxation time than the backbone carbons over the entire relaxation range. This was observed before. A second longer relaxation time is found for both backbone and methyl carbons below glass transition temperature. This has been attributed to the anchoring

effect of the crosslinker on the chain, as described earlier This second relaxation time is only observed for the PPG1000 and 2000 samples. It appears not to be present at all in the PPG400 networks, while the number of chains affected in the PPG3000 networks is too small to be detected.

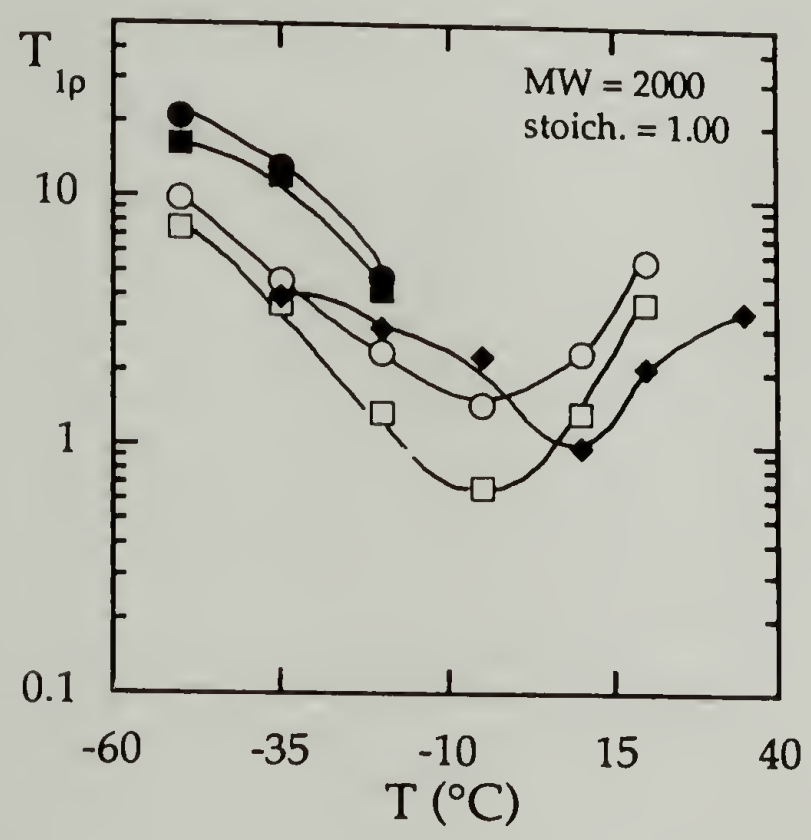

Figure 5.7 $T_{1\rho}$ relaxation times in msec vs. temperature, for the PPG2000-DRF sample. Methyl groups: short, open circles; long , filled circles (^{13}C); backbone: short, open squares; long, filled squares (^{13}C); crosslink: filled diamonds (^{31}P). Molecular weight and stoichiometric imbalance indicated.

The temperature of the minimum ^{31}P relaxation time is higher for all samples measured. This was earlier attributed to the difference in frequency of reorientation between the chain and the crosslink point. A factor 3-5, depending

on the molecular weight of the PPG, was suggested. Our calculation shows a factor of approximately 10-12, depending on the stoichiometric imbalance, for the PPG400 networks, a factor 8 for the PPG1000 networks, and a factor 5 for the PPG2000. The slightly higher values found here could be due to the slightly different method of preparation between this and the previous study. The differences in the PPG400 network results serve to show that at this molecular weight the network properties are far more easily influenced by the crosslinker. Figure 5.8 shows a plot of ^{13}C-$T_{1\rho}$ relaxation times vs. temperature for PPG-DRF3000 samples with stoichiometric imbalances. This plot was chosen because it shows the effect of stoichiometric imbalance most clearly. The same trends are present in all other PPG-DRF results, yet become less pronounced with lower molecular weight. The shape of the curves becomes narrower with stoichiometric imbalance. This indicated that an increase in activation energy of the motion occurs. In these samples the highest differences was observed. The change is on the order of a factor 2 from the stoichiometrically balanced to the stoichiometrically most imbalanced sample.

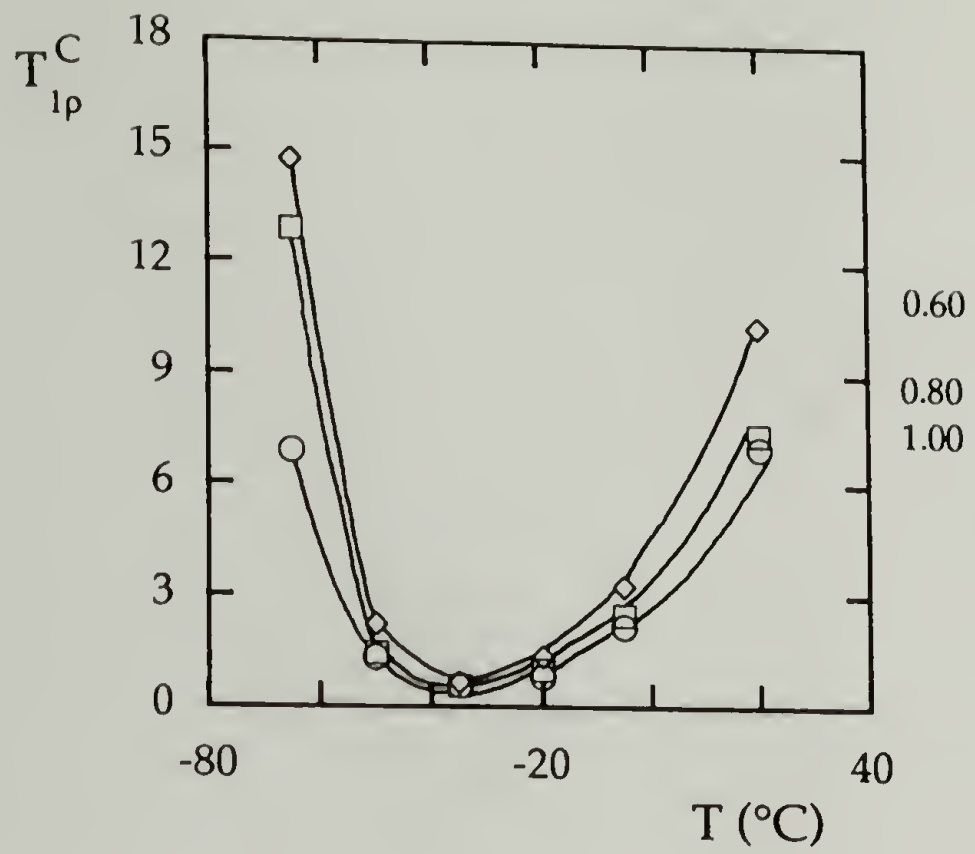

Figure 5.8 ^{13}C-$T_{1\rho}$ relaxation times vs. temperature for PPG-DRF3000 samples with stoichiometric imbalances

Figure 5.9 is a plot of ^{31}P-$T_{1\rho}$ relaxation times vs. temperature for stoichiometrically balanced PPG-DRF samples. The molecular weight of the PPG is indicated. A shift in the temperature of the minimum is observed. The order of magnitude corresponds closely with the shift in Tg found by DSC. It needs to be noted that the frequency of the rotating frame is 50 kHz. A similar plot could be made for the backbone and methyl carbons. It was omitted for the reason that it shows the same shift, with the only difference that the absolute values of the Tg are different.

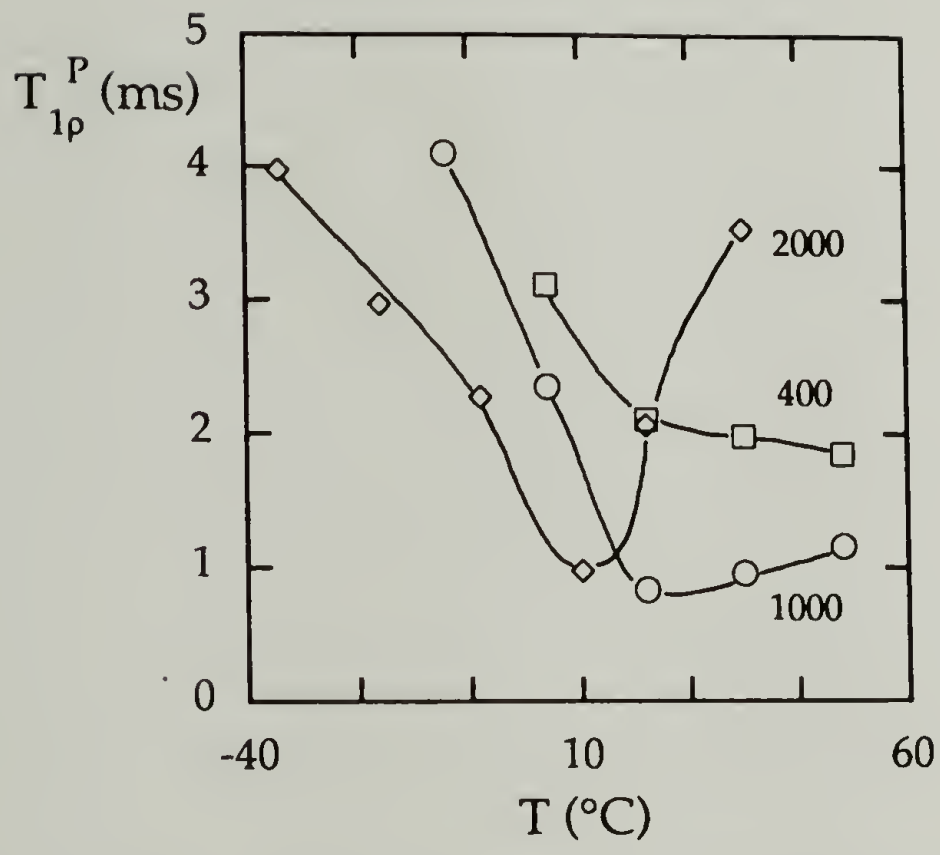

Figure 5.9 ^{31}P-$T_{1\rho}$ relaxation times vs. temperature for stoichiometrically balanced PPG-DRF samples. Molecular weight of the PPG is indicated.

Figure 5.10 shows the ^{13}C -$T_{1\rho}$ relaxation times in msec vs. temperature, for the stoichiometrically balanced PIP2201-HDI. This plot is indicative of the ones for all samples of the PIP-HDI system.

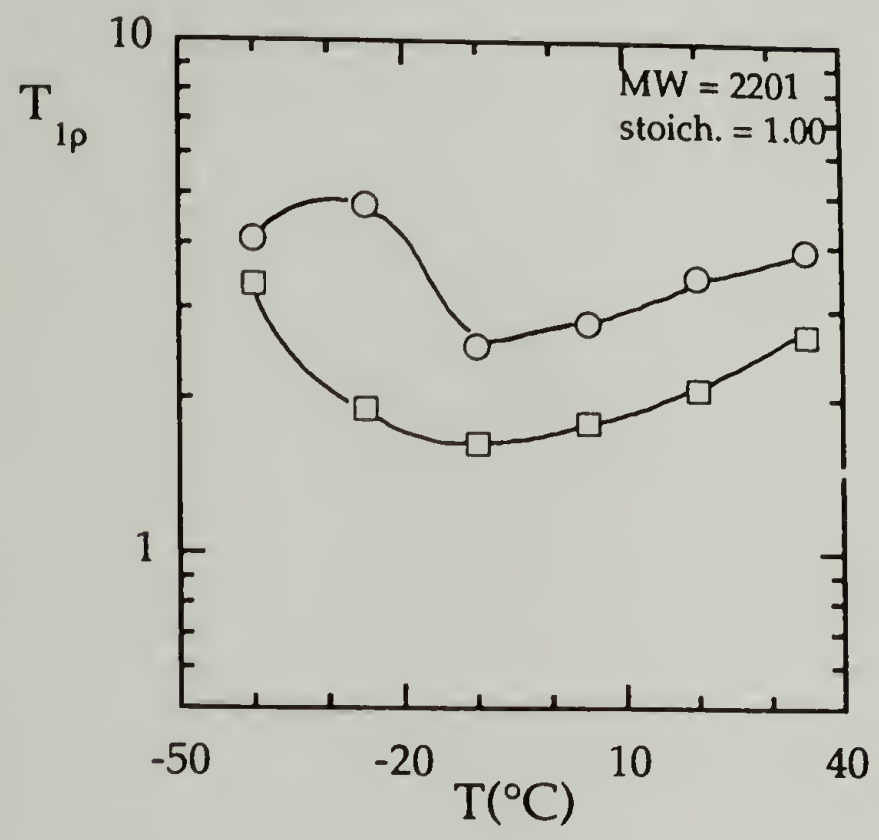

Figure 5.10 ^{13}C -$T_{1\rho}$ relaxation times in msec vs. temperature, for the stoichiometrically balanced PIP2201-HDI. Methyl groups: open circles; backbone: open squares.

The methyl relaxation was measured for the two peaks at 17 ppm and 21 ppm, corresponding to the 1,4 propagated isoprene methyl and the 3,4 propagated isoprene, respectively. Around the glass transition these two peaks were not resolved. Where they were discernible, their relaxation times were the same within experimental error. The methylene region contains a multitude of peaks that are not resolved. A peak in this unresolved region is usually observed

around 33 ppm over the entire temperature range. This peak corresponds to the $-CH_2-$ in the backbone. The relaxation times reported for the backbone are for this peak. Where more peaks could be resolved, it was determined that all the methylene relaxations have approximately the same relaxation time, within experimental error. The double bonded carbon region (90-150 ppm) shows a number of peaks, all of which become unresolved around the glass transition. Where they could be resolved it was found that the relaxation times of the carbons in a branch (3,4 and 1,2 PIP or 1,2 PBD) have approximately the same relaxation time as the methyl groups, while the double-bonded carbons in the show the same relaxation time as the methylene backbone carbons. In summary, the backbone carbons (of any kind) give rise to the lower relaxation time, while the higher relaxation time stems from all branch carbons (of any kind). Both relaxation phenomena show a minimum at the same temperature, analogously to the PPG-DRF system. The order of magnitude of the relaxation times is the same as for the PPG-DRF system. No second longer relaxation time could be found. This indicated that the absence of the bulky crosslinker increases homogeneity in the network system.

Figure 5.11 is a plot of ^{13}C-$T_{1\rho}$ relaxation times vs. temperature for PIP-HDI samples with different molecular weights for the backbone carbons. A similar plot can be drawn for the methyl carbons, as well as for the stoichiometrically imbalanced networks. It can be seen that the activation energy of the motion increases with molecular weight. This also occurs in stoichiometrically imbalanced samples of a particular molecular weight. In addition to this change

in activation energy, a decrease of the minimum relaxation time is observed with increasing molecular weight. The same occurs on a smaller basis in the PPG-DRF system. This decrease can be described as a difference in the reorientation factor (σ_{pa} - σ_{pe}) in the theoretical description. If the motion of the molecular fixed axis system, drawn theoretically, does not move through a full 90° this factor becomes too large to achieve the minimum accessible relaxation time. If motion is more restricted, the relaxation time can never reach its minimum value.

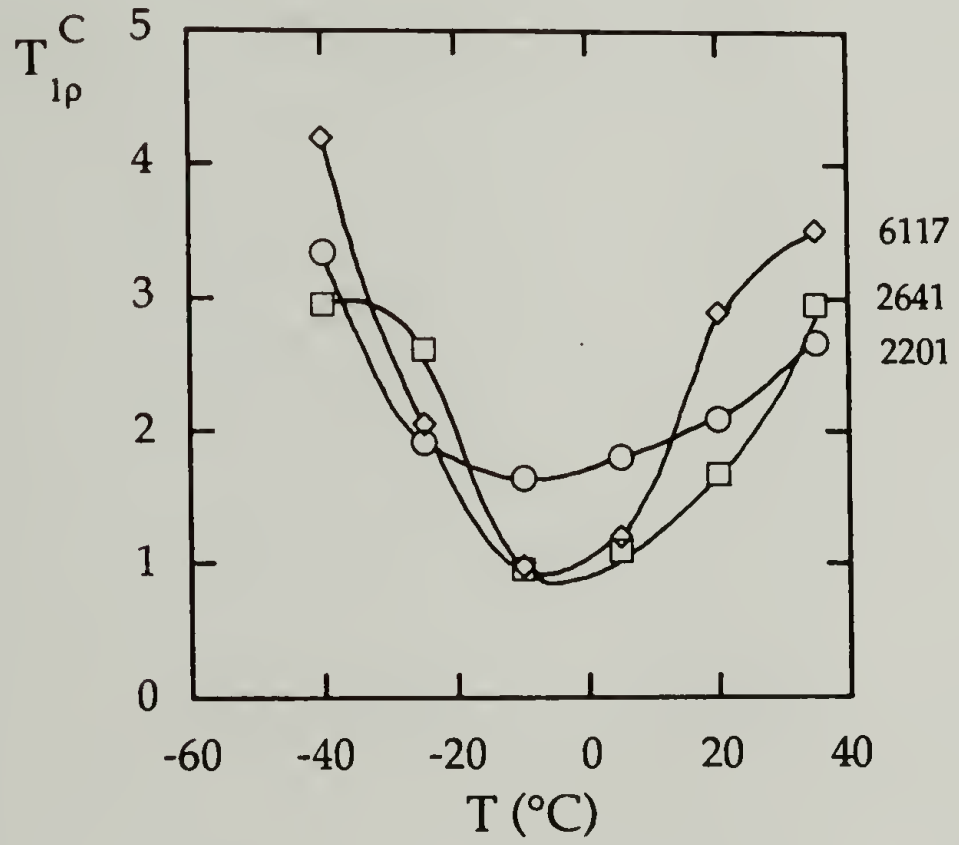

Figure 5.11 ^{13}C-$T_{1\rho}$ relaxation times vs. temperature for PIP-HDI samples with different molecular weights for the backbone carbons.

Conclusions

In summary it can be said that all samples of both network systems are homogeneous on the molecular level, with some reservations for the PPG-DRF system. The bulkiness of the DRF crosslinker has a profound effect on both the dielectric relaxation and the ^{13}C NMR relaxation. The absence of that bulkiness in the PIP-HDI system removes these effects. The explanation of Havriliak of previous dielectric data can be correlated with the NMR data to show that the crosslinker indeed has an anchoring effect on the network chain, as was shown before.

The temperature shift with molecular weight and stoichiometric imbalance of the Tg as observed by these techniques is similar to that found by DSC measurements. Plasticizer effects can account for the broadening of the tan δ (DMTA) and tan ε (DETA) spectra for both networks. This broadening is more pronounced in the PPG-DRF system than in the PIP-HDI system. This can be explained by the difference in the molecular weight of the soluble fraction, and the amount of free end groups present in the network.

References

1. J. J. Aklonis, W. J. MacKnight, Introduction to Polymer Viscoelasticity, J. Wiley & Sons (1983)

2. J. D. Ferry, Visocelastic Properties of Polymers, John Wiley & Sons, New York, (1980)

3. K. Ichikawa, W. J. MacKnight, submitted for publication

4. H. Frolich, Theory of dielectrics, 2nd ed., Oxford University Press (1958)

5. S. Havriliak Jr., personal communication

6. S. Havriliak Jr.,Macromolecules, 23, 2384 (1990)

7. S. Havriliak Jr., S. J. Havriliak, Polymer, 33, 938 (1992)

8. L. C. Dickinson, P. L. Morganelli, C. W. Chu, Z. Petrovic, W. J. MacKnight, J. C. W. Chien, Macromolecules, 21, 338, (1988).

9. L. C. Dickinson, J. C. W. Chien, W. J. MacKnight, 23, 1279 (1990)

CHAPTER 6

SWELLING IN MIXED SOLVENTS

Introduction

When a linear polymer is submersed in a solvent it will dissolve if the free energy of mixing ΔG_{mix} is negative. A linear polymer in a "good" solvent can be described as an open thermodynamic system: it can be stated that the polymer dissolves in the solvent and that the solvent dissolves in the polymer, with equal accuracy. The thermodynamic system composed of a network polymer and a solvent is a semi-open one. Upon submersion of the network, the solvent may enter the network structure, resulting in a swollen network. The polymer is distinctly confined to one of the two phases. A similarity exists with the case where the polymer is confined to one of two or more phases by a membrane. The network surface is comparable with the membrane.

The process of swelling is dependent on a number of variables: temperature, solvent activity, polymer-solvent interactions, etc. Swelling is useful in the assessment of either the crosslink density or the solvent-polymer interaction parameter, given that one is known.

The first theoretical treatment of swollen networks was proposed by Flory and Rehner[1]. It is based on the now generally accepted assumption that the Gibbs free energy of swelling is the sum of the free energy of mixing, ΔG_{mix}, and the elastic free energy, ΔG_{el}. Equilibrium swelling will be reached when the energy contribution of the solvent-polymer interaction is offset by the contribution of the

elastic forces. Lattice theory of solution is at the basis of the free energy of mixing, while the elastic free energy is taken from the rubber elasticity theory (Chapter 4).

When analyzing the contribution of the elasticity to the swelling the train of thought is similar to the one followed in Chapter 4. The different considerations involving the Constrained Chain, Constrained Junction and other rubber elasticity models are of importance here. The permanent topological constraints, like trapped entanglements are thought to have an effect on the swelling equilibrium. In studying the polymer-solvent interactions, it is often assumed that the network is perfect which may be erroneous. The influence of the crosslinker is not well understood. Chemically, the crosslinker is often different in structure from the polymer chain. It was found that for the PPG-DRF system the swelling behavior needs to take into account not only the interaction parameters of PPG with the solvent and DRF with the solvent separately, but also the interaction parameter between PPG and DRF[2]. The network clearly behaves like a copolymer in this case. A swelling study in mixed solvents was done, and while an explanation of the data on the basis of solubility parameters offered fair agreement with the general tendencies of the swelling behavior, further theoretical considerations were warranted. It became clear that a swelling equation based on a system of a copolymer with two solvents needed to be derived. In this study, this equation is derived and applied to swelling data of the PPG-DRF stoichiometrically balanced samples of different molecular weights, swollen in mixtures of benzene and methanol.

The general structure of the PIP-HDI system can be described as a copolymer as well. The system lacks the difference in structure at the crosslink point: a true point crosslink is found. However, the network chain is a block copolymer of polybutadiene (approximately 5-6 repeat units) and polyisoprene. The argument can be made that the polyisoprene is also a random copolymer of 1,4-, 1,2-, and 3,4-propagated units. As will be shown, the actual surface area of the unit is the same for all cases, and hence the interaction parameter will be similar for each unit. Possible differences will be ignored. The same can be said for the polybutadiene portion which is a copolymer of 1,2- and 1,4- segments. Structurally, the difference between polybutadiene and polyisoprene is a mere methyl group. This difference however translates in a 22% difference in surface area of the repeat unit, which is one of the important parameters in the theoretical treatment. It will be of interest to characterize the influence of this structural characteristic.

The solvents chosen for the study are methanol and benzene. This offers the opportunity to examine the effect of a polar solvent and an apolar one on what is, in its roughest approximation , a polar and a non-polar network. The parameters needed to calculate the interaction between the two solvents are well characterized and available in the literature. A number of assumptions will be needed to translate this information to the appropriate interaction parameters.

Theoretical background and its application

For the purpose of introducing the new equation for the condition of equilibrium swelling of the system of a copolymer in two solvents, a quick overview of the basic theoretical considerations is warranted.

The Gibbs free energy of swelling is generally defined as a linear combination of the free energy of mixing ΔG_{mix} (of the copolymer in two solvents) and the elastic free energy ΔG_{el} (of the network).

The Gibbs free energy of elasticity ΔG_{el}

The general expression[3] for the elastic free energy as it applies to the swelling condition is

$$\Delta G_{el} = \nu RT [(A/2 \sum \lambda_i^2 - 3) - B \ln \lambda_x \lambda_y \lambda_z] \quad (1)$$

All parameters have the same definition as in previous chapters. A and B are defined as (f-2)/f and 0 in the phantom limit, and 1 and 2/f for the affine limit in the Constrained Junction model, where f is the crosslink functionality. In the previous study of equilibrium swelling of PPG-DRF[2], the choice of the different models did not seriously affect the conclusion that the system behaved as a copolymer. This conclusion will be reassessed here. Also, considering the trapped entanglement contribution did not show to be of importance, even though it was thought to have an effect in the equilibrium modulus

measurements of PPO networks[4]. We shed a different light on that conclusion in Chapter 4. There, it was concluded that the Constrained Chain model explained the behavior well, and the direct contribution of trapped entanglements is negligible. In the case of swelling, chain constraints are largely neutralized by the separation due to the solvent. The chain constraints are expected to have little influence on the equilibrium swelling of these networks. This notion needs to be verified.

In the earlier article on PPG-DRF[2], it was suggested to investigate the possibility for A and B to depend on the swelling ratio. This dependency is complex[5], but a first approximation was checked there, as will be done here.

The Gibbs free energy of mixing ΔG_{mix}

In the following treatment the subscripts used need to be consistent. Several discrepancies exist between the nomenclature used in the different articles on which the derivations are based. Here, all parameters pertaining to the polymer will have subscript 3, while 1 and 2 will stand for two different solvents. When copolymer considerations are taken into account, a and b will designate the two components of the copolymer.

The general expression for the free energy of mixing for a polymer in a solvent, ΔG_{mix}, as derived by Flory[6] and Huggins[7] is

$$\Delta G_{mix} = RT\,[n_1 \ln \varphi_1 + n_3 \ln \varphi_3 + \chi_{13}\, n_1 \varphi_3] \qquad (2)$$

with φ_3 and n_3 the volume fraction and number of moles of the polymer, and φ_1 and n_1 the volume fraction and number of moles of the solvent in the solution, and χ_{13} the solvent-polymer interaction parameter. For future consideration it needs to be noted that mixing may occur when pure solvent and pure polymer are mixed. It is trivial that the Gibbs free energy of mixing of the pure solvent with itself and the pure polymer with itself is equal to 0. When the polymer is a copolymer, a deviation from this statement may occur since an interaction between the two copolymer components needs to be taken into account. This interaction was described in a previous treatment. For a copolymer in a single solvent the Gibbs free energy of mixing becomes:

$$\Delta G_{mix} = RT\,[n_1 \ln \varphi_1 + n_3 \ln \varphi_3 + (\varphi_a g_{1a} + \varphi_b g_{1b} - \varphi_a\varphi_b g_{ab}/\alpha)(n_1 m_1 \varphi_3/Q)] \quad (3)$$

Herein, φ_i are volume fractions, g_{ij} are interaction parameters, and m_i are molal volumes of the components designated by the appropriate subscript. Q is here defined as:

$$Q = \varphi_1 + (z_2/z_1)(\varphi_a + (z_3/z_2)\varphi_b)\,\varphi_3 \quad (4)$$

The theoretical expression of ΔG_{mix} of a copolymer in a mixture of solvents becomes increasingly complex. Krigbaum and Carpenter treated the simpler case of phase equilibria in polymer (3)-liquid (1)-liquid (2) systems thoroughly[8]. The basis for their treatment lies in the equilibrium between a binary phase and a

ternary phase. The binary phase consists of the two solvents before mixing with the polymer, while the ternary phase contains the polymer, diluted in the solvent mixture.

The total free energy of formation of the binary phase, ΔG_{mixb}, is given by:

$$\Delta G_{mixb} = RT [n_1 \ln \varphi_1 + n_2 \ln \varphi_2 + \chi_{12} \varphi_1 \varphi_2] \quad (5)$$

where φ's, n's, and χ_{12} are defined equivalently to previous definition. For the ternary phase, the free energy of dilution of the polymer, ΔG_{mixt}, becomes:

$$\Delta G_{mixt} = RT [n_1 \ln \upsilon_1 + n_2 \ln \upsilon_2 + \chi_{12}' \upsilon_1 \upsilon_2 + \chi_{13}' \upsilon_1 \upsilon_3 + \chi_{23}' \upsilon_2 \upsilon_3] \quad (6)$$

χ_{12}', χ_{13}', and χ_{23}' are the interaction parameters between solvent 1 and solvent 2, between solvent 1 and the polymer, and between solvent 2 and the polymer, all in the swollen state. υ_1, υ_2, and υ_3 are the volume fractions of solvent 1, solvent 2, and the network in the ternary phase, the swollen network. All other variables were defined earlier.

It needs to be pointed out here that the ratio of the volume fractions of the solvents in the ternary phase, as a measure of composition of the "total solvent fraction", may be different from that in the binary phase. The interaction parameters between solvents and polymers are usually considered to be constant vs. composition. The interaction parameter between the two solvents usually is not. Since the "total solvent fraction" composition is different between the two

phases, the solvent-solvent interaction parameter will likely be different in both phases.

As Krigbaum and Carpenter mentioned in their article, equation (6) is not equal to the representation of the total free energy of formation of the ternary phase. For the case of the linear polymer a term RT n_3 ln υ_3 needs to be added, in addition to a term describing the osmotic pressure since the polymer is restricted to the network phase. This term will cancel out of the final equation, as is shown for the elastic term in Appendix B It will therefore be omitted here for didactic reasons. The elastic term will be discussed.

The equilibrium swelling condition

The equilibrium swelling condition for a copolymer network swollen in a single solvent can be found following the procedure given by Flory and Rehner[1]. Combining equations 1 and 3, and taking the first derivative with respect to n_1 and setting it equal to 0 yields:

$$\ln (1-\varphi_3) + \varphi_3 + m_1 \chi_{13} \varphi_3^2 + \nu_e m_1 V_B (A\varphi_3^{1/3} - B\varphi_3) = 0 \qquad (7)$$

V_B is the volume of the basic volume unit.

For further determination of the equation describing the equilibrium condition of swelling of a copolymer network in a mixed solvent, the partial molal free energies of formation of the binary and ternary phase need be determined as follows

$$\Delta\mu_{mixb1} = \partial(\Delta G_{mixb})/\partial n_1 \quad (8a)$$

$$\Delta\mu_{mixt1} = \partial(\Delta G_{mixt} + \Delta G_{el})/\partial n_1 \quad (8b)$$

$$\Delta\mu_{mixb2} = \partial(\Delta G_{mixb})/\partial n_2 \quad (8c)$$

$$\Delta\mu_{mixt2} = \partial(\Delta G_{mixt} + \Delta G_{el})/\partial n_2 \quad (8d)$$

The equilibrium condition is found by considering a composition fluctuation arising from the exchange of δn moles of volume units of solvent 1 from the binary phase with δn moles of volume units of solvent 2 from the ternary phase, while keeping $\upsilon 3$ constant. The free energy change for this exchange is given by:

$$\delta G = [(\Delta\mu_{mixt1} - \Delta\mu_{mixb1}) - m_1(\Delta\mu_{mixt2} - \Delta\mu_{mixb2})]\delta n \quad (9)$$

Herein m_1 is defined as V_2/V_1, with V_1 and V_2 the molal volumes of solvent 1 and 2 respectively. At equilibrium, δG is equal to 0.

The equations describing the equilibrium condition of the Krigbaum-Carpenter treatment are different from the treatment needed here. Their equations do not take into account the copolymer contribution since neither was necessary for their experimental results. Both are essential in our treatment, and need to be introduced in equations 2-6.

To account for the copolymer behavior of our networks an expression for the interaction parameter was derived in previous work[2] for the PPG-DRF system

with a single solvent. The same approach can be used here. At the basis of the description of the interaction parameter is the basic assumption that the number of nearest-neighbor contacts is proportional to the surface area of the components of the system[9]. Starting from this assumption, a number of polymer blend and solvent-polymer systems have been described[10 11 12].. An equation for ΔG_{mixt} for the case of a copolymer in a mixture of solvents can be derived on the same basis, as is done in Appendix B. It is clear that equation (B8) in the appendix is equivalent to equation (6) with the following modifications:

$$\chi_{12}' = [g_{12}]/Q \qquad (10a)$$

$$\chi_{13}' = [\varphi_a g_{1a} + \varphi_b g_{1b} - \varphi_a \varphi_b g_{ab}/\alpha]/Q \qquad (10b)$$

$$\chi_{23}' = s_{21} [\varphi_a g_{2a} + \varphi_b g_{2b} - \varphi_a \varphi_b g_{ab}/\alpha]/Q \qquad (10c)$$

The condition of equilibrium swelling is then given by the following equation:

$$\delta G = \ln \{(\upsilon_1/\upsilon_2)/(\varphi_1/\varphi_2)\} + (1 - m_1) \ln (\upsilon_2/\varphi_2) + m_1 \upsilon_3 (\chi_{13}' - \chi_{23}')$$
$$+ m_1 \chi_{12} (\varphi_{22} - \varphi_{12}) - m_1 \chi_{12}' [\upsilon_3 (\upsilon_2 - \upsilon 1) + \upsilon_2^2 - \upsilon_1^2] = 0 \qquad (11)$$

This equation differs slightly from the equilibrium equation of Krigbaum and Carpenter. This difference stems from the assumption that the value of the interaction parameter between the two solvents is composition dependent. This is true for most solvent mixtures.

Practical and computational considerations

As explained in the earlier treatise[2], the complexity in the calculation of the effective interaction parameter χ_{ij} and equivalently of g_{ij} here stems from the inclusion of considerations of differences in surface area between the solvents and the network components. This intrinsically necessitates the knowledge of the volume and the relationship to the surface area. The Bondi[13] volumes of the PPO repeat unit, the PIP repeat unit, the PBD repeat unit, and the [OC_6H_4NCO] unit are, 34.39, 47.62, 37.42, and 64.55 cm^3/mol. The molal volumes of methanol and benzene were calculated from their densities and taken to be 40.39, and 88.99 cm^3/mol, respectively. The surface areas of all components can be calculated from Bondi's treatment and are applicable since in the theory only ratios of these surface areas are used and the absolute value is of no consequence. They are 3.58, 6.01, 4.65, 6.21, 4.86, and 7.2 10^9 cm^2/mol, for methanol, benzene, the PPO repeat unit, the PIP repeat unit, the PBD repeat unit, respectively. The trimerization of methanol[14] was shown to have an effect on the swelling behavior of the PPG-DRF system. Thus the surface area of the trimer, that can actually be in contact with the network and the other solvent, is smaller than expected. From the previous study[2] it can be concluded that the surface area of the trimer is approximately 6.00 10^9 cm^2/mol. This value will be used from here on in all calculations with methanol.

The hydrogen bonding present in both systems may have an influence on the swelling behavior. As noted in the previous study, there is no known procedure to include this in the calculations, and it will therefore be ignored.

A further difficulty in this calculation appears when an assessment of the value of the interaction parameter between the two solvents is made. In the literature, this problem is only addressed tangentially. As becomes clear when reading introductory texts on solvent-solvent and solvent-polymer interaction, different conventions are used. The main difficulty stems from the description of the combinatorial contributions. For solvent-polymer equations, these are expressed in terms of volume fractions, while mole fractions are used strictly for solvent-solvent equations. This poses an obvious problem of definition, and afterwards of conversion. In Appendix B, we treat this problem for the interaction parameter in function of the composition of the mixture for the case at hand, namely the methanol-benzene system.

Results and discussion

Figures 1 and 2 depict the degree of swelling for the PPG-DRF and PIP-HDI system at 25°C, respectively.

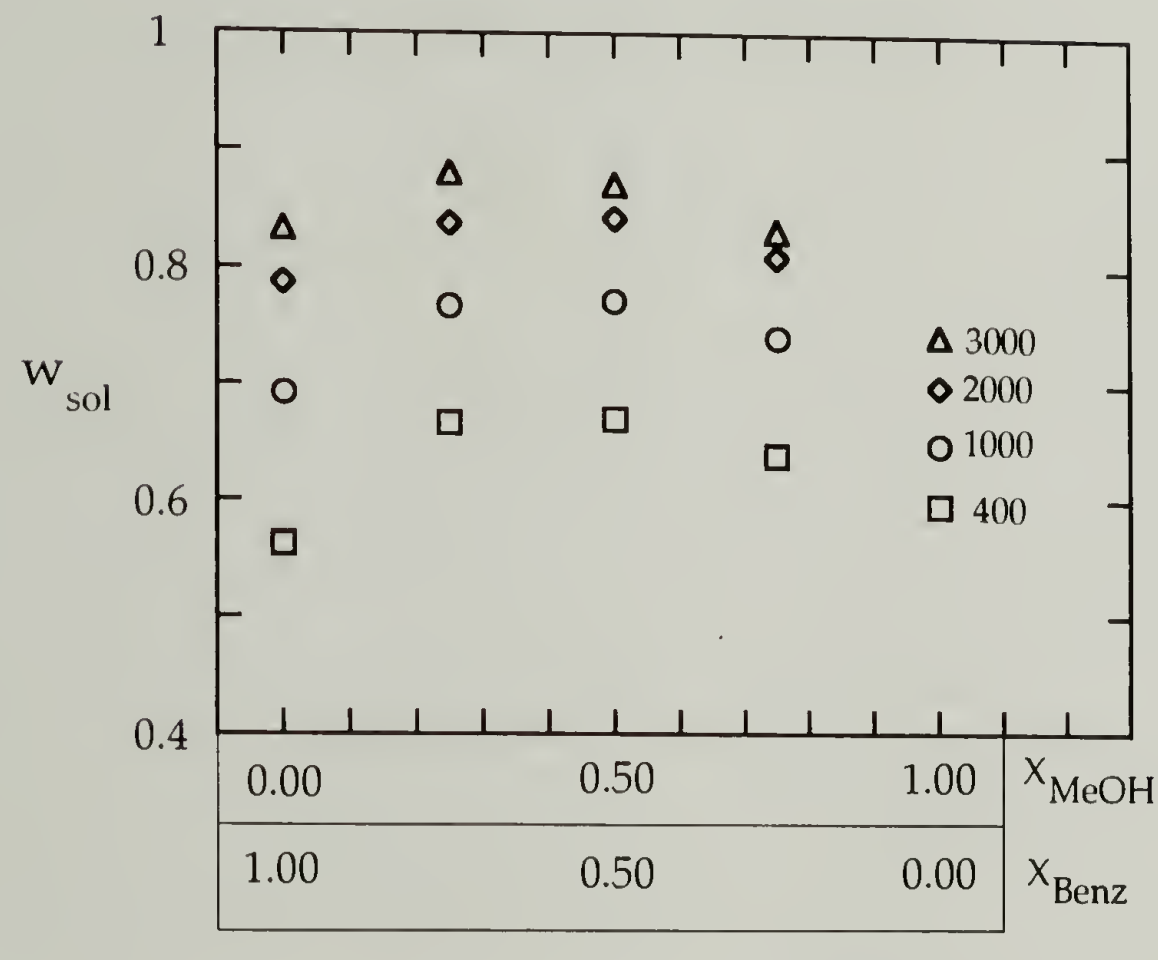

Figure 6.1 Degree of swelling in mixed solvents for PPG-DRF samples. Plot of the weight fraction of the solvent mixture vs. the mole fraction of methanol (x_{MeOH}) or benzene (x_{Benz}) in the solvent mixture for the PPG-DRF system. Molecular weights of the PPG indicated.

The general trends for both are clear and consistent. For the PPG-DRF system, the experimental swelling data are very similar to the data found for the swelling of other PPG-DRF networks in a toluene-methanol mixture[2]. A maximum is

found in the degree of swelling vs. composition. The maximum shifts slightly to compositions richer in benzene with molecular weight. The degree of swelling is directly proportional to the molecular weight of the PPG.

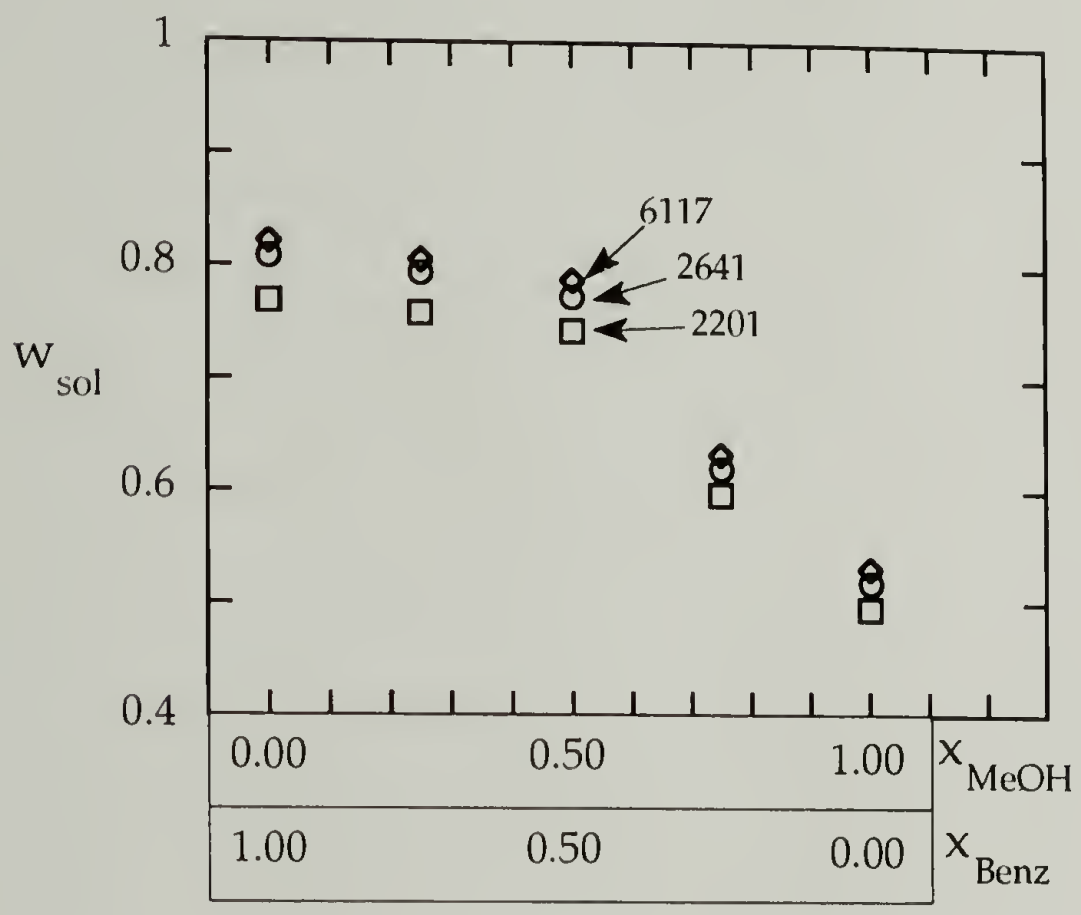

Figure 6.2 Degree of swelling in mixed solvents for PIP-HDI samples. Plot of the weight fraction of the solvent mixture vs. the mole fraction of methanol (x_{MeOH}) or benzene (x_{Benz}) in the solvent mixture for the PIP-HDI system. Molecular weights of the PIP indicated.

For the PIP-HDI system, no clear maximum in the degree of swelling with composition of the solvent is found, although such a trend is present. The increase in swelling with molecular weight is smaller than the one seen in the PPG-DRF system.

Qualitatively, some conclusions can be drawn. For the PPG-DRF system, at the basis of the shift of the maximum is a distinctive difference in interaction parameters between the crosslinker and the chain on one hand and the solvent on the other.

This observation can not be made clearly for the PIP-HDI system, although the calculations will need to be performed to in- or exclude copolymer effects. An apparent reversal of the magnitude in the degree of swelling with a change in solvent composition does seem to support the notion of a copolymer effect. The behavior in a single solvent, as described by the extremes in Figure 6.2, show no straight-forward relationship between the molecular weight of the tristar and the degree of swelling. It is actually remarkable that swelling occurred to the extent of 40-50% in methanol. Methanol is not a good solvent for PIP[15] nor for PBD[16]. Solutions over 5% of these homopolymers are difficult to obtain. The influence of the urethane groups on methanol swelling may therefore be far bigger than initially thought in the PIP-HDI system.

This was not found in the PPG-DRF system where the swelling data in pure methanol and benzene, could be fitted adequately with the theory described in the earlier paper, as will be shown further on. The effect of hydrogen bonding between the urethane group and methanol may be fully overshadowed in the PPG-DRF system by the multitude of favorable hydrogen bonding opportunities with the ether groups of the chain, while they are crucial in the PIP-DRF system. The "copolymer-in-solvents" equation may have to be written in a form to account for that, but at this point no reasonable way of addressing this problem seems eminent.

In the quantitative assessment of the equilibrium swelling behavior, a large number of parameters are to be determined from a relatively small number of experimental data. The entire behavior can only be described in terms of a multi-dimensional plane, of which a certain projection needs to correspond to another for verification of the entire approach. From a mathematical perspective it needs to be stated that this could lead to a "forest and trees" situation. One needs to be aware of the pitfalls of fitting data with the number of parameters present in this particular case. Also, the molecular weight between crosslinks range is relatively small, and is therefore a strain on the accuracy of the mathematical descriptions employed.

Keeping these factors in mind, the first step in the computation of the swelling behavior is to assess whether the notion of treating the PPG-DRF system as a copolymer is valid. Next, the determination of the interaction parameters between the two solvents separately with the two "copolymer" components needs to be made, in order for them to be used in a final step in the modified Krigbaum-Carpenter equation (11). The choice of the right interaction model for the determination of the interaction parameters is crucial. Also, the influence of the difference in elasticity models can be determined here.

The same steps need be performed for the PIP-HDI system.

In the following discussion, each aspect of the problem will be proved using highlights of the actual calculations. Full inclusion of available data is overkill, and is omitted for didactic purposes. The reader needs to be aware that the

trends and conclusions discussed are valid for the entire range of swelling addressed here.

Step 1: Is the copolymer approach valid? As was shown in the previous article[2], the swelling behavior in single solvents of the PPG-DRF system can be described adequately by assuming the copolymer effect to be applicable. A three parameter model was found to be appropriate from a plot of χ_{13} vs. φ_b. The plots were not linear, necessitating the description of χ_{13} as in equation (3), or with the regular three parameter equation[17]:

$$\chi_{13} = \varphi_a \chi_{1a} + \varphi_b \chi_{1b} - \varphi_a \varphi_b \chi_{ab} \qquad (12)$$

A similar plot was made here and represented in Figure 6.3. Similar behavior was found, and therefore determination of which three parameter model applies is warranted. This verification can only be made in conjunction with step 2.

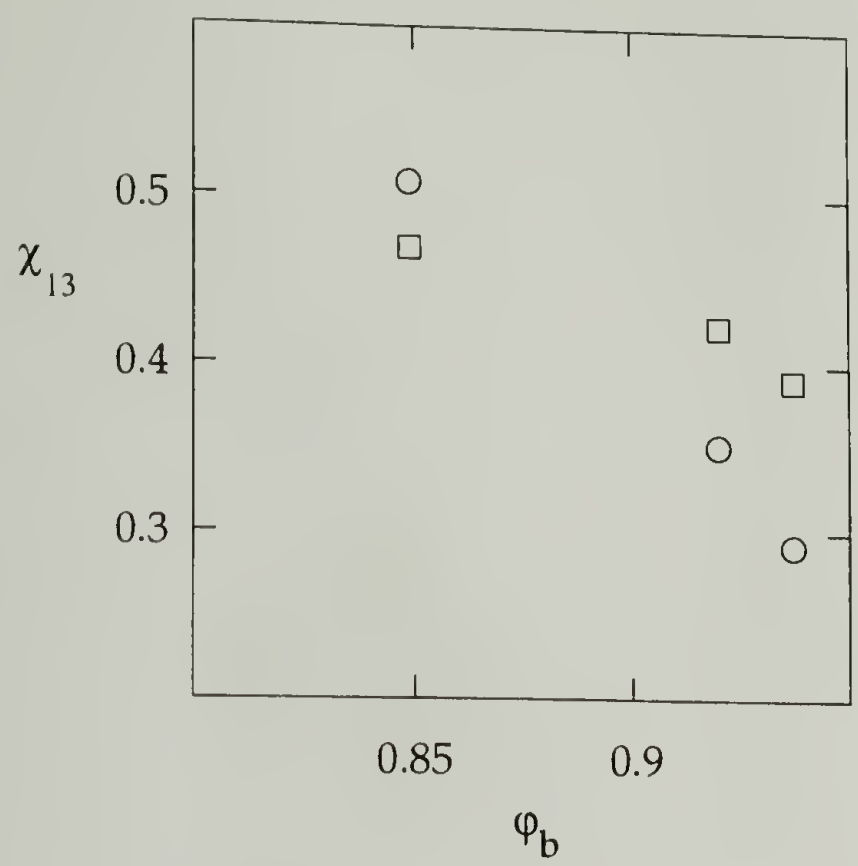

Figure 6.3 Plot of χ_{13} vs. φ_b for the PPG-DRF system at 25°C, extracted. Full line: best fit; dotted line: straight-line relationship.

Step 2: What are the appropriate values for the interaction parameters between all components involved? These again need to be determined from the single-solvent swelling behavior. The difficulty in this determination lies in the problem to determine these parameters independently with a different technique, since the polymer of the pure crosslinker cannot be made. The right values for the interaction parameters are assumed to be those for which, with the same elasticity model and three parameter model, the interaction parameter between the two network components, χ_{ab}, is the same for the case of both solvents.

First, it needs to be determined which elastic model needs to be applied. The number of elastically active network chains (EANCs) is of importance. The values obtained for χ_{ab} were relatively large when the networks were assumed not to be extracted (which does not correspond to reality, since all network were extracted before the swelling measurement). Values of between -14.49 and -51.63 were found. These are an order of magnitude larger than the χ_{ab} values found in the previous article[2]. The use of "unextracted" EANC values are thus discarded as invalid.

Second, the use of the swelling-dependent A and B in the elastic term needs to be addressed. Herein, A and B are defined as:

$$A = A_1 + A_2 \varphi_3; \qquad B = B_1 + B_2 \varphi_3 \qquad (13)$$

The boundary conditions for determination of A_1, A_2, B_1, and B_2 are A = 1 and B = 2/3 at $\varphi_3 = 1$, and A = 1/3 and B = 0 at $\varphi_3 = 0$.

When applying these values, χ_{ab} in the case of swelling in benzene is always positive, while for methanol it is always negative. This discrepancy does not occur in the case of the classical description of A = 1, and B =2/3.

Thirdly, the applicability of either three parameter model needs to be assessed. The values of χ_{ab} in the case of "extracted" EANCs and the affine model of elasticity are in the right order of magnitude for both models and both solvents over the entire temperature range used. Table 6.1 shows an overview.

Table 6.1 χ_{ab} for swelling in methanol and benzene. At 5°C, 25°C, and 45°C for the three parameter model (TPM) and the modified three parameter model (MTPM)

	5°C		25°C		45°C	
	TPM	MTPM	TPM	MTPM	TPM	MTPM
methanol	-9.5	-4.3	-7.2	-2.8	-10.8	-5.7
benzene	-4.6	-4.6	-2.3	-2.7	-5.5	-5.4

It is clear that for all temperatures the χ_{ab} values of the modified three parameter model are practically equal for both solvents, while rather large discrepancies do exist for the regular three parameter model.

It can be concluded that the modified three parameter model is applicable with the classical affine deformation model for the elasticity with account of the extraction to calculate the EANCs. The other interaction parameters are not given here for reasons explained later.

Step 3: Can the swelling behavior in mixed solvents be described with the Krigbaum-Carpenter equation (11)? To simplify calculations it is observed here that the mathematical expressions for χ_{13}' and χ_{23}' are equivalent to the equation for χ_{13} in equation (3) when s_{21} is equal to 1, which is the case for trimeric methanol and benzene as the solvent mixture. A complete list of χ_{13} values at different temperatures for different solvents and molecular weight between crosslinks is given in appendix B.

When solving the modified Krigbaum-Carpenter equation for the solvent composition in the swollen network, some interesting features appear. As a measure for solvent composition υ_1 is taken. To allow for a comparison with the solvent composition outside the network, the methanol volume fraction of the solvent fraction was calculated as $\upsilon_1' = \upsilon_1/(\upsilon_1 + \upsilon_2)$. In Table 6.2, the results of this calculation at 25°C are given.

The deviations from these results for different temperatures are small in absolute terms, but the trends stay the same over the entire range.

It can be concluded from this table that significant changes in solvent composition in- and outside the swollen network occur at the highest and the lowest methanol concentration. For the lowest methanol concentration in the solvent mixture outside the network, a higher methanol concentration is found inside the swollen network. For the highest methanol concentration in the solvent mixture outside the network, a lower methanol concentration is found inside the network. For the middle concentration, only a very small difference is observed.

This "azeotropic" behavior can possibly be explained by reviewing the starting assumptions by Krigbaum and Carpenter. Since the swelling of network polymers is a semi-open thermodynamic system, the surface of the network acts as a boundary between the binary and ternary phases. It is well known that benzene-methanol mixtures are azeotropic[18], meaning that the vapor phase can be more or less abundant of one component than the liquid phase. This same behavior is observed here, where the swollen network phase is more or less

Table 6.2 Solvent composition inside and outside the swollen PPG-DRF network at 25°C.

Composition $\varphi_1 = 0.1315$

MW(PPG)	υ_3	υ_1	υ_1'	χ_{12}	χ_{12}'
1002	0.2395	0.1576	0.2073	1.87	1.60
2004	0.1555	0.1554	0.1840	1.87	1.65
2910	0.1075	0.1522	0.1705	1.87	1.70

Composition $\varphi_1 = 0.3124$

MW(PPG)	υ_3	υ_1	υ_1'	χ_{12}	χ_{12}'
1002	0.2369	0.2462	0.3226	1.27	1.26
2004	0.1526	0.2641	0.3116	1.27	1.27
2910	0.1202	0.2732	0.3105	1.27	1.27

Composition $\varphi_1 = 0.5768$

MW(PPG)	υ_3	υ_1	υ_1'	χ_{12}	χ_{12}'
1002	0.2907	0.3840	0.5414	0.70	0.75
2004	0.1969	0.4383	0.5457	0.70	0.74
2910	0.1695	0.4556	0.5486	0.70	0.74

abundant than the solvent mixture phase. It appears that vapor-liquid equilibrium azeotropes cause swollen network-liquid azeotropes.

The notion of a copolymer effect and the azeotropic effect can be verified by repeating these calculations for the swelling of the PIP-HDI system.
Step1: Is the copolymer approach valid? To answer that question for this system is difficult because the difference in the two lowest molecular weights of the tristars is too small to determine linearity with reasonable accuracy. The differentiation may result from step 2.
Step 2: What are the appropriate values for the interaction parameters between all components involved? The same train of thought was followed as for the PPG-DRF system. For this system, it could also be concluded from the order of magnitude of the χ_{ab}'s found that the "extracted" EANCs need to be used. No significant difference could be found between χ_{ab}'s for different elastic models. The conclusion on the three parameter model could be confirmed here. The best agreement was again found for the modified three parameter model with the classical affine elasticity model. The values at 25°C are 0.14 for methanol, and 0.37 for benzene, while for the regular three parameter model these values were 0.94 and -0.20. The magnitude of the χ_{ab} values found here are an order of magnitude smaller than for the PPG-DRF system. The correspondence therefore can hardly be called remarkable for the MTP model. It is therefore still unclear whether the PIP-HDI system behaves like a copolymer with respect to swelling, but indications in that direction are found.

Additional information can be gotten from the interaction parameters between the individual solvents and the network PBD and PIP. The values of g_{1a} and g_{1b} for methanol are both 0.17. This indicates that methanol interacts with equally with PIP and PBD. For benzene a different picture is found: $g_{1a} = 0.33$ and $g_{1b} = 0.05$. For benzene, the PIP-HDI system does behave like a copolymer, while it does not in the case of methanol. It needs to be noted that the differences in all values are relatively small, that this conclusion can merely be a first look, and nothing more than a first approximation.

Step 3: Can the swelling behavior in mixed solvents be described with the Krigbaum-Carpenter equation (11)? Knowing whether the PIP-HDI system behaves like a copolymer in swelling experiments turns irrelevant when the surface areas of trimeric methanol and benzene are found to be practically equal. With this assumption, the PPG-DRF data could be described. Here we will assume the same to circumvent the lack of knowledge of copolymer behavior in PIP-HDI. Therefore the χ_{13} interaction parameters found for both benzene and methanol with equation (7) can be used directly in equation (11). The results are summed up in Table 6.3.

It is clear that exactly the same conclusions can be drawn from the calculations for PIP-HDI as for PPG-DRF with respect to the swelling in mixed solvents: The azeotropic behavior of the vapor-liquid equilibrium of the methanol-benzene mixture is found in the swollen network-liquid equilibrium of PIP-HDI networks.

Table 6.3 Solvent composition inside and outside the swollen PIP-HDI network at 25°C.

Composition $\varphi_1 = 0.1315$

MW(PIP)	υ_3	υ_1	υ_1'	χ_{12}	χ_{12}'
2201	0.1943	0.1462	0.1814	1.87	1.65
2641	0.1818	0.1319	0.1612	1.87	1.78
6117	0.1625	0.1293	0.1543	1.87	1.81

Composition $\varphi_1 = 0.3124$

MW(PIP)	υ_3	υ_1	υ_1'	χ_{12}	χ_{12}'
2201	0.1971	0.2481	0.3090	1.27	1.29
2641	0.1863	0.2404	0.2954	1.27	1.30
6117	0.1813	0.2326	0.2841	1.27	1.33

Composition $\varphi_1 = 0.5768$

MW(PIP)	υ_3	υ_1	υ_1'	χ_{12}	χ_{12}'
2201	0.2964	0.3690	0.5245	0.70	0.85
2641	0.3083	0.3502	0.5062	0.70	0.87
6117	0.3293	0.3267	0.4871	0.70	0.90

Relatively small deviations from these values were found upon use of different values for the surface area of methanol, but the conclusion of azeotropic behavior remained unchanged.

Conclusions

A number of interesting features of network swelling were highlighted in this chapter. That swelling of the PPG-DRF system needs to treated as swelling of a copolymer was confirmed. For the PIP-HDI system, this conclusion is uncertain for lack of an appropriate range of molecular weights of the PIP tristars. It appears that PIP-HDI behaves copolymeric for benzene and homopolymeric for methanol. For both systems, the classical affine elasticity model yielded the best results. Assuming A and B to be dependent on the degree of swelling was deemed fruitless. It was confirmed that the number of elastically active network chains needs to be calculated taking into account extraction.

The most remarkable conclusion can be drawn from the calculations on the swelling in mixed solvents. The azeotropic behavior of the vapor-liquid equilibrium of the methanol-benzene mixture is found in the swollen network-liquid equilibrium of both PPG-DRF and PIP-HDI network systems. The modified Krigbaum-Carpenter equation as it was used here opens interesting perspectives in separating the combinatorial part from the elastic part of the swelling equation, as it was defined by Flory and Rehner. This aspect will be studied in the future.

References

1. P. J. Flory, J. Rehner, J. Chem. Phys, 11, 521 (1943)

2. Z. S. Petrovic, W. J. MacKnight, R. Koningsveld, K Dusek, Macromolecules, 20, 1088 (1987)

3. K. Dusek, W. Prins, Adv. Polym. Sci., 6,1(1969)

4. M. Ilavsky, K. Dusek, Polymer, 24, 981 (1983)

5J. Queslel, J. E. Mark, Encycl. Polym. Sci. Technol., 5, 3625 (1986)

6. P. J. Flory, J. Chem. Phys. 9, 660 (1941)

7. M. L. Huggins, J. Chem. Phys. 9, 440 (1941)

8. W. R. Krigbaum, D. K. Carpenter, J. Pol. Sci., 24, 241 (1954)

9. A. J. Staverman, J.H. Van Santen, Recl. Trav. Chim. Pays-Bas, 60, 76 (1941)

10. A. Balazs, Macromolecules, 22, 4260 (1989)

11. R. Koningsveld, L. A. Kleintjes, Macromolecules, 18, 243 (1985)

12. R. Koningsveld, L. A. Kleintjes, G. Markert, Macromolecules, 10, 1105 (1977)

13. A. Bondi, J. Chem. Phys. 68, 441 (1964)

14. S. Glasstone, D. Lewis, Elements of Physical Chemistry, Macmillan, London (1946)

15. G. Gee, L. R. G. Treloar, Trans. Far. Soc., 36, 147 (1942)

16. J. Ferry, G. Gee, L. R. G. Treloar, Trans. Far. Soc., 41, 340 (1945)

17. G. ten Brinke, F. E. Karasz, W. J. MacKnight, Macromolecules, 16, 1827 (1983)

18. G. Scatchard, C. L. Raymond, J. A. C. S., 60, 1278 (1938)

CHAPTER 7

CONCLUSIONS

This work was designed to investigate the influence of molecular considerations on the glass transition, the equilibrium modulus, and the swelling behavior of two structurally different model network systems. A number of samples were prepared from the PPG-DRF system and the PIP-HDI system, with different molecular weights between crosslinks, and stoichiometric imbalance. Homogeneity on the molecular level of both systems was tested by DMTA, DETA, and NMR.

The analysis of the glass transition temperature shows that the copolymer effect is of crucial importance in the PPG-DRF system. The crosslinking effect governs the Tg of the PIP-HDI system. A new method was proposed to predict the Tg of networks. It assumes that the network is a copolymer of a "crosslinking unit" and a "chain unit". The crosslinking unit is defined as the crosslink with a portion of the chain corresponding to half of the lowest molecular weight between crosslinks available. In this way the Tg of the "linear equivalent" of the crosslinking unit is defined as the Tg of the network prepared with the lowest molecular weight between crosslinks. This approach predicts the Tg of all networks well with deviations for the lowest molecular weights and the highest stoichiometric imbalances. It also applies to other systems as described for methacrylate networks with tetrafunctional crosslinks. The effects of

crosslinking, hydrogen bonding, non-point crosslinks and other structural features can be successfully incorporated into the theoretical approach without identifying every aspect of the structure separately.

The notion that only elastically active crosslinks contribute to the Tg is refuted by this study. For lower molecular weights between crosslinks, essentially in epoxy resins, it is necessary to consider this feature.

The entire treatise confirms that an approach, based on the principle that Tg is an iso-free volume state, is valid and can be expanded to structural units larger than the polymer repeat unit or the crosslinker molecule.

The equilibrium modulus was measured to test the validity of certain assumptions in the molecular network theories of elasticity. The Constrained Chain model by Erman and Monnerie explained the experimental data well, except for the PPG400 networks, in the PPG-DRF system. No evidence to prove a contribution of trapped entanglements was found. This model explained the modulus dat of the PIP-HDI system perfectly, again without the contribution of trapped entanglements. This refutes earlier experiments on the PDMS system that clearly could be explained with the inclusion of a trapped entanglement contribution.

The erratic data observed for the PPG400 networks adds to the notion that these behave more like thermosets than like network polymers.

The influence of the bulky crosslinker in the PPG-DRF system has a profound effect on the DETA and NMR results, confirming an "anchoring" effect of the

crosslinker on the network chain. This effect was not seen in the PIP-HDI system. Therefore it was concluded that the PIP-HDI system is more homogeneous on a molecular level than the PPG-DRF system. Both systems produce homogeneous systems on a macroscopic scale. The influence of the anchoring effect on the glass transition and the equilibrium modulus is currently unclear at best.

Swelling of stoichiometrically balanced samples of both network systems was carried out in mixed solvents. The proposed copolymer-in-two-solvents theoretical approach seems to describe the degree of swelling in the PPG-DRF system and the PIP-HDI system consistently.

The conclusions drawn from earlier swelling experiments of the PPG-DRF system were confirmed. For both systems, the modified three parameter model yields the best results. The classical affine elasticity model is applicable, and the extraction is important in the calculation of the number of elastically active network chains.

The experimental results of the degree of swelling in mixed solvents can only be explained when taking into account a profound azeotropic effect in the swollen network-liquid equilibrium. This effect was found for both systems, and is consistent with the azeotropic effect of benzene-methanol mixture in vapor-liquid equilibria.

APPENDIX A

CALCULATION OF STRUCTURAL PARAMETERS OF POLYURETHANE NETWORKS

Petrovic et al[1]. applied the cascade theory of gelation to the PPG-DRF system for the case of stoichiometric amounts of network components. Introduction of stoichiometric imbalances leads to the following equations for the structural parameters of the system.

The extinction probability of a bond is the probability that the bond does not continue into a chain of infinite length. In our case v_H and v_I are the extinction probability of PPG and DRF, respectively. They are defined from the probability generation function (PGF) in the first generation.

$$v_H = (1 - p_H + p_H v_I) \qquad (A1)$$

$$v_I = (1 - p_I + p_I v_H)^2 \qquad (A2)$$

p_H and p_I are the conversions of the OH and NCO groups, respectively. In this case

$$p_H = p_I r_I \qquad (A3)$$

with

$$r_I = [NCO]/[OH] \qquad (A4)$$

the off-stoichiometric ratio. Solving for $(1-v_H)$ and $(1-v_I)$ from equations (A1) and (A2), taking into account (A3) gives

$$(1-v_I) = (2p_I^2.r_I - 1)/(p_I^4.r_I^2) \qquad (A5)$$

$$(1-v_H) = (2p_I^2.r_I - 1)/(p_I^3.r_I) \qquad (A6)$$

The conversion of reactive groups can be determined from the weight fraction of the sol, which is defined as:

$$w_S = m_H.x^2 + m_I.y^3 \qquad \text{(A7)}$$

with m_H and m_I the weight fraction of PPG and DRF, respectively:

$$m_H = n_H.M_H/M \qquad \text{(A8)}$$

$$m_I = n_I.M_I/M \qquad \text{(A9)}$$

n_H and n_I are the mole fractions of PPG and DRF and

$$M = (2.r_I.M_I + 3.M_H)/(3 + 2.r_I) \qquad \text{(A10)}$$

is the average molecular weight of the reaction mixture. x and y are defined as:

$$x = [1 - p_I\, r_I\, (1-v_I)] \qquad \text{(A11)}$$

$$y = [1 - p_I\, (1-v_H)] \qquad \text{(A12)}$$

Using equation (A7), p_I can be calculated from a determination of the weight fraction of the soluble fraction.

To calculate the Tg of the extracted sample, or gel fraction, using the modified copolymer approach, the weight fraction of DRF, w(g,I), and PPG, w(g,H), in the gel need to be determined. They can be defined as:

$$w(g,I) = m_I.(1 - y^3)/(1 - w_S) \qquad \text{(A13)}$$

$$w(g,H) = m_H\,(1 - x^2)/(1 - w_S) \qquad \text{(A14)}$$

The weight fraction of the "crosslinking unit" in the gel then is given by:

$$w(g,CLU) = w(g,I).\,(3.201 + 465)/465 \qquad \text{(A15)}$$

since each "crosslinking unit" consists of one DRF molecule, with molecular weight 465, plus 3 pieces of PPG chain, half the length of the shortest PPG chain with molecular weight of 402. The weight fraction of the "chain unit" is then defined as:

$$w(g,CU) = 1\text{-}w(g, CLU) \qquad \text{(A16).}$$

The number of unreacted hydroxyl and isocyanate end groups per gram of the unextracted samples is simply given as:

$$n_e = 6\,[1 + r_I - (2r_I p_I)]/(2r_I M_I + 3M_H) \qquad \text{(A17)}$$

For the extracted networks, the calculation is slightly more complex. The only hydroxyl groups still in the gel are of PPGs that have one, and only one OH group reacted. This is expressed by the fraction of unreacted OH end groups in the gel, f_{egH}:

$$f_{egH} = (1\text{-}p_H)\, p_H\, (1\text{-}v_I)/[1\text{-}(1\text{-}p_H\,(1 - v_I))^2] \qquad \text{(A18)}$$

For DRF the fraction of crosslinks that are connected to infinity and that have unreacted end groups are of two different kinds. The fraction of crosslinks that has two unreacted isocyanate groups is given by:

$$f_{egI2} = (1\text{-}p_I)^2\, p_I\, (1\text{-}v_H)/[1\text{-}(1\text{-}p_I\,(1 - v_H))^3] \qquad \text{(A19)}$$

and the fraction with one unreacted isocyanate group by:

$$f_{egI1} = (1\text{-}p_I)\, p_I^2\, (1\text{-}v_H)/[1\text{-}(1\text{-}p_I\,(1 - v_H))^3] \qquad \text{(A20)}$$

The number of unreacted end groups n_e of any kind per gram of network is then given by:

$$n_e = [(2f_{egI2} + f_{egI1})\, n_{Ig} + f_{egH}\, n_{Hg}]/M_g \qquad \text{(A21)}$$

Herein, n_{Hg} is defined as the mole fraction of PPG in the gel, which is given by:

$$n_{Hg} = w(g,H).M_I/(w(g,H).M_I + w(g,I).M_H) \qquad \text{(A22)}$$

and with nIg defined as the mole fraction of DRF in the gel, given by:

$$n_{Ig} = w(g,I).M_H/(w(g,H).M_I + w(g,I).M_H) \qquad \text{(A23)}$$

M_g can be defined as the average molecular weight of the network components in the gel, given by:

$$M_g = n_{Hg} . M_H + n_{Ig} . M_I \qquad \text{(A24)}$$

The number of elastically active network chains N_e can be found from the extinction coefficient using the following equation:

$$N_e = (3/2)\,(1 - v_H)^3\, p_I^3\, n_I \qquad \text{(A25)}$$

The equilibrium shear modulus G can then be defined as:

$$G = RT\,\rho\, N_e/M \qquad \text{(A26)}$$

with ρ the density of the network. The equilibrium shear modulus of the gel only can be defined as:

$$G_{gel} = G/(1 - w_s) \qquad \text{(A27)}$$

When the concentration of units with at least two bonds having infinite continuation are defined as $C_{I2(2)}$, $C_{I3(2)}$ $C_{I3(3)}$ and $C_{H2(2)}$, the trapping factor of trapped entanglements T_e becomes:

$$T_e = N^{-1}[C_{I2(2)} + C_{I3(2)} + C_{I3(3)} + C_{H2(2)}]^2 \qquad \text{(A28)}$$

The convention on the subscripts is clear. Each of these C's are defined as:

$$C_{I2(2)} = 3\, P_I\, n_I\, (1 - v_H)^2\, p_I^2\, (1 - p_I) \qquad \text{(A29)}$$

$$C_{I3(2)} = 3\, P_I\, n_I\, (1 - v_H)^2\, p_I^3\, v_H \qquad \text{(A30)}$$

$$C_{I3(3)} = 3\, P_I\, n_I\, (1 - v_H)^3\, p_I^3 \qquad \text{(A31)}$$

$$C_{H2(2)} = M_H\, n_H\, p_H^2\, (1-v_I)^2/M_{OH} \qquad \text{(A32)}$$

All parameters were defined before, except M_{OH}, which corresponds to the molecular weight of the PPG repeat unit, and P_I, which is the number of interacting segments in the DRF unit. In the calculations we assume its value to

be equal to 4, but the value affects the numerical outcome of the trapping factor only slightly. The normalization factor N is defined as:

$$N = [nI\ PI + M_H\ n_H/M_{OH}]^2 \qquad \text{(A33)}$$

The equivalent equations for the PIP-HDI system were calculated for a similar system by Dusek[2].

References

1. Z. S. Petrovic, J, Budinski-Simendic, T. Malavasic, W. J. MacKnight, Polymer, 31, 1514 (1990)

2. M. Ilavsky, K. Dusek, Polymer, 24, 981 (1983)

APPENDIX B

SWELLING OF A NETWORK IN A MIXTURE OF SOLVENTS, A THEORETICAL APPROACH

The Gibbs free energy of swelling of a copolymer network in two solvents

The system is composed of a copolymer network, consisting of two different units, and two solvents. For the description of the free energy of mixing of the ternary phase, we assume no crosslinking at this point. Subscripts used are defined in the main text, and more specifically as follows: a for the $[OC_6H_4NCO]$ unit or the PBD repeat unit; b for the PPG or PIP repeat unit; 1 for methanol; 2 for benzene and; 3 for the network. Each unit has a coordination number (average number of nearest neighbors) of z_i. The regular calculation of the number of contact pairs P_{ij} between all components yields $P_{ij} = N_i\theta_j$ for $i \neq j$, and $P_{ii} = N_i\theta_i$. $N_i = z_i n_i m_i$, with n_i the number of moles of species i, m_i the molar volume of species i in units of the basic volume unit, and θ_j is equal to $N_j/\Sigma N_i$.
The internal energy change of mixing can then be defined as

$$\Delta U = \Sigma\Sigma\, N_i\, \Delta P_{ij}\ \Delta\omega_{ij} \qquad \text{(B1)}$$

where ΔP_{ij} are the changes in the numbers of contact pairs, and $\Delta\omega_{ij}$ is the change in the contribution to the internal energy per contact. For our system this becomes:

$$\Delta U/N_\varphi RT = (N_a\theta_1/N_\varphi)(\Delta\omega_{a1}/RT) + (N_a\theta_2/N_\varphi)(\Delta\omega_{a2}/RT) + (N_b\theta_1/N_\varphi)(\Delta\omega_{b1}/RT) + (N_b\theta_2/N_\varphi)(\Delta\omega_{b2}/RT) + (N_1\theta_2/N_\varphi)(\Delta\omega_{12}/RT) + (N_{a(}\theta_b-\theta_b^\circ)/N_\varphi)(\Delta\omega_{ab}/RT) \qquad (B2)$$

with θ_b° defined as $N_b/(N_a + N_b)$. Then the switch is made to volume fractions of the components φ_i, combined with the simplified definition of the free energy per component $g_{ij} = z_j(\Delta\omega_{ij}/RT)$. This yields

$$\Delta U/N\varphi RT = [\varphi_1\varphi_2 g_{e12} + \varphi_1\varphi_3 g_{13} + \varphi_2\varphi_3 g_{23}]/Q \qquad (B3)$$

where Q, g_{12}, g_{13} and g_{23} are defined as

$$Q = \varphi_1 s_{1a} + \varphi_2 s_{2a} + \varphi_1 \alpha \qquad (B4)$$

$$g_{12} = g_{12} \qquad (B5)$$

$$g_{13} = g_{1a}\varphi_a + g_{1b}\varphi_b - g_{ab}\varphi_b\varphi_b/\alpha \qquad (B6)$$

$$g_{23} = s_{21}[g_{2a}\varphi_a + g_{2b}\varphi_b - g_{ab}\varphi_b\varphi_b/\alpha] \qquad (B7)$$

with $s_{ij} = z_i/z_j$, $\alpha = \varphi_a + \varphi_b s_{ba}$. Inherently included in this treatise is the assumption by Staverman[1] that the ratio of the coordination numbers is equal to the ratio of the surface areas of the components involved. The interaction parameters g_{13} and g_{23} are equal in form to the expression found for the interaction parameter found in a single solvent/polymer system, as described in a preceding article[2]. Subsequently, the Gibbs free energy of mixing , ΔG_{mix}, of n_1

moles of solvent 1 with n_2 moles of solvent 2 and n_3 moles of the copolymer is obtained by adding the entropic contribution to yield:

$$\Delta G_{mix}/RT = n_1 \ln \varphi_1 + n_2 \ln \varphi_2 + n_3 \ln \varphi_3 + [n_1 m_1 \varphi_2 g_{12} + n_1 m_1 \varphi_3 g_{13} + n_2 m_2 \varphi_3 g_{23}]/Q \qquad (B8)$$

The total free energy of swelling is obtained by combining equation (B8) with the elastic free energy change ΔA_{el}:

$$\Delta G_{el}/RT = \nu [(A/2 \sum \lambda_i^2 - 3) - B \ln \lambda_x \lambda_y \lambda_z] \qquad (B9)$$

The total energy of swelling is then defined as:

$$\Delta G_{sw}/RT = n_1 \ln \varphi_1 + n_2 \ln \varphi_2 + n_3 \ln \varphi_3 + [n_1 m_1 \varphi_2 g_{12} + n_1 m_1 \varphi_3 g_{13} + n_2 m_2 \varphi_3 g_{e23}]/Q + \nu [(A/2 \sum \lambda_i^2 - 3) - B \ln \lambda_x \lambda_y \lambda_z] \qquad (B10)$$

The methanol-benzene interaction parameter

The Gibbs free energy of mixing of a binary system is written as[3]

$$\Delta G_{mix} = G(n1, n2) - G°(n1) - G°(n_2) = n_1 (\mu_1 - \mu_1°) - n_2 (\mu_2 - \mu_2°) \qquad (B11)$$

As defined by Krigbaum and Carpenter in terms of volume fractions this is equal to[4]:

$$\Delta G_{mix} = RT [n_1 \ln \varphi_1 + n_2 \ln \varphi_2 + \chi_{12} \varphi_1 \varphi_2] \qquad (B12)$$

and the partial molar quantity $(\mu_1 - \mu_1^\circ)$ is given by taking the first derivative with respect to n_1 and is

$$(\mu_1 - \mu_1^\circ) = RT [\ln\varphi_1 + (1-m_1)\varphi_2 + m_1 \chi_{12} \varphi_2^2] \qquad (B13)$$

The difference between μ_1 and μ_1° can be expressed in terms of activity a_1 of species 1. From the theoretical description of the vapor-liquid equilibrium of solvent mixtures, these difference in chemical potentials can be defined as follows[5]

$$(\mu_1 - \mu_1^\circ) = RT \ln (P\, y/P_1) + (\beta_1 - V_1)(P - P_1) \qquad (B14)$$

In this equation P is the vapor pressure of the mixture, y is the mole fraction of component 1 in the vapor, P_1 is the vapor pressure of the pure component 1, β_1 is the limit at zero pressure of the difference between the molal volume of the vapor and that of a perfect gas, and V_1 is the molal volume of the pure liquid, all at the same temperature and pressure. In the literature, tables of vapor composition and vapor pressure at different compositions of the solvent mixtures can be found for methanol-benzene mixtures[6].

From equations B13 and B14, the interaction parameter between methanol and benzene can be calculated at different temperatures, using painstaking interpolation procedures and conversion methods of the raw data given by Scatchard[6]. This was performed and the results are plotted in Figure B.1.

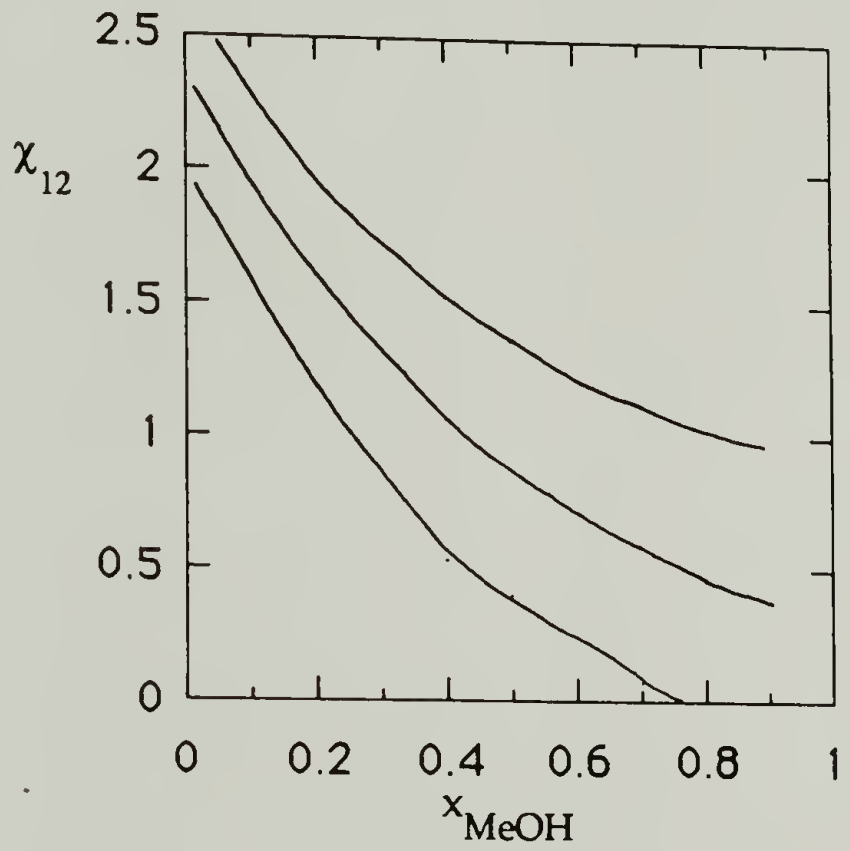

Figure B.1 χ_{12} for the methanol-benzene mixture. In function of mole fraction of methanol, while taking into account the trimerization of methanol.

References

1. A. J. Staverman, J.H. Van Santen, Recl. Trav. Chim. Pays-Bas, 60, 76 (1941)

2. Z. S. Petrovic, W. J. MacKnight, R. Koningsveld, K Dusek, Macromolecules, 20, 1088 (1987)

3. "Macromolecules, an Introduction to Polymer Science", Ed. by F. A. Bovey, F. H. Winslow, p. 275-288 (1979), Academic Press Inc., New York

4. W. R. Krigbaum, D. K. Carpenter, J. Pol. Sci., 24, 241 (1954)

5. G. Scatchard, C. L. Raymond, J. A. C. S., 60, 1278 (1938)

6. G. Scatchard, S. E. Wood, J. M. Mochel, J. A. C. S., 68, 1957 (1946)

BIBLIOGRAPHY

Aklonis, J. J. and MacKnight, W. J. (1983). Introduction to Polymer Viscoelasticity. John Wiley & Sons, New York.

Bovey, F. A. and Winslow, H. (1979). Macromolecules, an Introduction to Polymer Science. Academic Press, New York.

Chompff, A. J. and Newman, S., eds. (1971). Polymer Networks: Structure and Mechanical Properties. Plenum, New York.

Dusek, K. (1986). Adv. Polym. Sci., **78**, 1.

Dusek, K. and Prins, W. (1969). Adv. Polym. Sci., **6**, 1.

Labana, S. S., ed. (1977). Chemistry and Properties of Crosslinked Polymers. Academic Press, New York.

Labana, S. S. and Dickie, R. A., eds. (1984). Characterization of Highly Crosslinked Polymers. ACS Publications, Washington DC.

Mark, J. E. (1981). J. Chem. Educ., **58**, 898.

Mark, J. E. and Erman, B. (1988). Rubberlike Elasticity: a Molecular Primer. John Wiley & Sons, New York.

Mark, J. E. and Lal, J., eds. (1982). Elastomers and Rubber Elasticity. ACS Publications, Washington DC.

Mark, J. E. and Lal, J., eds. (1986). Advances in Elastomers and Rubber Elasticity. Plenum, New York.

Queslel, J. P. and Mark, J. E. (1987). J. Chem. Educ., **64**, 491.